Surface Friction Measurements of Fine-Graded Asphalt Mixtures

MBTC 2066
Final Report

by

Stacy G. Williams, Ph.D., P.E.
Research Assistant Professor
Department of Civil Engineering
University of Arkansas
700 Research Center Blvd.
Fayetteville, AR 72701
479-575-2220
479-575-7639 (FAX)
sgwill@uark.edu

June 2008

ABSTRACT

Skid resistance is generated by the development of friction between the vehicle tire and roadway surface, and is partially dependent upon the characteristics of the pavement texture. Microtexture and macrotexture are the critical components of pavement surface friction. Microtexture is the dominant characteristic at low speeds, and at high speeds, microtexture and macrotexture are both necessary. While these parameters are very important, neither is considered during the design of an asphalt mix.

In this project, mixture design parameters were investigated to determine what features of 4.75mm hot-mix asphalt (HMA) mixtures significantly influenced skid resistance. The British Pendulum Test (BPT) was used to quantify microtexture, and a sand patch test (modified for laboratory use) was used to measure macrotexture in terms of texture depth. Mixture properties and aggregate properties were also analyzed in order to develop relationships and guidelines for producing skid resistance during the design phase of an HMA construction project. Additional considerations involved comparisons with traditional surface mixes of larger nominal maximum aggregate size, and the effects of aging and wear on the long-term skid resistance of 4.75mm mixtures.

In general, mixture properties did not provide significant relationships to skid resistance (microtexture or macrotexture). Aggregate properties, however, did significantly correlate to measures of macrotexture. Specifically, the most influential variables were fine aggregate angularity, percent passing the #30 sieve, bulk specific gravity of the aggregate blend, and two-dimensional particle shape (as measured by the Aggregate Imaging System). Aggregate gradation was also significant in that a gap-graded aggregate blend appeared to increase both microtexture and macrotexture.

When compared to 9.5mm and 12.5mm mixes, the 4.75mm mixes possessed the greatest levels of microtexture. Thus, it was concluded that 4.75mm mixes did provide adequate skid resistance for low-speed roadways. The macrotexture of 4.75mm mixes was significantly less than that for a more traditional 12.5mm surface mix. Thus, if 4.75mm mixes are desired for use on high-speed roadways, the effects of roadway geometry on pavement drainage should be carefully considered.

ACKNOWLEDGMENTS

The author would like to gratefully acknowledge the Mack-Blackwell Transportation Center (MBTC) and the Arkansas Highway and Transportation Department (AHTD) for their funding and support of this project. Special thanks is also given to the Federal Highway Administration for their assistance with the aggregate imaging data. The efforts of Leela Bhupathiraju and Samatha Narra are deeply appreciated. Finally, the author wishes to recognize the residents of Hot Springs Village, Arkansas for committing to the 4.75mm HMA mixture application and serving as willing participants in the field trial.

TABLE OF CONTENTS

INTRODUCTION

Hot-mix asphalt (HMA) mixtures having a nominal maximum aggregate size (NMAS) of 4.75mm have been shown to provide significant advantages in a number of situations, including maintenance and resurfacing applications. *(1)* The small aggregate particles in these mixes will allow for placement of lifts as thin as 3/4 inch, which is much less than the typical 1-1/2-inch to 2-inch thickness used in traditional surface applications. This allows for significant savings in terms of costs, materials, and construction time. Also, this type of mix creates a smooth and tight surface that is aesthetically pleasing to the general driving public. These mixes certainly possess many advantageous characteristics, but some concern has been expressed that their smooth surfaces could also create an increased potential for skidding accidents.

Skid resistance is becoming increasingly important as it is a critical property for preventing accidents on wet roadways. *(2)* Skid resistance is provided by the friction developed between the roadway surface and the vehicle tire. This friction is significantly influenced by a number of factors including roadway geometry, the environment, and pavement surface characteristics. Geometric features of the roadway such as turning radius, design speed, frequency of intersections, and superelevation affect the ability of the driver to maneuver safely. Environmental features affect driver safety in that water and high temperatures decrease skid resistance. *(3)* The surface characteristics of the roadway are obviously important in that the friction that provides resistance to skidding takes place at the interface between the vehicle tire and pavement surface. Thus, it is reasonable that hot mix asphalt (HMA) mix designers could have some influence over the surface characteristics if this factor were considered during the mixture design process. Currently, skid resistance is not considered to be a standard design parameter for HMA mixes; however, support is growing for the inclusion of this item into standard mixture design criteria. *(4, 5)*

In this project, a number of mixture design parameters were investigated in order to determine what measures could be taken during the mixture design process to increase the effective skid resistance of 4.75mm HMA mixes. Mixture properties and aggregate properties were considered with an aim to correlate these characteristics with the amount of skid resistance generated. In addition, the skid resistance of 4.75mm mixes was compared to that of 9.5mm and 12.5mm NMAS mixes of similar material compositions. The effect of aging on skid resistance was also explored.

BACKGROUND AND LITERATURE REVIEW

Pavement friction is a measure of the force generated when a tire slides on a pavement surface, and is dependent on a large number of factors, including the road, vehicle tire, vehicle suspension, speed, ambient temperature, and the presence of contaminants such as oil and water. Skid resistance is the contribution of the roadway surface to the development of this friction, and is determined by examining the interaction between the pavement surface and the vehicle tires. The measurement of this friction is often represented by a friction number, or skid number. *(2, 3, 6, 7, 8)*

Climate

Typically, the skid resistance on a dry pavement is relatively high, and the skid resistance on a wet or damp pavement is somewhat lower and more variable. Thus, routine skid performance testing involves the application of water to the surface prior to testing. Rainfall activity will also affect skid resistance measurements. Interestingly, increased amounts of rainfall will create an increase in skid resistance. The results of a study in Maryland indicated that a 0.1 inch increase of daily average rainfall could lead to a 1.25 increase in friction number. *(2)* During dry periods, dust and oil collect on the surface. When water is applied for skid testing, the friction is reduced by these contaminants. Greater rainfall totals tend to clean the pavement surface and thus, measurements taken shortly after a rain are affected less by contaminants and result in higher skid numbers. *(2, 3, 7, 8)* It has also been noted that the extent to which moisture and contaminants affect skid resistance is dependent upon the surface type. *(2, 8, 9)*

In terms of temperature, skid resistance is typically less at higher temperatures. *(2, 7)* Seasonal variations can affect friction such that measurements made in spring or early summer may be higher than those measured for the same pavement in late summer or fall. In fact, a one degree F increase in average daily temperature can decrease friction number by one unit. *(2)* Also during the summer months, the pavement surface is continuously abraded, producing a coating of loose fines that reduce skid resistance. Thus, most skid resistance specifications require that routine testing be performed during the summer months in order to simulate worst case conditions. *(3)* During the winter months, skid resistance can be higher because the application of sand and salt used to prevent icy roads contaminates the surface. The subsequent removal of these contaminants roughens the surface, creating additional skid resistance. *(8)*

Traffic

Traffic also has a significant effect on skid resistance. Increases in traffic generate decreases in skid resistance. This is primarily due to the erosive action of vehicle tires on the surface texture of the roadway. Because urban roadways typically carry more traffic, they have been shown to deteriorate at a faster rate than rural roadways. In addition, when other parameters generate differences in skid resistance, this difference decreases as traffic level increases. *(7)*

Texture

Friction at the pavement's surface is generated by a combination of two primary components - microtexture and macrotexture. *(3, 7, 8, 9, 10)* Microtexture is the fine scale texture on the surfaces of individual aggregate particles, which is supplied primarily by the fine aggregate in the asphalt mixture. *(10)* This texture is produced by the microscopic irregularities in the exposed aggregate on the roadway surface, typically consisting of wavelengths ranging from 1μm to 0.5mm (0.0004 in. to 0.02 in.). *(7, 11)*

Macrotexture, or texture depth, is the larger texture generated by significant deformities in particle shape, as well as the spaces between aggregate particles. Wavelengths from 0.5 to 15mm are characteristic of macrotexture. Aggregate size and gradation are the primary factors affecting macrotexture. *(10, 11)*

Wavelengths larger than 15mm are commonly referred to as megatexture. This term describes the longitudinal profile of the pavement, and is often associated with pavement roughness. *(7, 12)* This texture is not beneficial to pavement skid resistance, and can create very uncomfortable driving conditions. In fact, a large megatexture can actually reduce the skid resistance of a roadway because less contact area is available to the vehicle tire.

Microtexture and macrotexture both contribute to skid resistance, and this relationship is dependent upon vehicle speed. At low speeds, microtexture dominates the skid resistance of the surface. In fact, microtexture alone may provide adequate skid resistance on low speed roadways. *(3, 8)* As the vehicle tire contacts the pavement, the tiny irregularities of the microtexture temporarily penetrate the tire and generate adhesive forces, creating a bond between the tire and pavement surface. *(5)* During this process, the tire deforms to take on the shape of the individual aggregate particles, creating a loss of energy known as hysteresis. The combination of hysteresis and adhesion generates the friction necessary to stop a skidding vehicle. *(13)*

At low speeds, surfaces with increased microtexture have higher wet skid resistance because the microtexture is able to absorb the thick water films that form on the surface of the pavement and break the films that coat the individual aggregate particles, thereby allowing for more direct contact between the tire and roadway surface. *(9, 10, 14)* As speed increases, the time of contact is shorter and there is a decrease in the amount of time available for adhesion and hysteresis to develop, resulting in an overall decrease of effective microtexture. During rain events there is less time for water films to be broken and to escape from the vehicle/surface contact area. In fact, just 0.025 to 0.23mm of water on the surface has been reported to reduce dry pavement friction by as much as a 20 to 30 percent. *(15)* Thus, microtexture alone may not provide adequate skid resistance at high speeds.

At higher speeds, the macrotexture of the roadway surface becomes increasingly important. *(3, 9, 10)* Larger texture depths generate larger deformations in the vehicle tire, increasing the amount of friction developed. The macrotexture of the pavement is also important in that it supplies a pavement with the ability to provide storage for water during rain events, as well as avenues to facilitate the removal of this water. In this way, drainage of the roadway is facilitated without disrupting the roadway/tire interaction, reducing the risk of hydroplaning. *(7, 11, 14, 16)* At higher speeds, there is greater potential for water pressure buildup, which is a component of hydroplaning. Also, hysteresis is more likely to develop in coarse aggregate texture at higher speeds. *(17)* For these reasons, an increase in macrotexture has been shown to decrease the frequency of fatal accidents in both wet and dry conditions. *(7)*

It is generally accepted that macrotexture has the greatest effect on the change of friction with speed; as speed increases, the effects of macrotexture become more important. However, there is some controversy as to the speed at which it begins to dominate. Most believe that texture depth becomes significant at speeds ranging from 40 mph (64 km/hr) to 50 mph (81 km/hr), *(6, 8, 17)* while others claim that macrotexture is significant at speeds as low as 31 mph (50 km/hr). *(3, 7, 18)*

In reality, the combined effects of microtexture and macrotexture are necessary to provide adequate skid resistance. A pavement having good microtexture and macrotexture maintains a high level of skid resistance regardless of speed. A pavement having good microtexture and poor macrotexture may have an equivalent amount of skid resistance at low speeds, but skid resitance decreases as speed increases. A pavement having poor microtexture and good macrotexture starts with a lesser amount of skid resistance, but maintains that level of skid resistance as speed increases. A pavement having poor microtexture and poor macrotexture will have a lesser resistance to skidding at lower speeds, and will exhibit a reduction in skid resistance as speed increases. *(6, 7, 8)* This phenomenon is presented in Figure 1. While microtexture alone may provide adequate skid resistance at low speeds, macrotexture alone cannot provide sufficient skid resistance at high speeds.

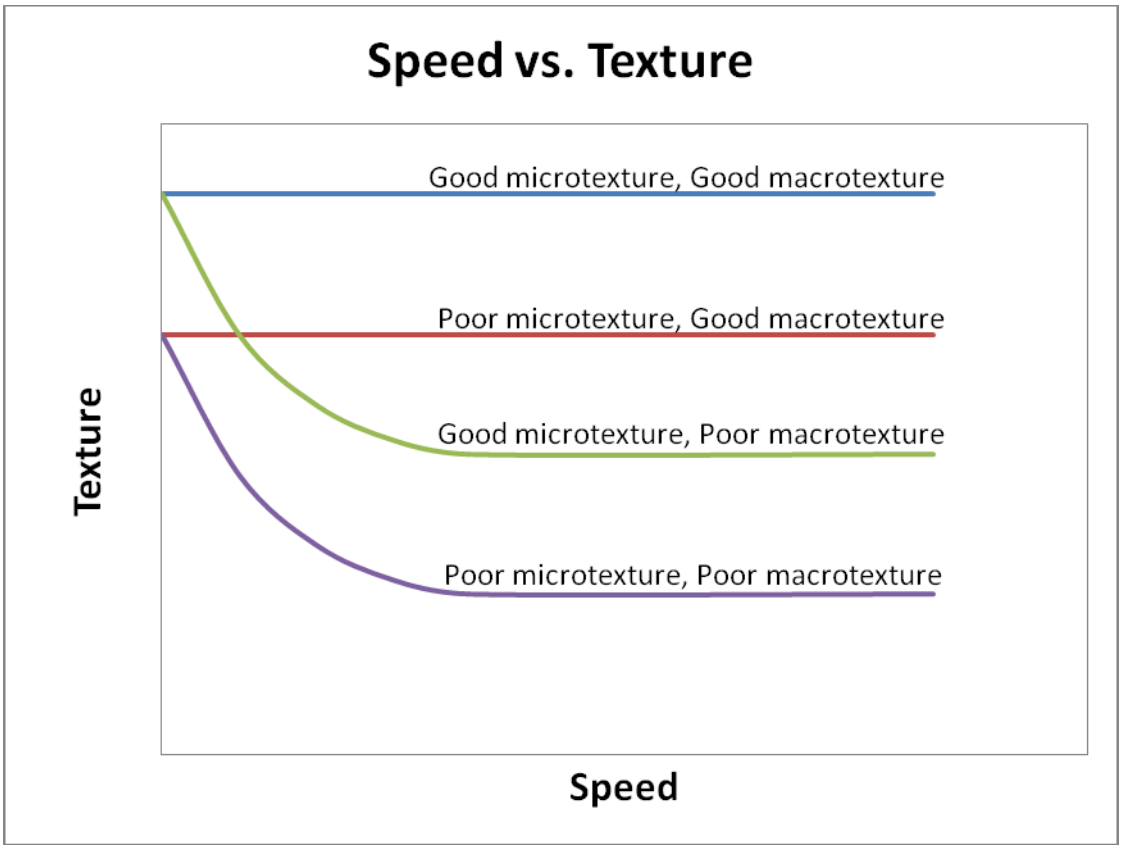

Figure 1. Relationship of Speed and Texture

Pavement texture can be either positive or negative, as illustrated in Figure 2. Positive texture is created by aggregate particles that protrude from the surface profile of the pavement. This type of texture is exhibited in chip seals, slurry seals, and some dense grade HMA mixtures. When a vehicle traverses a positive texture pavement, aggregate embeds into the tire, and the aggregate microtexture is exposed, creating hysteresis and adhesion (i.e., friction).

Negative texture is created by void spaces at the surface of the pavement. Negative texture surfaces are exemplified in open graded friction courses (OGFC), stone matrix asphalt mixes (SMA), porous asphalt mixes, and other coarse graded mixes. These types of mixes typically have thick coatings of binder and coarse-graded or gap-graded aggregate blends. Negative texture mixes are gaining popularity because they possess a number of advantages relating to fatigue, long-term durability, rutting resistance, splash and spray, rolling resistance, and noise. *(4, 7, 19)* Although the thick binder coatings aid in solving many durability issues face by the pavement industry, they may actually be detrimental to skid resistance. Negative texture contains less protruding aggregate particles, which reduces the amount of embedment of aggregate into the vehicle tire. In addition, the thick asphalt coatings prevent thorough contact between the microtexture and tire. Thus, the contribution of hysteresis is reduced and less overall

friction is generated, especially during emergency braking action. *(4, 20)* Another point of caution regarding negative texture mixes is that only the points on the aggregate contacting vehicle tires are considered as part of the microtexture measurement. The microtexture existing in the negative spaces does not contact the vehicle tires, and therefore does not provide any additional skid resistance.

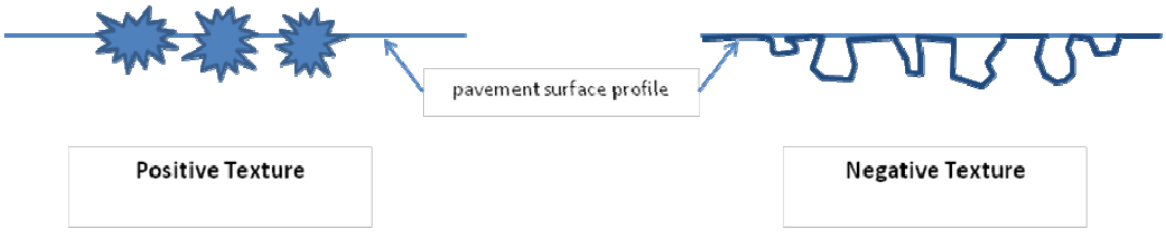

Figure 2. Positive vs. Negative Texture

Methods of Measurement

Most friction testing is performed as part of a routine pavement maintenance program as a means for managing the risk of wet skidding accidents, and in some cases, it is performed for forensic purposes. *(3)* For this reason, skid testing is most often considered to be a field test. Because skid resistance is dependent on both microtexture and macrotexture, which is significantly affected by speed, most skid testing programs involve a measure of both parameters. Most skid tests are performed using either the British Pendulum Tester (BPT) or a skid trailer according to one of the test methods listed in Table 1, then supplemented with a measure of texture. In general, field tests used to characterize skid resistance produce a frictional coefficient. This value is then multiplied by 100 and reported as the skid number.

Type of Device	Typical Equipment
British Pendulum	ASTM E 303 Tester
Locked Wheel Device	ASTM E 274 Trailer
Side Force Devices	Sideway-force Coefficient Routine Investigation Machine (SCRIM) MuMeter
Fixed Slip Devices	Griptester
Variable Slip Devices	ASTM E 1859 ASTM E 1337 Norsemeter ROAR

Table 1. Summary of Most Common Field Skid Testers in Use

The BPT is the most commonly used device for measuring microtexture, and has several advantages in that it is portable, relatively inexpensive, can serve as either a laboratory or field test, and the results can be mathematically adjusted to account for the

effects of temperature. *(10, 14)* In this method, a rubber foot attached to a pendulum is released from a starting position. As the arm is released, the potential energy in the system is converted to kinetic energy, which is then dissipated by friction on the rubber foot as it slides over the pavement surface. This method can only account for low-speed skidding, and is less accurate for samples having a very coarse macrotexture. Therefore it is not recommended for the measurement of macrotexture, or for testing surfaces having high macrotexture. *(8)*

One alternative to the BPT is the North Carolina State University variable-speed friction tester. It is very similar to the BPT but has a locked-wheel smooth rubber tire at the bottom of the pendulum and can simulate variable vehicle speed. It is also applicable to samples of a coarse or open-graded nature. The test results provide a 'variable speed number' (VSN) which has been shown to relate well to field skid numbers. *(8)*

Because so many field tests exist, extensive field trials have been performed in order to correlate skid numbers. *(7, 21)* One of the most notable was performed by the World Road Association, previously referred to as the Permanent International Association of Road Congresses (PIARC). *(7)* From the data collected during these field trials, the concept of the international friction index (IFI) was proposed, which is a process for correlating the effects of speed and friction from the various devices.

A number of models have attempted to relate the effects of speed and friction. An early model was developed at Penn State in which the relationship of friction to slip speed was described. Another model, the Rado model, was developed based on the peak friction developed during the braking action of a vehicle having anti-lock brakes. In developing the IFI, PIARC adopted the Penn State model but changed the intercept to 60 km/hr. It was felt that a model would be more approprate if more than one speed were considered to describe skid resistance because speed can have such a profound influence over skid resistance for a given texture.

The IFI is a function of friction number *(F60)* and a speed constant *(S_p)*, and is calculated according to Equation 1 for a device operating at slip speed *(S)*. Slip speed is defined as the relative velocity of the tire of a locked wheel over the pavement surface. At low slip speeds, microtexture dominates the measurement; and at high slip speeds, the macrotexture becomes increasingly important. *(22)* The slip speed of the BPT method is usually assumed to be about 6 mph (10 km/hr). Because this speed is very low, the BPT measure of skid resistance should only be treated as a measure of microtexture and is used as a surrogate measure of this property. This is very useful because actual microtexture measurements are extremely difficult to quantify. *(7)*

$$F(S) = F60e^{\frac{60-S}{S_p}} \qquad \textit{Equation 1}$$

The critical feature of the IFI is that it is based upon both friction and texture measurements. This is important because both microtexture and macrotexture must be considered in order to adequately characterize pavement friction. Friction number and speed constant are calculated according to ASTM E 1960. *(23)* In the calculation, a constant is necessary to describe the type of tire used in the friction test because smooth tires are more sensitive to macrotexture than patterned or ribbed tires.

The friction number *(F60)* is a harmonized level of friction for a slip speed of 36 mph (60 km/hr), and is calculated by Equation 2 where A, and B are calibration constants, and C is a constant which is dependent upon the method used to determine macrotexture.

$$F60 = A + B\ FRS\ e^{\frac{S-60}{S_p}} + C\ TX \qquad \textit{Equation 2}$$

The speed constant *(S_p)* is derived from the macrotexture measurement that indicates the speed dependence of friction, and is related to the macrotexture measurement *(TX)* by Equation 3, where a and b are constants that must be determined for each type of macrotexture measurement.

$$S_p = a + b\ TX \qquad \textit{Equation 3}$$

Historically, the American Association of State Highway and Transportation Officials (AASHTO) has recommended volumetric techniques for measuring macrotexture. This recommendation was published in 1976, and there has been no update to these guidelines since that time. Volumetric methods include the sand patch method, the grease patch method, the glass beads method, and the silicone putty method – all of which rely on physical measurements of a volume of material required to fill the texture spaces in a circular area in the surface of the pavement. *(14, 21)* A newer proposed method is the Mean Profile Depth (MPD), which is described in ASTM E 1845. *(24)* In this method, the MPD is calculated by dividing the measured profile into segments having a length of 100 mm (4 inches). The slope of each segment is set to zero using linear regression techniques, which creates a zero mean profile. Next, the segment is divided in half and the height of the highest peak in each half is calculated and the average height of the two peaks is the mean segment depth. The MPD is reported as the average for all of the mean segment depths, which can be related directly to the speed constant *(Sp)* or used to estimate mean texture depth (MTD).

Other methods for quantifying texture depth include the Circular Texture Meter (CTMeter), which is a relatively new device used for the measurement of MPD, the Kansas linear traverse method, the Texas texturemeter, light sectioning methods, and stereo photography. *(7, 8)*

The Dynamic Friction Tester (DFT) is a relatively new method for measuring frictional properties. This method, developed in Japan, is a portable device which allows for the measurement of surface friction of a variety of pavement types in either the laboratory or field setting. The DFT is affected by both microtexture and macrotexture, and can be used in combination with mean profile depth measurements in order to determine IFI. It also has the advantage of being able to directly measure friction as a function of speed. The DFT value at 12 mph (20 km/hr) in combination with a texture measurement has been demonstrated to provide a good estimate of IFI. *(7)* In another study, the DFT correlated well with the BPT while also displaying lesser testing variability. *(10)*

HMA Properties and Skid Resistance

Both the binder and aggregate components of an HMA mix contribute to its skid resistance. When a pavement is new, the binder coatings are still present on the surfaces of the aggregates, and it is the friction generated by the binder that contributes to skid resistance. Thus the binder properties are most important when the pavement is new. As traffic begins to wear the pavement's surface, the binder coatings are worn away and the aggregate is exposed. Because aggregate has a much greater microtexture and macrotexture than binder, the skid resistance of the pavement can sharply increase, reaching a maximum level as the aggregate characteristics begin to govern. As the aggregate is exposed, its microtexture improves the overall skid resistance of the mix. As the pavement ages, the aggregates begin to polish and degrade, resulting in a subsequent loss of skid resistance. Aggregate polishing is primarily responsible for losses of microtexture, and aggregate degradation is largely responsible for losses of macrotexture. For most roadways, friction changes over time such that it generally follows a logarithmic trend of decreasing, then leveling out at a terminal friction level. After that time, the friction level remains relatively constant. *(2, 7, 25)* In general, the friction level of a pavement is believed to reach a relatively steady state within the first one to two years of service, with some pavements losing as much as 50 percent of the initial skid resistance. *(2, 17, 26)*

Binder Considerations

Mixes having greater binder contents are more likely to experience bleeding, flushing, and rutting; and are prone to lower skid resistance. In essence, excess binder at the pavement surface acts as a contaiminant and disrupts the contact between the vehicle tire and pavement texture. Bleeding binder in a mix can be tracked by vehicles if it has a high temperature or a low viscosity. This tracking can transfer excess binder to other locations on the pavement surface, masking the microtexture of aggregates and decreasing skid resistance. *(12, 27)* Flushing is a related problem, and is defined as the upward migration of binder. Flushed binder fills the macrotexture space and lowers the overall roadway surface texture. If temperatures are high and the surface tension of this excess binder is broken, bleeding and tracking can also occur – again resulting in a reduction of macrotexture and surface texture. *(12)* Skid resistance can also be reduced

by pavement rutting. When an HMA mix ruts, the aggregate particles shift within the aggregate matrix. This reorientation results in an unstable mix and decreased frictional resistance. *(28)*

Excess films of binder can also lead to a problem known as 'bituplaning'. This phenomenon is similar to hydroplaning, but occurs on a dry surface when binder films (rather than water) interrupt the hysteresis and subsequent adhesion between the tire and pavement surface. *(19, 20)* In come cases, pavements having adequate wet surface friction may be prone to bituplaning.

Binder grade is also a factor that affects skid resistance. Modified binders take longer to wear away from the aggregate surfaces, and thus take longer to reach the maximum skid resistance condition. Unmodified binders tend to be softer and weaker than modified binders, so they wear away more quickly and expose the aggregate earlier during the life of the pavement. Therefore, aggregate quality quickly gains importance for unmodified mixes. In some cases, a pavement that contains weaker, stripping-susceptible aggregates may develop greater early skid resistance than that of a mix containing higher quality aggregates, simply because of the premature aggregate exposure. *(4, 27)*

Aggregate Considerations

Aggregates that are strong, durable, and abrasion-resistant are believed to the the best performers with respect to long term skid resistance. *(29)* Hard aggregates, such as feldspar and quartz, assist in supplying good skid resistance. Sandstone and slag are other hard aggregate types that also possess good microtexture. Specifically, materials having a minimum Moh's hardness of 5 to 6 are recommended for use in surfacing materials. *(6, 17)* Alternatively, weak aggregates tend to quickly lose friction if the tiny sharp edges that generate friction are not durable. *(28)* When these portions of the aggregate break, the frictional resistance provided by microtexture is no longer available. This action is characteristic of aggregate polishing, which is source dependent, and has been cited as the parameter most responsible for reductions in skid resistance. *(10, 26)*

The polish resistance of an aggregate is usually measured by establishing the initial skid resistance of the material, conditioning the sample by subjecting it to a series of polishing cycles, then determining the skid resistance of the conditioned samples. The BPT is often used in conjunction with the British Polishing Wheel in order to characterize the reduction in microtexture due to aggregate polish. Other methods for polishing include the small-wheel circular track wear and polish machine, the Georgia skid tester, and the French high-pressure water application. *(8)*

In Europe, the British Polishing wheel is commonly used to measure the Polished Stone Value (PSV) of aggregate sources because it is generally accepted that high PSV aggregates generate greater skid resistance. Some states in the U.S. also specify this

method for qualifying an aggregate source. A Maryland study reported that mixes containing aggregates with a PSV greater than 6 had friction numbers that were approximately 3 unites higher than mixes containing aggregates with a PSV less than 6. *(2)* While PSV can be used as a significant indicator of aggregate quality, researchers in the U.K. caution that mix designers should consider more than just PSV and texture depth because high PSV does not guarantee early-life skid resistance. The true relationships are complicated and a number of factors must be balanced. *(4)*

Aggregate particle size and gradation are also known to affect skid resistance. As aggregate size decreases, friction increases. *(2, 18, 29)* This is partly because fine aggregate is the primary contributor to microtexture; and microtexture is often the true parameter being measured by "friction" tests. Gradation is important to skid resistance in that as aggregate spacing decreases, friction increases. *(30)* Fine-graded aggregate blends contain a large portion of small aggregate particles with small void spaces, or gaps, which are likely to exhibit closer aggregate spacings. These fine aggregates also generate microtexture, which increases total friction. Conversely, coarse-graded aggregate blends contain a large proportion of large particles such that the void spaces, or gaps between them, are also relatively large. Large void spaces can create significant areas of the pavement surface which do not contact the vehicle tire, and thus do not contribute to microtexture. Again, this relationship is likely affected by the fact that most friction tests primarily detect microtexture.

Effects of Mix Design

In many areas of Europe and the U.S., skid testing is being implemented as a routine tool for pavement maintenance. While this practice is indicative of the high importance of frictional characteristics, this type of testing is performed only after construction is complete. In other words, no specific design procedures are incorporated. *(31)* In order for skid resistance properties to be optimized prior to construction, many feel that there is a great need to incorporate specific skid resistance components into current design procedures. *(4, 27)*

When an HMA mix is developed, designers consider a number of factors including structural performance and durability, skid resistance, noise, splash and spray, rolling resistance, and tire wear. Most designers feel that structural performance and durability are most important, and skid resistance ranks as a close second because of the inherent safety issues involved. *(7)* While a multitude of design requirements are specified to ensure structural pavement performance, skid resistance is not a formal part of the design process. In most cases, adequate skid resistance is ensured simply by requiring the use of good quality coarse aggregate with a satisfactory performance history. For example, Indiana accepts an aggregate source based on historical data, and then requires skid test monitoring according to ASTM E 524 for two years following construction. *(32, 33, 34)*

Some design procedures are based on the assumption that since aggregate durability and skid resistance are interrelated (i.e., aggregate polishing and degradation are signs of low durability as well as poor frictional characteristics), specifications relating to aggregate durability also prevent the use of low friction aggregates. *(7)* Others do not feel that there is a skid resistance test method available that is appropriate for design specifications. Nevertheless, no HMA mixture design methodologies used in the U.S. include procedures for the consideration of frictional resistance and texture, and only a few exist in other countries. *(5, 7)*

In the United Kingdom, a minimum macrotexture depth (MTD) of 1.5mm is *preferred* for new pavements. *(7)* In New Zealand, a surface texture of 0.6mm is required. *(27)* The Quebec Ministry of Transportation uses image analysis for HMA fine aggregates to distinguish roundness and angularity, which provides a surrogate measure of aggregate quality relating to skid resistance. *(8)*

In the U.S., HMA mixtures are designed primarily to be durable, and to resist the primary failure modes of rutting and cracking. *(35)* Recent design methodologies encourage the use of coarse-graded aggregate blends to strengthen the stone-to-stone sturctural skeleton, along with rich performance-graded binder coatings that enhance durability. These types of mixtures usually produce a surface having negative texture. These mix types are increasing in popularity because they are durable, good for fatigue, and reduce road noise. However, the thicker binder coatings tend to mask the aggregate microtexture, lowering the wet skid resistance. Also, negative texture mixes may be prone to bituplaning, or dry friction problems, as discussed earlier. *(19)*

Although HMA mixture properties are known to affect pavement skid resistance; the interrelationships are complicated by aggregate type, binder, composition, surface texture, time of year, roadway geometry, and traffic. Additional complications arise when elements such as production factors, construction factors, inservice factors, and environmental factors are considered. *(4, 6, 29)* With so many influential variables, it is not surprising that numerous research efforts have been unable to completely quantify the relationship of these effects for incorporation into HMA design specifications.

Several trends, however, have been reported. *(4, 5, 27, 36)*

- As binder content increases, skid resistance decreases.
- As voids in the mineral aggregate (VMA) increase, macrotexture may increase while microtexture decreases.
- As the percent passing the 4.75mm (#4) sieve increases, microtexture increases, but macrotexture decreases.
- As the fineness modulus of the aggregate blend increases, macrotexture increases and microtexture decreases.
- As the relative density of the compacted material increases, microtexture increases and macrotexture decreases.

In a 2004 study, a three dimensional finite element model was developed in order to predict the skid resistance value of a surface generated by microtexture. *(37)* The intention of this model was to eliminate the need to perform the BPT test. However, microtexture alone is not an adequate measure of skid resistance. In New Zealand, a procedure has been proposed which calculates mean profile depth as a function of aggregate gradation and binder content. *(27)*

When attempting to incorporate a mixture parameter into a design scheme, a laboratory test method (rather than field method) must be used. This poses the natural question: does the test method performed in the laboratory accurately reflect the performance that might be expecte in the field? A study was performed to investigate the use of laboratory skid tests during the design of HMA mixes. *(5)* For dense-graded, 12.5mm NMAS Superpave and SMA designs, laboratory and field skid resistance data was collected. In general, the top sides of the gyratory-compacted specimens had greater skid resistance than the bottom sides. Overall, the laboratory specimens exhibited greater skid resistance than the field mixes, but the bottom sides more closely correlated with field skid resistance values. Differences in laboratory and field data led to the conclusion that the laboratory compaction mechanism is not equivalent to that of field compaction. It was suspected that the intense pressure applied during laboratory compaction caused aggregate surfaces at the top of the specimen to become exposed, and therefore offer increased skid resistance. This situation also indicated that field compaction equipment is not as harsh as that used in the laboratory. Although predictive relationships were not yet recommended for use during design, the following factors were found to have the greatest impact on the skid resistance of a mixture: the fineness modulus of the aggregate blend, the bulk relative density of the compacted mix, the percent passing the No. 4 (4.75mm) sieve, and binder content.

OBJECTIVES

The primary objective of this research project was to determine whether fine-graded HMA mixtures, specifically 4.75mm mixes, possess safe and desirable levels of skid resistance, and to determine what steps could be taken during the mixture design process in order ensure adequate skid resistance.

During mixture design, mix proportions are adjusted in order to meet specification requirements for a number of mix parameters. Mixture characteristics such as air void content, binder content, voids in the mineral aggregate, voids filled with aggregate, and level of compaction are known to affect pavement performance, and are considered throughout the mixture design process. In this project, a number of mixture design parameters were investigated so that their relationships to skidding performance could be established, and a potential mechanism could be generated for the purpose of considering skid resistance during the design of asphalt mixtures.

In addition, natural variation in mixture parameters can directly affect performance. In most cases, mix property variations are related to structural pavement performance (i.e., rutting and cracking). Skidding performance, however, has most often been related to other signs of pavement distress rather than actual mixture properties. The intention of this project was to directly relate the effects of variations in mixture properties to changes in skid resistance.

Aggregate properties such as toughness, abrasion resistance, durability, soundness, shape, and texture are known to have a significant effect on skid resistance. Therefore, a number of aggregate properties were investigated for a range of aggregate types to relate mixture skidding resistance to aggregate characteristics that are commonly measured. These relationships could also prove valuable if used as an aid during the HMA mix design process.

Because the intention of this project was to determine ways to design HMA mixtures with adequate skid resistance, all test methods investigated were laboratory methods. Also, since skid resistance is not currently measured during design, there was no published value for judging the adequacy of skid resistance. Thus, 9.5mm and 12.5mm HMA mixtures were evaluated in order to provide a comparative sense of the frictional characteristics of typical surface mixtures.

Additional aims of this project included comparisons of field and laboratory measures of skid resistance, a consideration of the loss of skid resistance over the life of the pavement, and an investigation of the effects of drainage issues on skid resistance.

RESEARCH METHODS

In this study, three aggregate sources were used to design a number of 4.75mm mixtures. The effects of specific design parameters, as well as the effects of other properties that were varied as a result of the design process, were analyzed with respect to skid resistance. A discussion of the mixtures and test methods used is included in this section.

Mixture Properties

To assess the effects of design parameters on the skid resistance of 4.75mm mixes, mix designs were produced at various combinations of design air void content and design compaction levels. According to AASHTO M 323, HMA mixtures are to be designed at 4.0 percent air voids. (*38*) However, previous research has demonstrated that the rutting performance of 4.75mm mixes can be improved when designed at higher air void contents. *(1, 39)* In Arkansas, standard HMA mixtures containing PG 70-22 binders are designed at 4.5 percent air voids. *(40)* Therefore, two design air void contents (4.5 and 6.0 percent) were chosen for this portion of the study. Because 4.75mm mixtures have many possible applications and could be used to serve a wide range of traffic levels, three design levels of compaction were chosen (N_{design} = 50, 75, and 100 gyrations). All samples were compacted in the Superpave gyratory compactor (SGC) according to AASHTO T 312 and contained PG 70-22 binder. Three aggregate sources were used to generate the mixtures – limestone (LS), sandstone/gravel (SG), and syenite (SY). The combinations of air voids, compaction level, and aggregate type resulted in a total of 18 mixtures. Replicate samples were fabricated for each design. A complete summary of each mix design and its associated properties is shown in Tables 2 - 4.

	Limestone					
Design Air	4.5	4.5	4.5	6.0	6.0	6.0
Design VMA	16.0	16.0	16.0	18.0	18.0	18.0
Ndes	50	75	100	50	75	100
Job Mix Formula (%)						
LS12				7	7	7
LSsc				43	43	43
LSgs				50	50	50
LSbc	5	5	5			
LScl	55	54	54			
LSms	30	41	41			
NS	10					
Blend Gradation						
% Passing						
½"	100.0	100.0	100.0	100.0	100.0	100.0
3/8"	100.0	100.0	100.0	99.0	99.0	99.0
No. 4	92.5	92.9	92.9	92.6	92.6	92.6
No. 8	71.5	72.1	72.1	72.7	72.7	72.7
No. 16	45.2	42.4	42.4	49.2	49.2	49.2
No. 30	26.5	23.0	23.0	32.4	32.4	32.4
No. 50	16.0	15.3	15.3	19.8	19.8	19.8
No. 100	10.8	11.3	11.3	12.2	12.2	12.2
No. 200	8.2	8.6	8.6	8.6	8.6	8.6
Binder Content (%)	7.2	7.5	7.1	8.7	8.5	8.4
Actual Air (%)	4.3	4.4	4.5	6.0	6.0	6.1
VMA (%)	16.9	17.3	16.3	20.0	19.5	19.5
VFA (%)	74.8	74.6	72.4	69.9	69.4	68.7
Gsb	2.551	2.551	2.551	2.500	2.500	2.500
Gse	2.665	2.658	2.658	2.647	2.647	2.647
DP	1.43	1.30	1.39	1.38	1.36	1.37
Pbe (%)	5.7	6.6	6.3	6.2	6.2	6.3
%D @ Nini	83.9	84.2	83.8	84.9	84.3	84.3
Film Thickness (microns)	7.4	8.0	7.3	8.1	7.8	7.7

Table 2. Mix Design Summary for Limestone Aggregate Source

	Sandstone / Gravel					
Design Air	4.5	4.5	4.5	6.0	6.0	6.0
Design VMA	16.0	16.0	16.0	18.0	18.0	18.0
Ndes	50	75	100	50	75	100
Job Mix Formula (%)						
SSsc	50		50	40	30	40
SSws		50				
SSgc	50	50	50	60	70	60
NS						
Blend Gradation						
% Passing						
½"	100.0	100.0	100.0	100.0	100.0	100.0
3/8"	100.0	100.0	100.0	100.0	100.0	100.0
No. 4	94.5	96.3	94.5	95.6	96.7	95.6
No. 8	58.9	58.5	58.9	58.7	58.6	58.7
No. 16	41.2	37.9	41.2	40.1	39.1	40.1
No. 30	32.5	28.0	32.5	30.9	29.4	30.9
No. 50	27.0	22.1	27.0	25.2	23.4	25.2
No. 100	17.7	13.4	17.7	16.2	14.7	16.2
No. 200	9.4	6.3	9.4	8.2	7.1	8.2
Binder Content (%)	8.4	8.0	7.8	8.3	8.0	7.5
Actual Air (%)	4.4	4.6	4.7	5.9	6.0	6.0
VMA (%)	17.1	16.2	16.8	19.6	18.4	18.1
VFA (%)	74.5	71.3	71.8	70.1	67.2	67.0
Gsb	2.479	2.451	2.479	2.472	2.448	2.472
Gse	2.624	2.624	2.624	2.592	2.587	2.592
DP	1.48	1.18	1.65	1.25	1.20	1.44
Pbe (%)	6.4	5.3	5.7	6.6	5.9	5.7
%D @ Nini	78.7	77.9	76.8	77.4	76.5	76.3
Film Thickness (microns)	6.8	7.4	6.1	7.6	7.5	6.6

Table 3. Mix Design Summary for Sandstone/Gravel Aggregate Source

	Syenite					
Design Air	4.5	4.5	4.5	6.0	6.0	6.0
Design VMA	16.0	16.0	16.0	18.0	18.0	18.0
Ndes	50	75	100	50	75	100
Job Mix Formula (%)						
SY12	20	18	18	20	16	18
SYsc	38	33	33	38	42	33
SYms	20	23	23	20	20	23
NS	22	26	26	22	22	26
Blend Gradation						
% Passing						
½"	100.0	100.0	100.0	100.0	100.0	100.0
3/8"	98.9	99.0	99.0	98.9	99.1	99.0
No. 4	89.3	90.3	90.3	89.3	90.2	90.3
No. 8	71.6	60.0	60.0	71.6	72.3	60.0
No. 16	56.7	74.2	74.2	56.7	57.2	74.2
No. 30	41.9	44.9	44.9	41.9	42.2	44.9
No. 50	23.4	25.0	25.0	23.4	23.5	25.0
No. 100	12.4	13.3	13.3	12.4	12.4	13.3
No. 200	7.3	7.9	7.9	7.3	7.3	7.9
Binder Content (%)	8.2	7.6	7.3	7.8	6.8	6.7
Actual Air (%)	4.4	4.6	4.5	5.8	6.1	6.1
VMA (%)	17.8	19.2	18.6	18.9	19.2	18.8
VFA (%)	75.5	76.1	76.0	69.4	68.0	67.3
Gsb	2.574	2.571	2.571	2.574	2.573	2.571
Gse	2.632	2.627	2.627	2.632	2.629	2.627
DP	1.07	1.16	1.22	1.13	1.15	1.32
Pbe (%)	6.8	6.8	6.5	6.5	6.4	6.0
%D @ Nini	80.8	80.2	79.6	79.5	79.9	78.2
Film Thickness (microns)	8.8	7.6	7.2	8.3	7.0	6.5

Table 4. Mix Design Summary for Syenite Aggregate Source

Aggregate Properties

In addition to mixture properties, aggregate properties were also investigated because they are known to affect the long-term skid resistance of a pavement. In the Superpave mixtures design method, the source and consensus properties of the aggregate are considered. *(35)* The source properties include toughness, soundness, and deleterious materials. The consensus properties are coarse aggregate angularity, fine aggregate angularity, flat and elongated particles, and clay content. These properties were included in the Superpave design method because they are believed to be critical to the performance of HMA mixtures. These properties are already a part of HMA mix design, and thus correlating these characteristics to skid resistance would be significant step toward the inclusion of skid resistance considerations during the mix design process. Because the focus of the project was on 4.75mm mixes, only the fine aggregate properties were considered. The Micro-Deval and sodium sulfate soundness tests were performed to characterize toughness, durability, and soundness. Fine aggregate angularity tests and aggregate imaging techniques were used to characterize aggregate shape and texture.

Micro-Deval

The ability of the aggregate to resist wearing relates to skid resistance. The Micro-Deval method was used to assess aggregate toughness and durability. This method is most often a coarse aggregate test, so an adjusted procedure for fine aggregate was used. In this method, a specific grading of aggregate is placed in a cylindrical canister with water and rotated on its side, such that the aggregate particles tumble over each other in the presence of water. This is similar to the L.A. Abrasion test, which is used by many states for coarse aggregate toughness, but the interactions of the aggregate particles during the test are not subjected to impact interactions, and testing is performed in the presence of water. Upon completion of the Micro-Deval test, the percent loss is calculated based on the change in material gradation after testing. The Micro-Deval apparatus is shown in Figure 3.

Figure 3. Micro-Deval Apparatus

Sodium Sulfate Soundness

The ability of an aggregate to resist the degrading forces of the environment also relates to skid resistance. The sodium sulfate soundness test, as outlined in AASHTO T 104, was used to assess the durability and soundness of the aggregates by simulating the resistance of aggregate to degradation from environmental factors. In this test, a specific grading of aggregate is subjected to cycles of soaking in a sodium sulfate solution, then dried. During the soaking period the salt solution swells and simulates the expansive forces developed in the aggregate when water freezes in the pores. During the drying period, the salt is precipitated from the solution, which simulates the removal of these forces during thawing. The repeated cycles represent the performance of the aggregate during repeated seasons of freezing and thawing. After five cycles of soaking, the gradation of the aggregate sample is determined and the amount of aggregate breakdown is report as the percent loss. The equipment used in the sodium sulfate soundness test is shown in Figure 4.

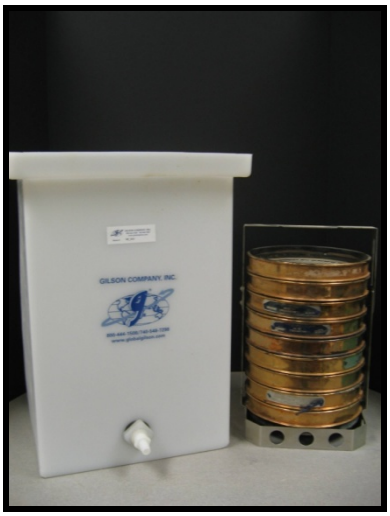

Figure 4. Sodium Sulfate Soundness Testing Equipment

Fine Aggregate Angularity

Fine aggregate angularity is affected by the shape and texture of the aggregate surfaces, which also contributes to skid resistance. The fine aggregate angularity test, detailed in AASHTO T 304, is a method for quantifying this shape and texture. In this method, a specifically graded sample of fine aggregate is prepared, and allowed to freefall through a funnel into a calibrated cylindrical cup. Based on the volume of the cup, the weight of the material in the cup, and the bulk specific gravity of the fine aggregate, the percent of uncompacted voids is calculated. The more angular and textured the material, the less the material will consolidate in the cup, thereby increasing the volume of void spaces in the sample. Thus, higher values of uncompacted voids indicate greater angularity. The fine aggregate angularity device is shown in Figure 5.

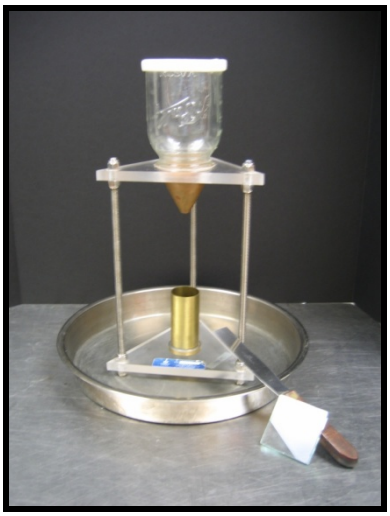

Figure 5. Fine Aggregate Angularity Apparatus

Aggregate Imaging System

The Aggregate Imaging System (AIMS), shown in Figure 6, is a digital imaging process combined with a statistical analysis method used to determine the form and angularity of aggregates. *(41)* This system is based on the components of aggregate shape, which include the properties of form, angularity, and texture. Form describes the large scale shape of the particle, using proportional dimensions to provide a value relating to features such as flat and/or elongated particles. Angularity describes shape in a smaller scale and in greater detail, and focuses on the variations of the aggregate at the corners of the particle. The shape features described by angularity are such that there is little to no interaction with aggregate form. Surface texture is the third level of description for aggregate shape, which describes surface irregularities that are too small to affect form or angularity. Texture measurements are only applicable to coarse aggregates.

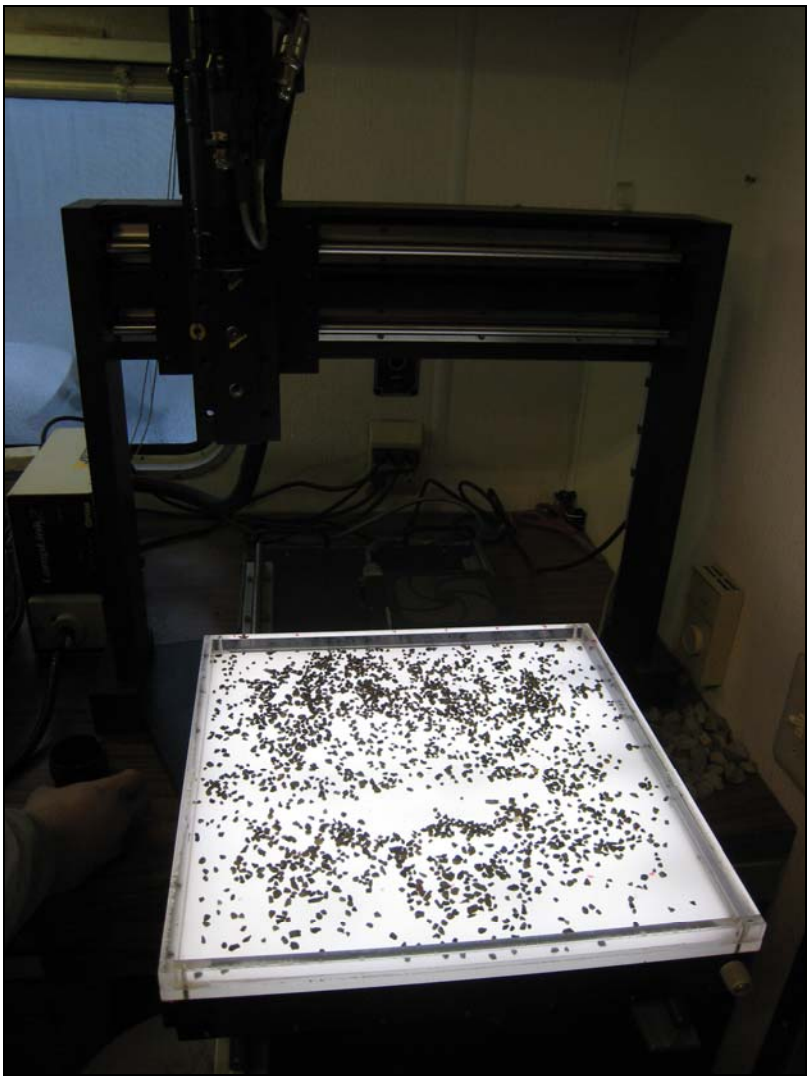

Figure 6. Aggregate Imaging System (AIMS)

The AIMS uses a camera and special lighting to capture aggregate images, and then employs image analysis techniques to measure aggregate shape properties. Fine aggregates are analyzed for form and angularity by using black and white images generated from the camera and a backlit tray. Approximately 200 grams of fine aggregate are arranged randomly on the tray, and the camera moves incrementally in the x and y directions to capture images at specified intervals for the entire tray area.

Angularity of fine aggregate is determined by two methods. The gradient method utilizes vector analysis to determine the rate of change of vectors to adjacent points on the particle edge. The direction of the gradient vector changes quickly for angular particles, but changes slowly for rounded particles. The angularity index by the gradient method is separated into categories describing particle shape as given in Table 5.

Angularity Classification	Gradient Angularity Index
Rounded	<2100
Sub-Rounded	<3975
Sub-Angular	<5400
Angular	<10,000

Table 5. Particle Angularity Classifications for AIMS Gradient Angularity

The radius method for angularity compares the radii of the particle's shape in various directions to that of an equivalent ellipse. Greater differences between particle shape and the ellipse indicate greater angularity. Ranges of radius angularity index values corresponding with various aggregate shapes are presented in Table 6.

Angularity Classification	Radius Angularity Index
Rounded	<8
Sub-Rounded	<10.65
Sub-Angular	<15.25
Angular	<20

Table 6. Particle Angularity Classifications for AIMS Radius Angularity

Aggregate form is computed using one of two methods – a three-dimensional measure of sphericity, or a two-dimensional index. Fine aggregate form is determined using the two-dimensional method, which is determined by incremental changes in particle radius. The form index of a perfect circle would be zero, and the index values increase as aggregate shape becomes less circular. Particle shape classifications are given in Table 7.

Particle Shape	Two-Dimensional Form Index
Circular	<6.5
Semi-Circular	<8
Semi-Elongated	<10.75
Elongated	<20

Table 7. Particle Shape Classifications for AIMS Two-Dimensional Form

Microtexture

The British Pendulum Tester, shown in Figure 7, is often used to describe the skid resistance of a surface. The device was originally developed to describe the frictional properties of roadway surfaces, but has since been used for many other surfaces, including flooring and pedestrian walkways. *(42)* In this method, described in AASHTO T 278 and ASTM E 303, an asphalt sample is placed under a pendulum arm and rubber slider foot, then aligned such that the length of contact between the rubber foot and sample is between 124 and 127 mm. The geometry of the testing configuration is such

that a gyratory-compacted specimen with a 150 mm diameter is suitable for the test. After the specimen is carefully aligned, the pendulum arm is released from a fixed position and the rubber foot skids across the sample. In order to simulate a wet pavement (i.e., worst case condition), the surface of the test sample is sprayed with water just prior to releasing the arm. The measurement obtained from the scale represents the skid resistance of the material tested such that higher values indicate greater skid resistance. The measured value, or British Pendulum Number (BPN) is approximately 100 times the coefficient of friction. *(42)* For a single test result, a total of 5 swings of the pendulum are required. The result of the first swing is not recorded. The readings from the remaining 4 swings are then averaged to generate a single test result.

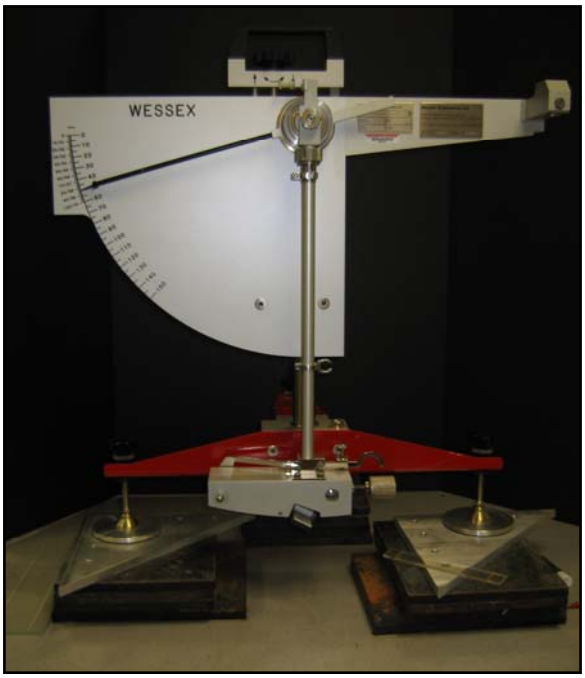

Figure 7. British Pendulum Tester

According to Wessex Engineering in the United Kingdom, roadways are categorized into three primary groups based on geometry and traffic level. *(42)* Category A is defined as roadways having a tight turning radius, steep grades and intersection approaches. Skid resistance is most critical for these situations, and a minimum BPN of 65 is recommended. Category B is comprised of roadways in urban areas that experience significant traffic levels (>2000 vehicles per day). For category B, the skid resistance needs based on the quantity of traffic are more dominant than resistance needs created by difficult roadway geometry. The required skid resistance in these situations is governed by the need to stop suddenly or other quick-response braking motions. A BPN of 55 is recommended for category B roadways. For all other roadways, skid resistance considerations do not include severe extenuating circumstances, and a minimum BPN of 45 is recommended.

The British Pendulum Test provides primarily a measure of microtexture. This test is typically assumed to exhibit a slip speed of 6 mph (10 km/hr), and microtexture is believed to govern for low-speed applications. For high-speed roadways it is recommended that a texture measurement also be performed.

Macrotexture

The sand patch test is a volumetric method often used in conjunction with the BPT for field measurement of macrotexture. In this method, a known volume of sand is spread in a circular shape on the surface of a pavement. The diameter of the circular patch is measured, and the area of the circle is calculated. Next, the volume and area of sand are used to estimate texture depth. Texture depth describes macrotexture, and represents the amount of space in the surface of the roadway that could be used to store water.

This test is usually performed using fine sand according to ASTM E 965, however, other materials have been used including glass beads, grease, and silicone putty. Regardless of the material used, macrotexture depth, or mean texture depth (MTD), is calculated based on the volume of material used and the diameter of the area of coverage, according to Equation 4.

$$MTD = \frac{4V}{\pi D^2} \qquad \textit{Equation 4}$$

where: MTD = mean texture depth
V = test material volume
D = average diameter material area

No states currently specify minimum requirements for macrotexture, however, this parameter is being used in some European countries. Texture depths over 0.80 mm are considered excellent, and in the U.K, values of 1.5 mm are desirable for new pavements. Values less than 0.70 mm are unacceptable and can lead to slippery conditions. *(7, 43)* Sand patch texture measurements require wind protection, and a minimum of three texture measurements should be tested for each test surface. *(44)*

Since the intention of the texture measurement in this study was for the purpose of design, a modified procedure was developed for estimating the texture depth of laboratory-compacted specimens. This procedure is outlined in Table 8 and illustrated in Figure 8.

Modified Sand Patch Test for Laboratory-Compacted Cylindrical Specimens	
Step 1	Determine the bulk specific gravity of a finely graded sand
Step 2	Determine the average of 4 evenly spaced diameters on the test specimen
Step 3	Calculate the surface area of the specimen
Step 4	Determine the mass of the compacted specimen
Step 5	Carefully brush the sand onto the surface of the specimen and strike off such that the surface voids become essentially filled with sand
Step 6	Carefully brush excess sand from the sides of the specimen
Step 7	Without losing sand from the surface of the specimen, determine the mass of the "sanded" specimen
Step 8	Subtract the mass of the clean specimen from that of the "sanded" specimen to determine net mass of sand used to fill the surface voids.
Step 9	Calculate the volume of sand used to fill the surface voids (weight/density)
Step 10	Estimate the texture depth of the specimen (volume/area)

Table 8. Summary of the Modified Sand Patch Test Procedure

Figure 8. Modified Sand Patch Test

Specimen Conditioning

Many methods have been used for simulating the long-term effects of aggregate wear and polish on the skid resistance of HMA mixes. Most involve a polishing device, such as the British Polishing Wheel, or a wheel tracking tracking system. *(8)* In this study, the samples were conditioned using the Evaluator of Rutting and Stripping in Asphalt (ERSA). ERSA is a wheel-tracking device that is most often used to test for the rutting and stripping resistance of asphalt mixtures while loaded with a steel wheel. *(45)* For conditioning skid test specimens, ERSA was retrofitted with high-density polyethylene (HDPE) wheels approximately 3.0 inches in width. The wheel assemblies and additional

weights placed a 62.5 lb load on each sample. The contact length of the wheel was approximately 0.3 inches, resulting in a total contact pressure of approximately 70 psi. Each sample was conditioned with a series of loading cycles, and was tested in the BPT after 0, 50, 150, 650, 1650, and 6650 cycles. The ERSA device fitted with the conditioning wheels is shown in Figure 9.

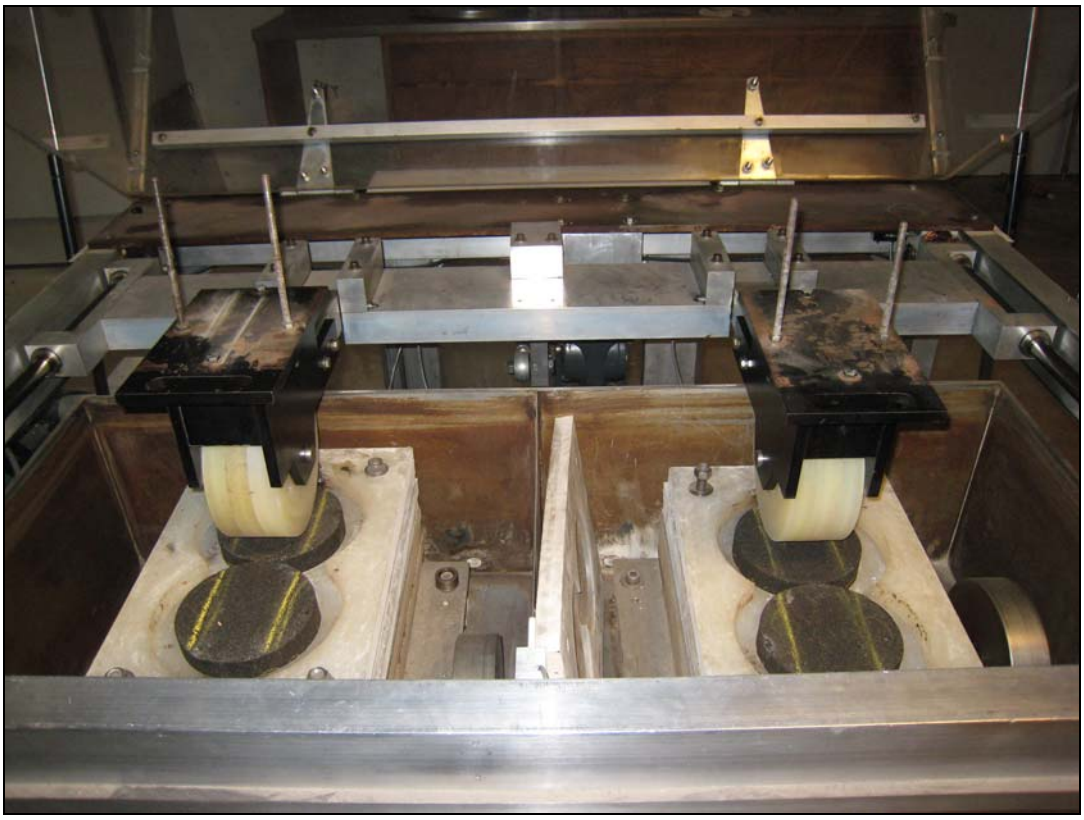

Figure 9. ERSA Device Retrofitted with Conditioning Wheels

DATA ANALYSIS AND DISCUSSION

Mix Design

The mix design parameters of air void content and compaction level were intentionally varied and evaluated with respect to their effects on skid resistance according to the experimental summary in Table 9. All statistical analyses were performed using a 95 percent level of significance (α = 0.05).

Factor	Levels of Variation
Aggregate Type	3 (LS, SG, SY)
Design Air Voids	2 (4.5%, 6.0%)
Compaction Level	3 (Ndes = 50, 75, 100)

Table 9. Summary of Factors for Mix Design Analysis

Microtexture

Four replicate microtexture tests were performed for each of two samples from each mix design using the British Pendulum. Two surfaces (top and bottom) were tested for each sample, resulting in a total of 16 measures of skid resistance for each sample type. Table 10 provides a summary of results for the BPT testing for this analysis, including average BPN, standard deviation, and coefficient of variation (COV). For 288 tests, the average BPN for all samples was 67.6, with individual values ranging from 52.2 to 76.9. When separated by aggregate source, the average BPN was 63.5 for the limestone source, 71.6 for the sandstone/gravel source, and 67.8 for the syenite source. The average standard deviation for all mix types was 3.11, and the average COV was 4.6 percent. This level of variability is similar to that found in a previous study, in which standard deviations ranged from 2.0 to 5.8. *(46)* The low coefficient of variation (<5 percent) supports the conclusion that the BPT method is reasonably consistent.

Aggregate Source	Design Air (%)	Compaction Level (Ndes gyr)	Sample #	Side	BPN Mean	BPN Std. Dev.	BPN COV (%)
SG	4.5	50	1	Bottom	71.25	2.76	3.88
SG	4.5	50	1	Top	71.75	3.09	4.31
SG	4.5	50	2	Bottom	71.13	2.22	3.12
SG	4.5	50	2	Top	68.19	2.65	3.88
SG	4.5	75	1	Bottom	76.94	1.38	1.79
SG	4.5	75	1	Top	73.88	1.27	1.71
SG	4.5	75	2	Bottom	67.19	2.16	3.22
SG	4.5	75	2	Top	66.38	1.92	2.89
SG	4.5	100	1	Bottom	72.38	1.79	2.47
SG	4.5	100	1	Top	71.44	2.91	4.07
SG	4.5	100	2	Bottom	72.56	2.73	3.76
SG	4.5	100	2	Top	74.56	3.40	4.56

SG	6.0	50	1	Bottom	74.19	1.03	1.39
SG	6.0	50	1	Top	74.44	0.90	1.21
SG	6.0	50	2	Bottom	73.81	1.91	2.58
SG	6.0	50	2	Top	72.81	2.70	3.70
SG	6.0	75	1	Bottom	71.13	1.71	2.41
SG	6.0	75	1	Top	70.56	1.13	1.59
SG	6.0	75	2	Bottom	71.94	2.83	3.94
SG	6.0	75	2	Top	72.06	2.38	3.31
SG	6.0	100	1	Bottom	71.00	3.77	5.32
SG	6.0	100	1	Top	65.56	2.10	3.20
SG	6.0	100	2	Bottom	70.88	4.04	5.71
SG	6.0	100	2	Top	72.81	4.34	5.96
SY	4.5	50	1	Bottom	70.19	4.20	5.98
SY	4.5	50	1	Top	70.31	4.49	6.39
SY	4.5	50	2	Bottom	73.69	3.01	4.08
SY	4.5	50	2	Top	70.69	3.67	5.18
SY	4.5	75	1	Bottom	72.06	2.29	3.18
SY	4.5	75	1	Top	71.06	6.88	9.68
SY	4.5	75	2	Bottom	70.69	3.20	4.53
SY	4.5	75	2	Top	73.19	5.09	6.96
SY	4.5	100	1	Bottom	72.06	1.66	2.31
SY	4.5	100	1	Top	72.13	5.80	8.04
SY	4.5	100	2	Bottom	72.31	2.70	3.74
SY	4.5	100	2	Top	69.25	5.41	7.82
SY	6.0	50	1	Bottom	57.50	2.51	4.30
SY	6.0	50	1	Top	58.50	1.22	2.11
SY	6.0	50	2	Bottom	52.25	1.52	2.88
SY	6.0	50	2	Top	54.75	1.67	3.02
SY	6.0	75	1	Bottom	66.56	2.86	4.30
SY	6.0	75	1	Top	65.19	2.41	3.70
SY	6.0	75	2	Bottom	66.13	2.98	4.50
SY	6.0	75	2	Top	66.19	3.11	4.70
SY	6.0	100	1	Bottom	72.00	3.89	5.40
SY	6.0	100	1	Top	69.25	2.64	3.81
SY	6.0	100	2	Bottom	71.19	3.00	4.21
SY	6.0	100	2	Top	69.50	4.52	6.51
LS	4.5	50	1	Bottom	65.75	1.00	1.52
LS	4.5	50	1	Top	65.75	2.07	3.11
LS	4.5	50	2	Bottom	65.00	0.89	1.37
LS	4.5	50	2	Top	59.25	0.55	0.92
LS	4.5	75	1	Bottom	63.94	5.46	8.54
LS	4.5	75	1	Top	61.81	7.11	11.51
LS	4.5	75	2	Bottom	64.75	8.82	13.63

LS	4.5	75	2	Top	60.56	4.28	7.07
LS	4.5	100	1	Bottom	62.50	3.95	6.32
LS	4.5	100	1	Top	61.06	3.70	6.07
LS	4.5	100	2	Bottom	65.69	7.67	11.68
LS	4.5	100	2	Top	65.44	3.72	5.68
LS	6.0	50	1	Bottom	64.42	0.80	1.25
LS	6.0	50	1	Top	61.25	5.00	8.17
LS	6.0	50	2	Bottom	60.63	1.13	1.86
LS	6.0	50	2	Top	62.88	3.90	6.21
LS	6.0	75	1	Bottom	67.88	4.56	6.71
LS	6.0	75	1	Top	61.31	0.75	1.22
LS	6.0	75	2	Bottom	62.56	7.62	12.18
LS	6.0	75	2	Top	60.19	1.68	2.78
LS	6.0	100	1	Bottom	62.50	2.19	3.50
LS	6.0	100	1	Top	65.56	0.47	0.72
LS	6.0	100	2	Bottom	65.38	4.25	6.49
LS	6.0	100	2	Top	67.19	4.21	6.27

Table 10. Summary of BPN Results for 4.75mm Mix Design Analysis

Since a previous study had determined that the top and bottom sides of SGC-compacted samples do not necessarily provide similar results for 12.5mm specimens, the effect of sample side was investigated. *(5)* For the 4.75mm samples tested in this study, the average BPN for all bottom sides was 68.9, which was slightly higher than that for all top sides, which had an average BPN of 67.8. Statistically, the ANOVA confirmed that the effect compaction side was not significant for the 4.75mm mixtures tested. Thus, all data points were combined for further analysis.

Next, analysis of variance (ANOVA) was used to determine whether changes in the design parameters of air voids and compaction level generated significant changes in skid resistance properties as measured by the BPT. The effect of aggregate type was separated from the factors of interest for the analysis. Statistically, the only significant factor of interest was design air void content. Compaction level did not significantly affect the microtexture of the samples nor did it interact with design air void content. It was noted that aggregate source was indeed a significant factor. Average BPT values for the LS, SG, and SY aggregate sources were 63.4, 71.6, and 69.3, respectively. The results of the ANOVA are shown in Table 11.

Factor	**df**	**F-calc**	**P-value**
Aggregate Source	2	79.15	<0.0001
Design Air Voids	1	5.80	**0.0167**
Compaction Level	2	2.31	0.1015

Air*Compaction	2	0.36	0.7014
Error	255		

Table 11. ANOVA Results – Effects of Mix Design Parameters on BPT

Samples designed at 4.5 percent air voids had a slightly greater skid resistance than those designed with 6.0 percent air voids, having average BPN values of 68.8 and 67.5, respectively. While the difference of 1.3 units may be considered statistically significant, it may not warrant practical significance. Therefore, while a lower design air void content may generate slightly greater microtexture, a large increase should not be expected. Thus, no design changes are recommended based solely on skid resistance considerations as measured by the BPT. Microtexture appears to be much more affected by aggregate source than by the design features of the mix.

Macrotexture

Macrotexture was measured using the adjusted sand patch method previously described. Triplicate measurements were made for each of 72 samples, resulting in a total of 218 measures of macrotexture. The summary results, including standard deviation and COV, for texture depths based on the modified sand patch test are given in Table 12. The results for five samples were excluded due to damaged surface condition. The average MTD was 0.149 mm, with individual values ranging from 0.065 to 0.234. When separated by aggregate source, the average MTD was 0.161 for the limestone source, 0.185 for the sandstone/gravel source, and 0.097 for the syenite source. The average standard deviation for all mix types was 0.007, and the average COV was 5.134 percent. This level of variation was less than that reported in the literature, where standard deviations for the standard sand patch test for field pavements ranged from 0.05 to 0.20. *(46)* The low coefficient of variation (approximately 5 percent) indicates that the modified sand patch test is fairly precise.

Aggregate Source	Design Air (%)	Compaction Level (NDes gyr)	Sample #	Side	MTD Mean	MTD Std. Dev.	MTD COV (%)
SG	4.5	50	1	Bottom	0.181	0.004	2.21
SG	4.5	50	1	Top	0.173	0.006	3.22
SG	4.5	50	2	Bottom	0.174	0.006	3.20
SG	4.5	50	2	Top	0.145	0.006	4.05
SG	4.5	75	1	Bottom	0.179	0.003	1.61
SG	4.5	75	1	Top	0.186	0.002	1.24
SG	4.5	75	2	Bottom	0.198	0.005	2.27
SG	4.5	75	2	Top	0.195	0.001	0.59
SG	4.5	100	1	Bottom	0.208	0.008	3.91
SG	4.5	100	1	Top	0.214	0.007	3.05
SG	4.5	100	2	Bottom	0.151	0.007	4.40
SG	4.5	100	2	Top	0.175	0.009	5.32

SG	6.0	50	1	Bottom	0.208	0.006	2.68
SG	6.0	50	1	Top	0.166	0.010	5.74
SG	6.0	50	2	Bottom	excl.	excl.	excl.
SG	6.0	50	2	Top	excl.	excl.	excl.
SG	6.0	75	1	Bottom	0.192	0.008	3.98
SG	6.0	75	1	Top	0.171	0.006	3.26
SG	6.0	75	2	Bottom	0.193	0.004	2.16
SG	6.0	75	2	Top	0.151	0.007	4.52
SG	6.0	100	1	Bottom	0.234	0.007	2.78
SG	6.0	100	1	Top	0.201	0.004	2.07
SG	6.0	100	2	Bottom	0.162	0.004	2.47
SG	6.0	100	2	Top	0.213	0.007	3.20
SY	4.5	50	1	Bottom	0.128	0.009	6.72
SY	4.5	50	1	Top	0.116	0.005	3.99
SY	4.5	50	2	Bottom	0.138	0.010	7.10
SY	4.5	50	2	Top	0.096	0.006	5.72
SY	4.5	75	1	Bottom	0.087	0.008	8.89
SY	4.5	75	1	Top	0.070	0.010	13.66
SY	4.5	75	2	Bottom	0.087	0.008	8.81
SY	4.5	75	2	Top	0.106	0.012	11.05
SY	4.5	100	1	Bottom	0.094	0.008	8.63
SY	4.5	100	1	Top	0.080	0.008	9.43
SY	4.5	100	2	Bottom	0.089	0.007	7.68
SY	4.5	100	2	Top	0.075	0.009	11.85
SY	6.0	50	1	Bottom	excl.	excl.	excl.
SY	6.0	50	1	Top	excl.	excl.	excl.
SY	6.0	50	2	Bottom	excl.	excl.	excl.
SY	6.0	50	2	Top	excl.	excl.	excl.
SY	6.0	75	1	Bottom	0.098	0.008	7.95
SY	6.0	75	1	Top	0.089	0.009	9.52
SY	6.0	75	2	Bottom	0.192	0.004	2.17
SY	6.0	75	2	Top	0.083	0.006	7.09
SY	6.0	100	1	Bottom	0.079	0.008	9.71
SY	6.0	100	1	Top	0.065	0.005	7.70
SY	6.0	100	2	Bottom	0.084	0.006	7.25
SY	6.0	100	2	Top	0.079	0.005	5.96
LS	4.5	50	1	Bottom	excl.	excl.	excl.
LS	4.5	50	1	Top	excl.	excl.	excl.
LS	4.5	50	2	Bottom	excl.	excl.	excl.
LS	4.5	50	2	Top	excl.	excl.	excl.
LS	4.5	75	1	Bottom	0.175	0.003	1.75
LS	4.5	75	1	Top	0.173	0.014	8.11
LS	4.5	75	2	Bottom	0.181	0.007	3.87

LS	4.5	75	2	Top	0.180	0.010	5.39
LS	4.5	100	1	Bottom	0.186	0.004	2.23
LS	4.5	100	1	Top	0.183	0.005	2.47
LS	4.5	100	2	Bottom	0.210	0.009	4.06
LS	4.5	100	2	Top	0.171	0.008	4.72
LS	6.0	50	1	Bottom	0.140	0.009	6.06
LS	6.0	50	1	Top	0.155	0.003	1.87
LS	6.0	50	2	Bottom	0.144	0.007	4.63
LS	6.0	50	2	Top	0.139	0.015	10.89
LS	6.0	75	1	Bottom	0.137	0.005	3.79
LS	6.0	75	1	Top	0.149	0.006	4.03
LS	6.0	75	2	Bottom	0.130	0.006	4.52
LS	6.0	75	2	Top	0.159	0.007	4.20
LS	6.0	100	1	Bottom	0.158	0.004	2.63
LS	6.0	100	1	Top	0.174	0.011	6.22
LS	6.0	100	2	Bottom	0.149	0.007	4.38
LS	6.0	100	2	Top	0.137	0.005	3.66

Table 12. Summary of Texture Depth Results for 4.75mm Mix Design Analysis

By initial observation, the values for texture depth were somewhat lower than the values reported in the literature. Two reasons for this may exist. First, the mixes tested in this study are not consistent with those tested in the other projects; and second, the modified laboratory method developed for use in this research may have created some bias in the data.

As with the mix design analysis using the BPT test, compaction side was analyzed for the modified sand patch data. Previous research had indicated that the top side of SGC-compacted specimens more closely matched field values for 12.5mm mixes. For the 4.75mm samples tested in this study, the average MTD for all top sides was 0.144 mm and the average MTD for all bottom sides was 0.154 mm. Although the bottom side had a slightly greater MTD than the top, the ANOVA indicated that this difference was not statistically significant. Therefore, the entire dataset was combined for further analysis.

Analysis of variance was next used to evaluate the effects of design air void content and compaction level on the texture depth of 4.75mm samples. As with the BPT analysis, design air void content was the only statistically significant factor. Compaction level was not a significant factor, and there was no significant interaction between design air void content and compaction level. The effect of aggregate type, however, was significant. Average values of MTD were 0.162 mm, 0.184 mm, and 0.095 mm for the limestone, sandstone/gravel, and syenite aggregate sources, respectively. The results of the ANOVA are given in Table 13.

Factor	df	F-calc	P-value
Aggregate Source	2	212.20	<0.0001
Design Air Voids	1	6.77	**0.0100**
Compaction Level	2	0.59	0.5538
Air*Compaction	2	0.44	0.6438
Error	178		

Table 13. ANOVA Results – Effects of Mix Design Parameters on MTD

Samples designed with 4.5 percent air voids had a slightly greater texture depth than those designed with 6.0 percent air voids. Average MTD values were 0.152 mm for the mixes designed at 4.5 percent air voids, and 0.142 mm for mixes designed at 6.0 percent air voids. While statistically significant, it is certainly arguable that the 0.01 mm difference may not be practically significant. Aggregate type appears to have the most significant influence.

Previous research regarding design of 4.75mm mixtures has indicated that rutting resistance is significantly affected by changes in design air void content. *(1)* Specifically, mixes designed at 50 and 75 design gyrations exhibit greater rutting resistance when designed at an air void content of 6.0 percent. Mixes designed at 100 design gyrations were more resistant to rutting when designed at 4.5 percent air voids. While designing 4.75mm at a lower air void content may increase microtexture and macrotexture by a small amount, this difference is not felt to warrant any procedural design changes.

Other Mix Properties

Although the parameters which were varied intentionally in the previous analysis were not determined to have a significant effect on microtexture or macrotexture, other parameters were measured as a part of the mixture design and characterization process. These were:

- Binder content (Pb)
- Effective binder content (Pbe)
- Voids in the mineral aggregate (VMA)
- Voids filled with aggregate (VFA)
- Dust Proportion (DP)
- Percent compaction at $N_{initial}$ (%D@N_{ini})
- Film Thickness

Microtexture

The relationships of microtexture to these mixture properties are shown graphically in Figures 10 through 16. Summary information for individual regression analyses is presented in Table 14.

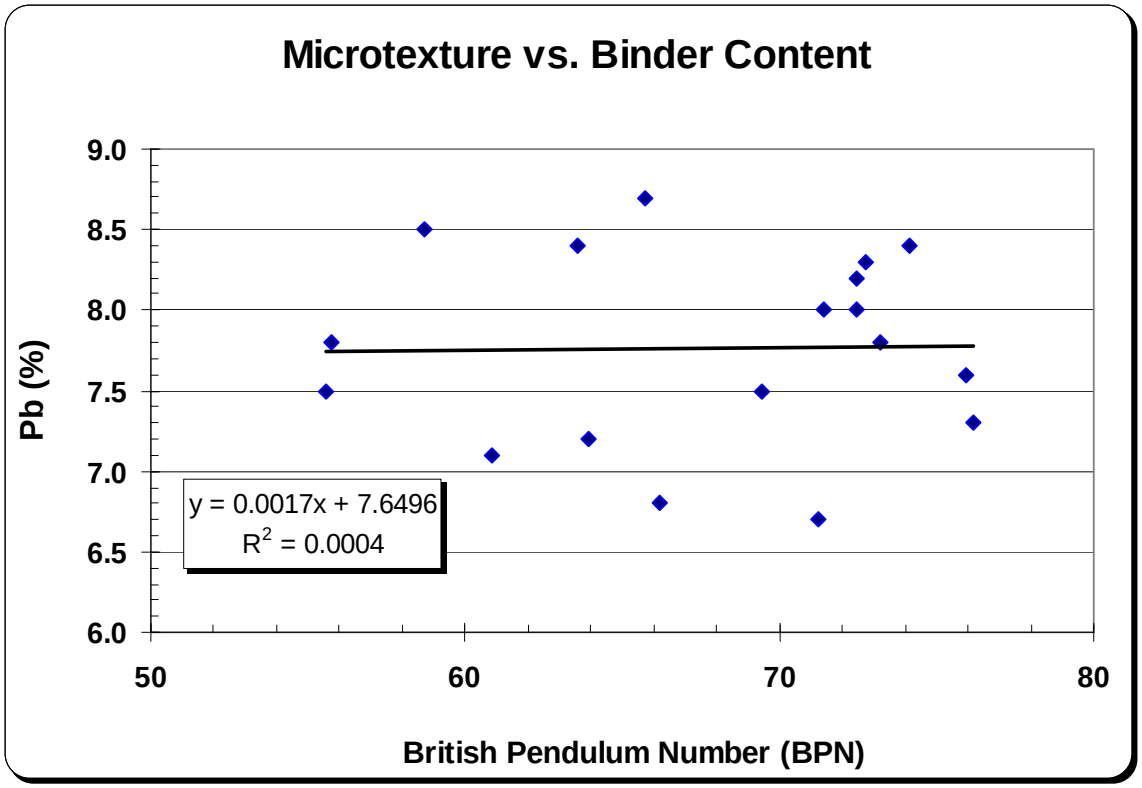

Figure 10. Relationship of Binder Content to Microtexture

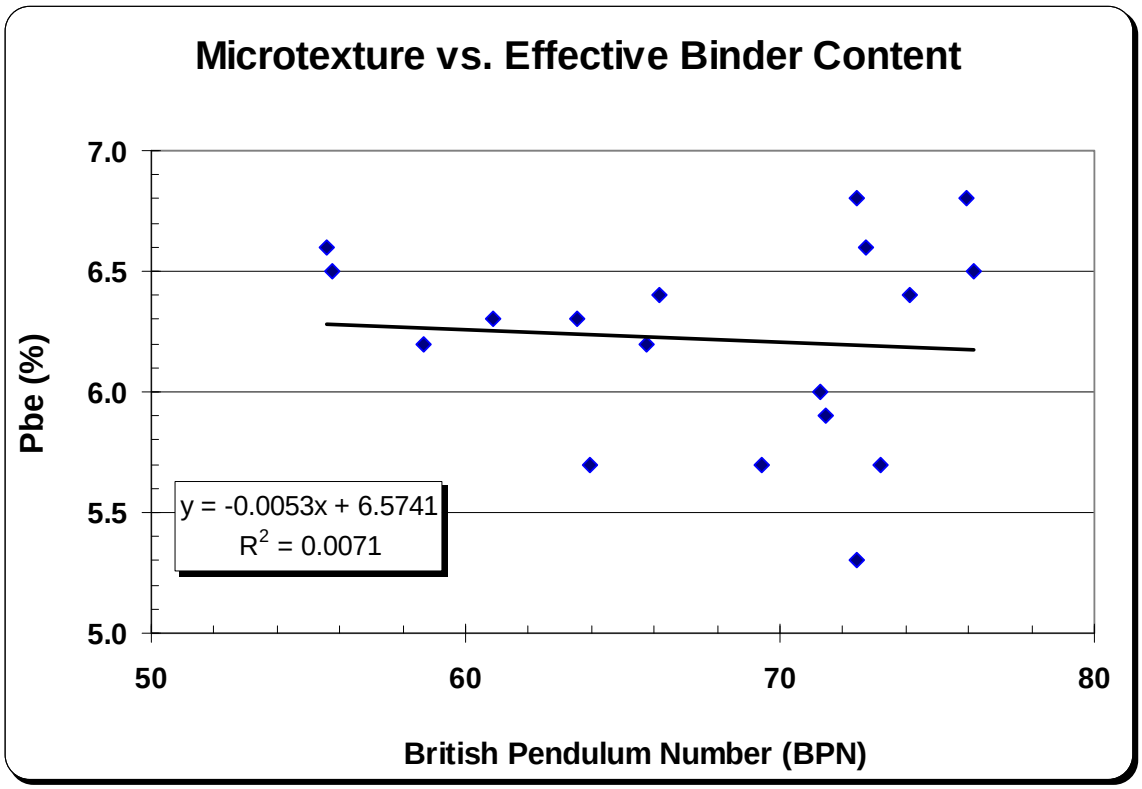

Figure 11. Relationship of Effective Binder Content to Microtexture

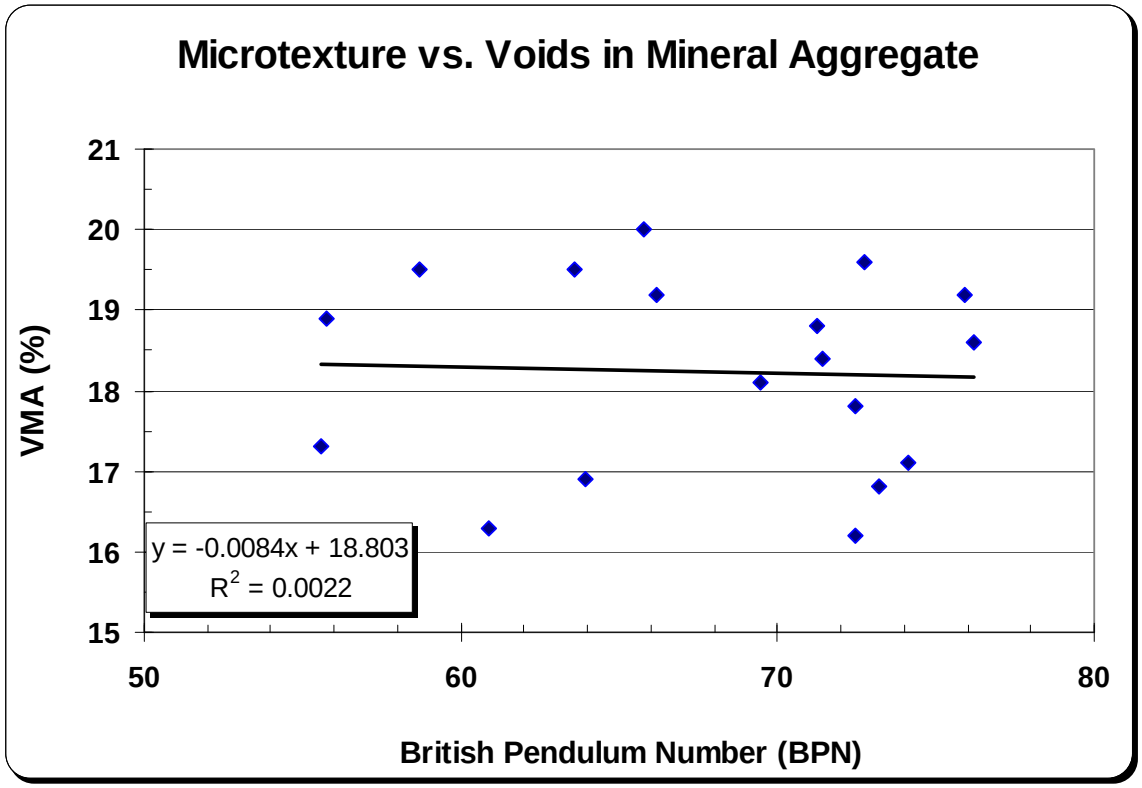

Figure 12. Relationship of Voids in Mineral Aggregate (VMA) to Microtexture

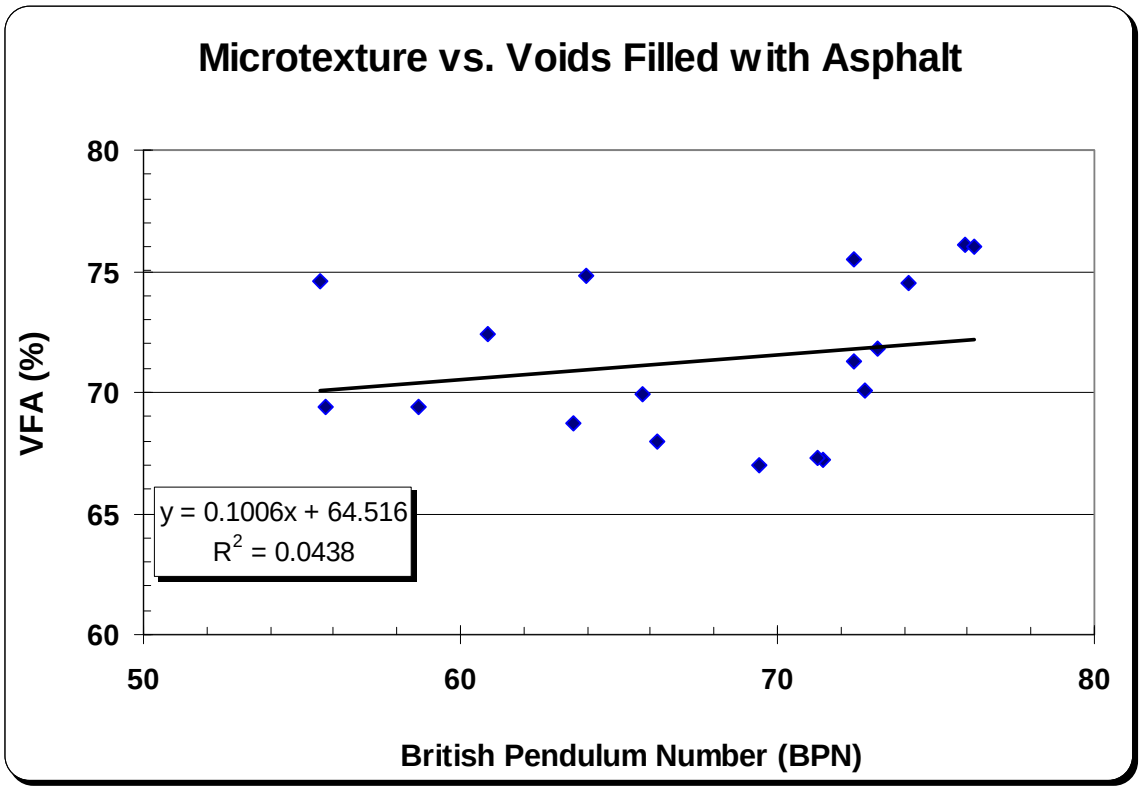

Figure 13. Relationship of Voids Filled with Asphalt (VFA) to Microtexture

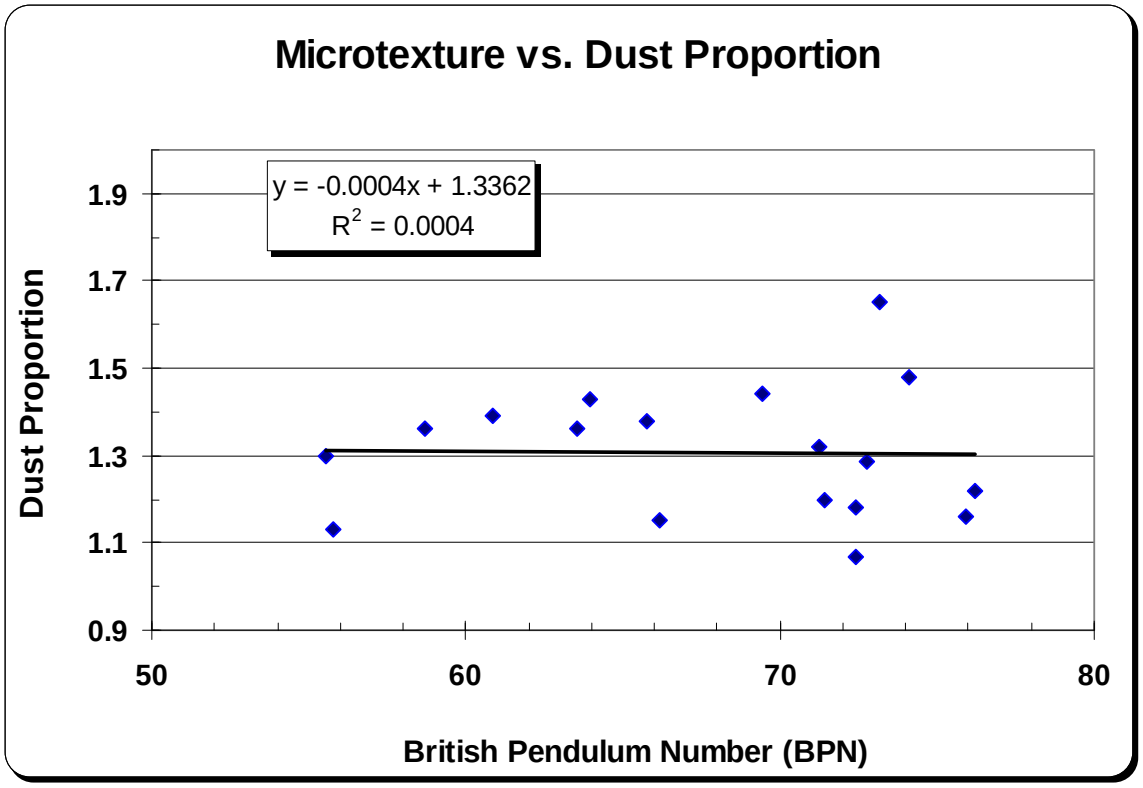

Figure 14. Relationship of Dust Proportion to Microtexture

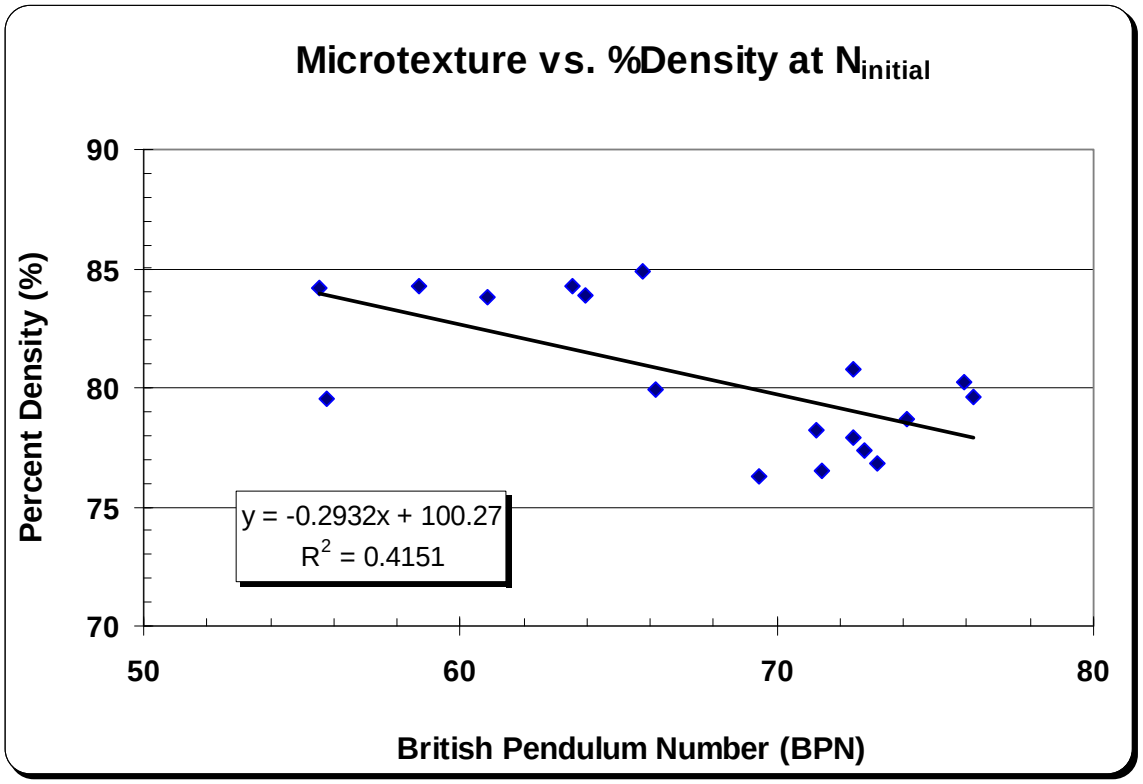

Figure 15. Relationship of Percent Density at $N_{initial}$ to Microtexture

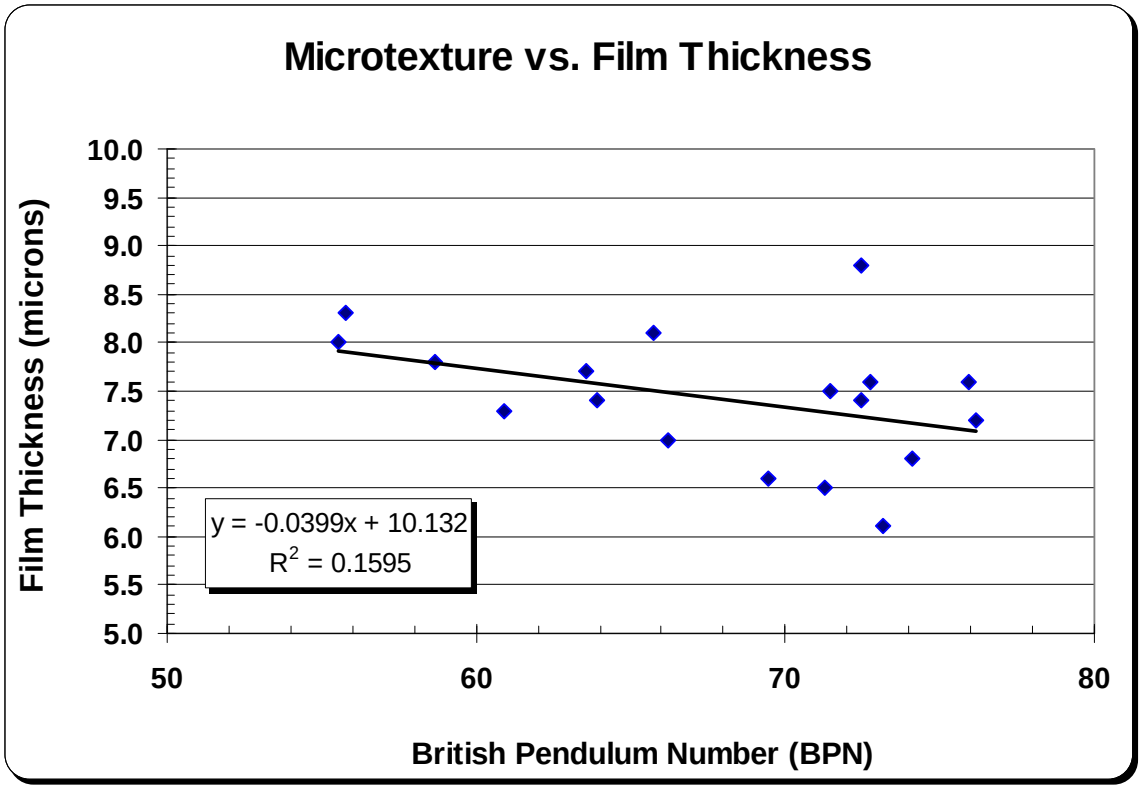

Figure 16. Relationship of Film Thickness to Microtexture

Property	Slope	Intercept	R^2
Binder Content (Pb)	0.0017	7.6496	0.0004
Effective Binder Content (Pbe)	-0.0053	6.5741	0.0071
Voids in Mineral Aggregate (VMA)	-0.0084	18.803	0.0022
Voids Filled with Asphalt (VFA)	0.1006	64.516	0.0438
Dust Proportion (DP)	-0.0004	1.3362	0.0004
Percent Density at $N_{initial}$ (%D@N_{ini})	-0.2932	100.27	0.4151
Film Thickness (FT)	-0.0399	10.132	0.1595

Table 14. Summary of Regression Variables for Relationships of Mixture Properties to Microtexture (BPN)

Based on the evaluation of the effects of individual mixture parameters on BPN, it was evident that the mixture characteristics did not significantly affect microtexture. The slope values for the regression relationships were very low, meaning that microtexture was not sensitive to variations in the mixture parameters. In fact, the relationships to Pb, Pbe, VMA, and DP, exhibited a very flat slope, indicating virtually no relationship. This conclusion is further indicated by the small coefficient of determination values (R^2 values). There was a slight positive correlation between VFA and BPN such that

increased VFA generated increased BPN. However, this relationship was not statistically significant. Film thickness was negatively correlated to BPN, so reductions in film thickness increased the microtexture of the mix. This is reasonable because thinner films of binder should wear away more quickly, exposing the microtexture of the aggregate particles. The percent compaction at $N_{initial}$ was the most influential single variable, in that higher densities generate lower BPN values. The relationship had a slope of -0.2932 and an R^2 of 0.4151, meaning that the values for $\%D@N_{ini}$ could mathematically explain just over 41 percent of the variability in the BPN values.

Macrotexture

Single regression was also used to analyze the macrotexture data for each mix parameter. These relationships are illustrated in Figures 17 through 23, and the regression coefficients are summarized in Table 15.

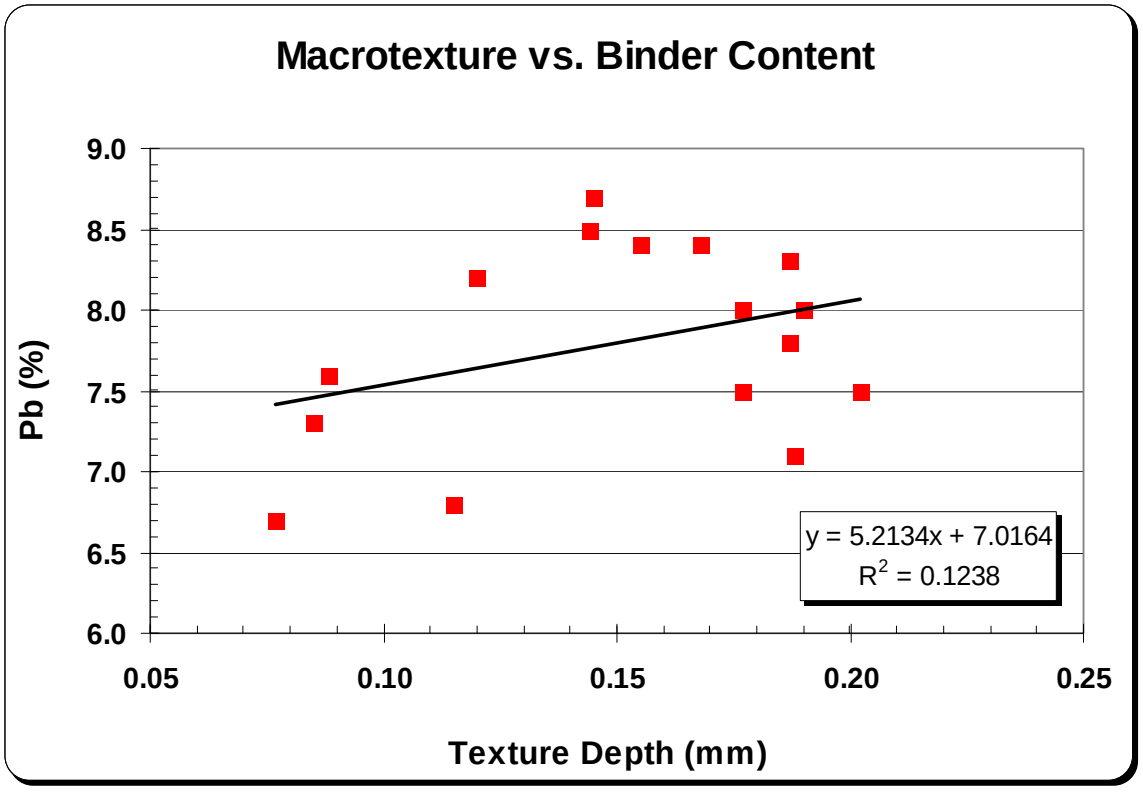

Figure 17. Relationship of Binder Content to Macrotexture

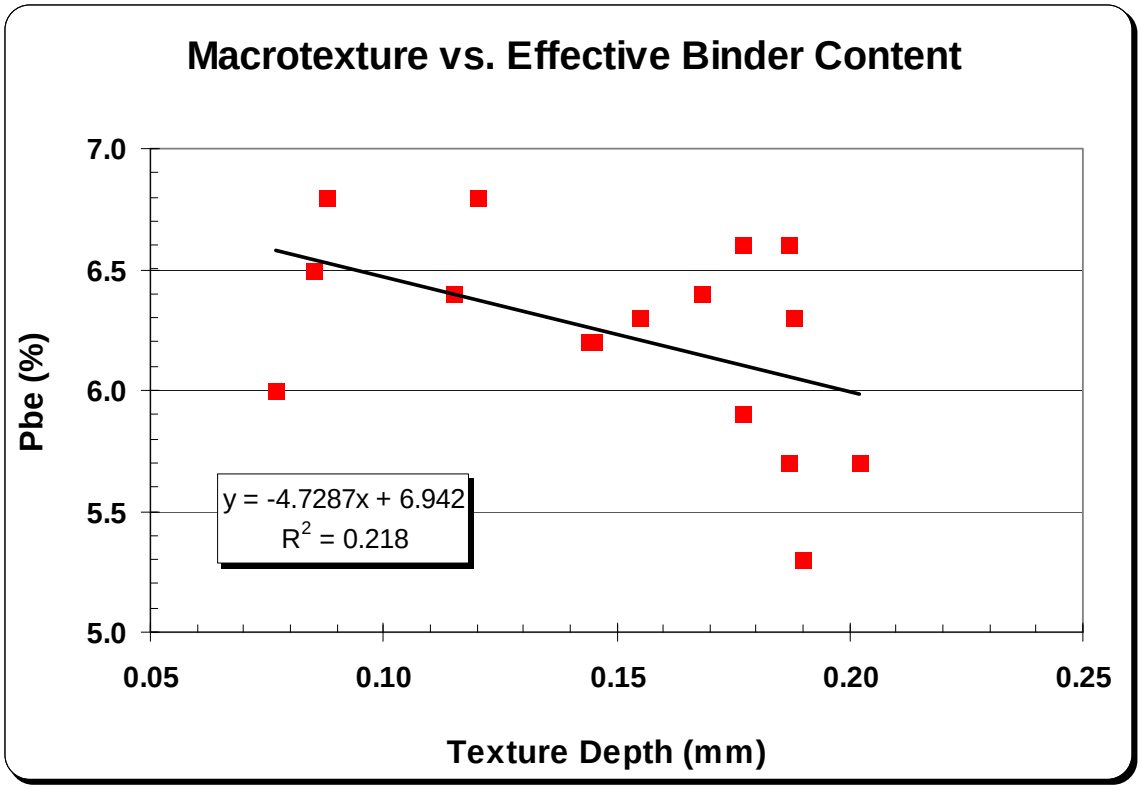

Figure 18. Relationship of Effective Binder Content to Macrotexture

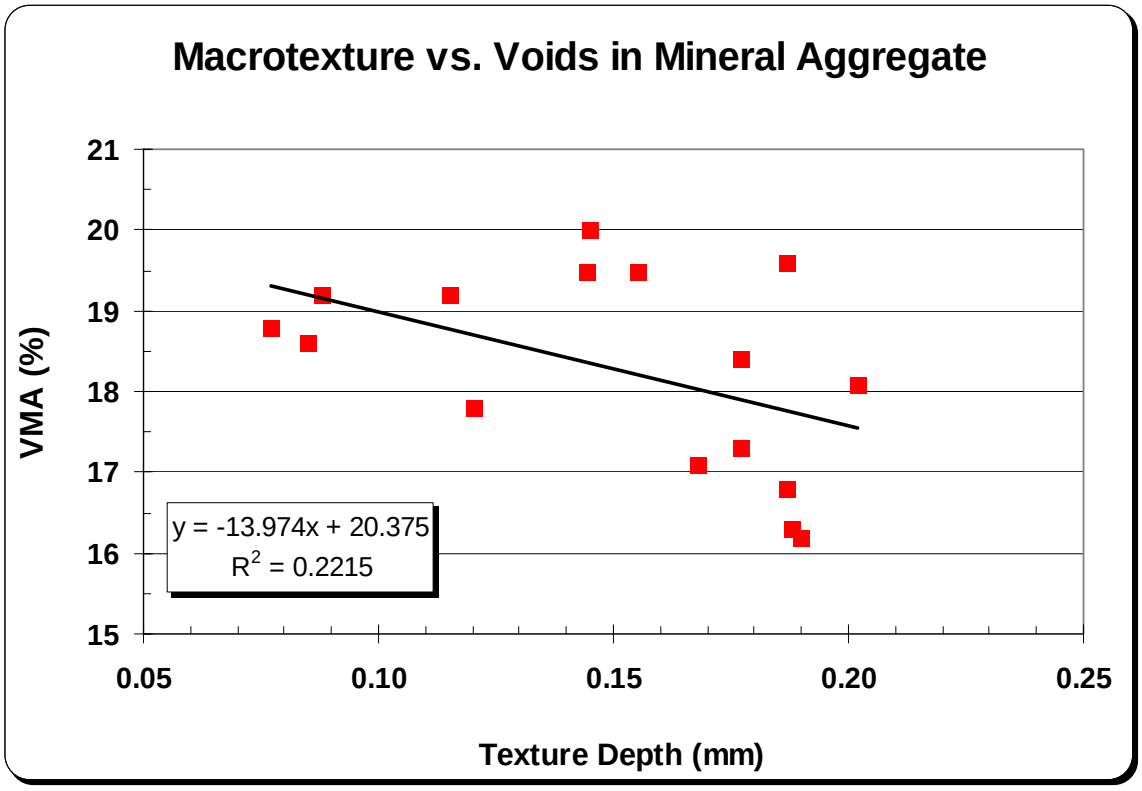

Figure 19. Relationship of Voids in Mineral Aggregate (VMA) to Macrotexture

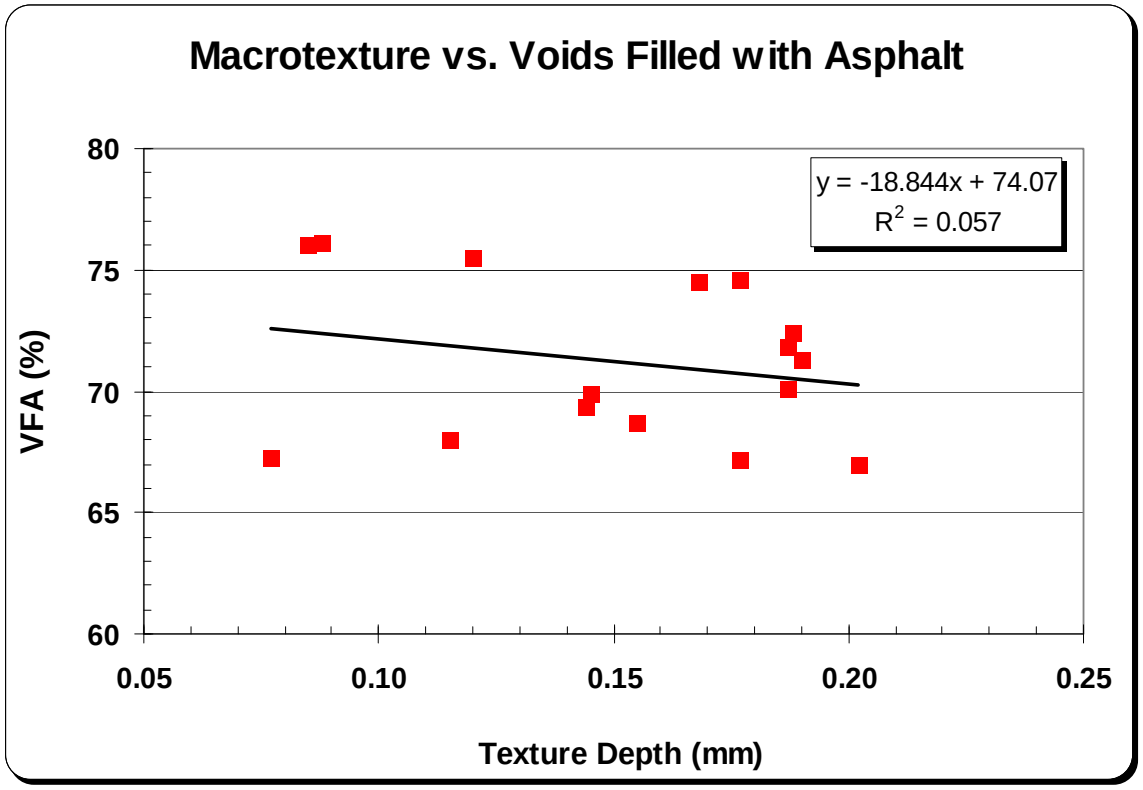

Figure 20. Relationship of Voids Filled with Asphalt (VFA) to Macrotexture

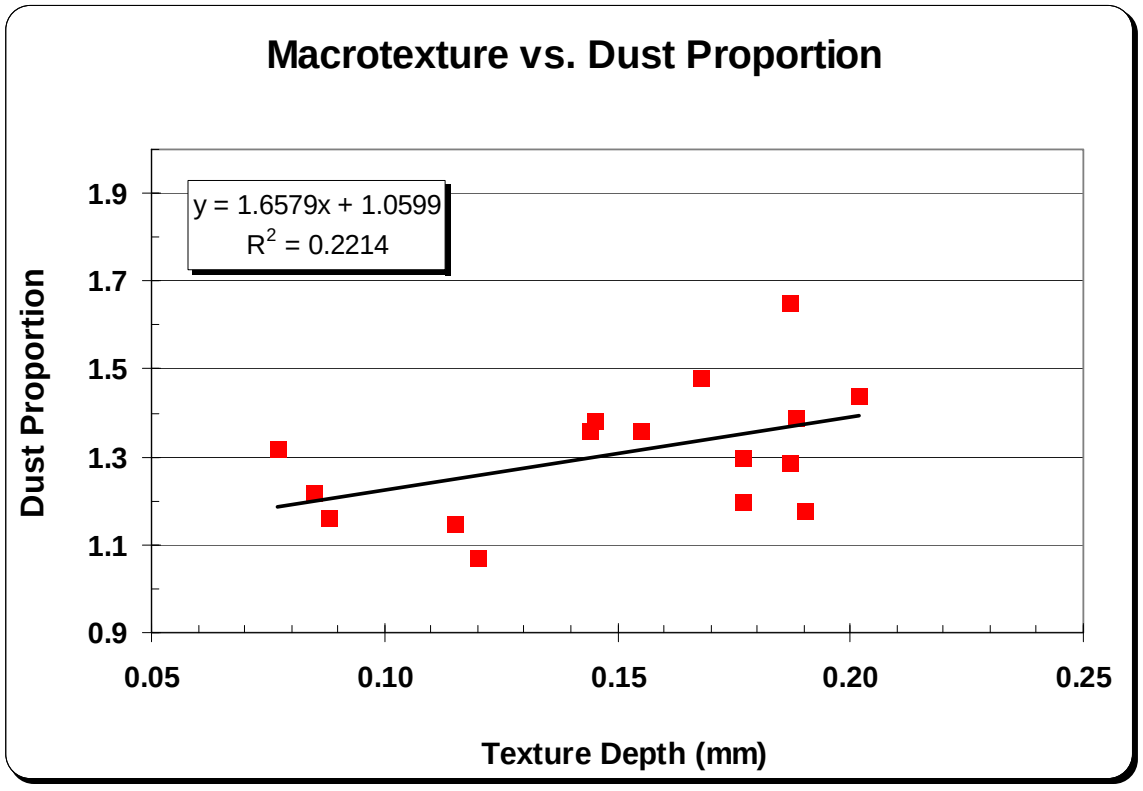

Figure 21. Relationship of Dust Proportion to Macrotexture

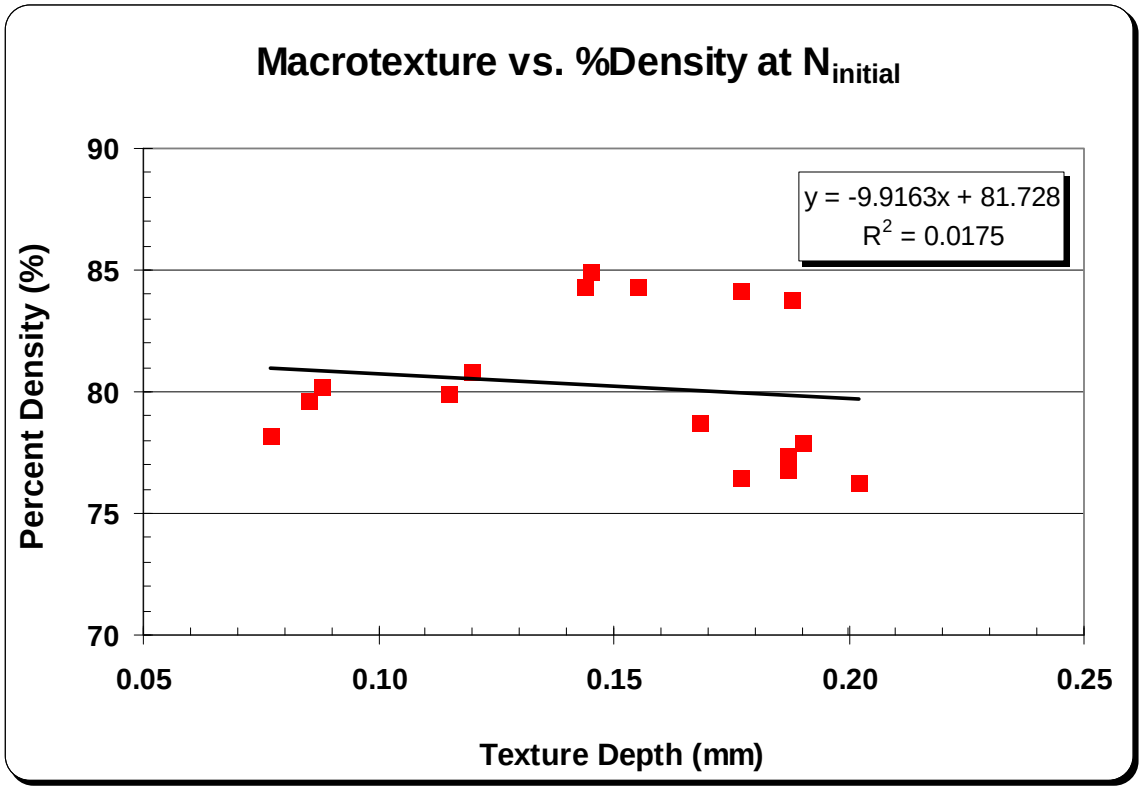

Figure 22. Relationship of Percent Density at $N_{initial}$ to Macrotexture

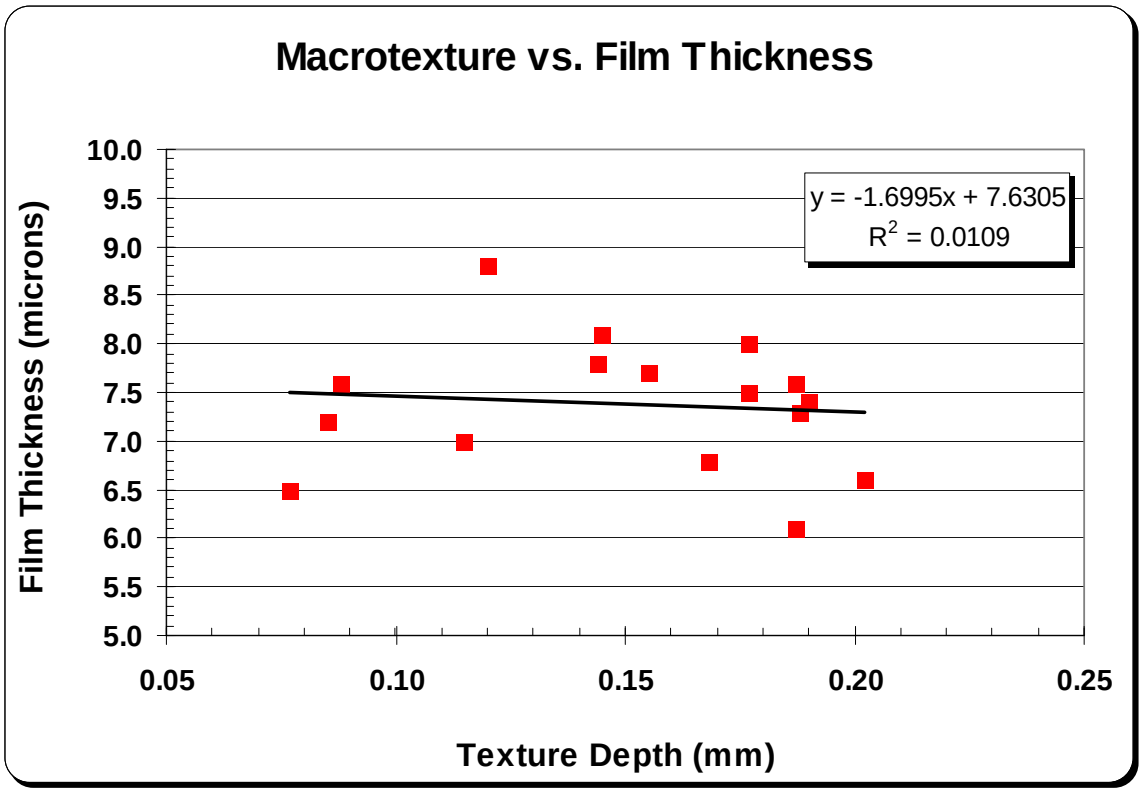

Figure 23. Relationship of Film Thickness to Macrotexture

Property	Slope	Intercept	R^2
Binder Content (Pb)	5.2134	7.0164	0.1238
Effective Binder Content (Pbe)	-4.7287	6.942	0.218
Voids in Mineral Aggregate (VMA)	-13.974	20.375	0.2215
Voids Filled with Asphalt (VFA)	-18.844	74.07	0.057
Dust Proportion (DP)	1.6579	1.0599	0.2214
Percent Density at $N_{initial}$ (%D@N_{ini})	-9.9163	81.728	0.0175
Film Thickness (FT)	-1.6995	7.6305	0.0109

Table 15. Summary of Regression Variables for Relationships of Mixture Properties to Macrotexture (MTD)

Macrotexture did not appear to be significantly dominated by any single mixture property. In fact, VFA, %D@N_{ini} and film thickness had essentially no effect at all. Binder content and dust proportion were positively correlated with macrotexture, such that binder content appeared to be the more sensitive of the two. Effective binder content and VMA displayed negative correlation. It was noted that binder content and effective binder content displayed conflicting trends with respect to macrotexture. Although neither trend was significant, it may be an indication that aggregate absorption affects skid resistance.

Overall, it was concluded that no single mixture parameter was able to significantly microtexture or macrotexture.

Aggregate Properties

Because the ANOVA indicated that aggregate source was significant in the initial mix design evaluation, and the regression analyses showed that no individual mixture property was significantly related to skid resistance, aggregate characteristics were further evaluated. A number of properties were investigated for each aggregate source, relative to microtexture and macrotexture, including:

- Fine aggregate angularity
- Micro-Deval abrasion
- Sodium sulfate soundness
- Bulk specific gravity
- Effective specific gravity
- Gradation
- Fineness modulus
- Particle Shape

Fine Aggregate Angularity

In some respects, fine aggregate angularity is a measure of particle shape, which could be expected to have a significant effect on skid resistance. Fine aggregate angularity was measured for each aggregate blend, and related to the average skid resistance for each mix. The results for microtexture are shown in Figure 24, and those for macrotexture are shown in Figure 25.

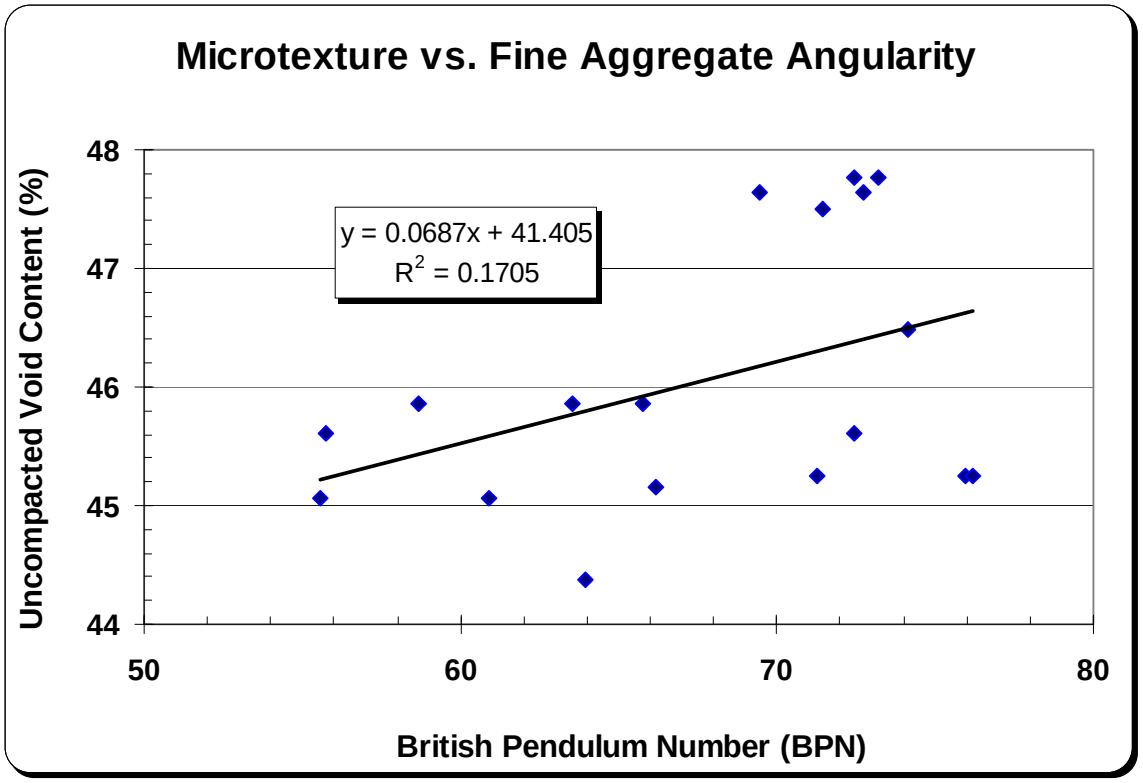

Figure 24. Relationship of Fine Aggregate Angularity to Microtexture

The relationships were weak, but did follow a trend of positive correlation such that as uncompacted void content increased, microtexture and macrotexture both increased. This was consistent with expected results, however the R^2 values were very low, and therefore no predictive relationships should be based on this dataset. The R^2 value for microtexture was just 17 percent, and it was noted that a BPN of 65 units corresponded with approximately 46 percent uncompacted voids. The R^2 value for macrotexture was somewhat better at 46 percent, meaning that fine aggregate angularity affects macrotexture more than microtexture. This was reasonable since angularity relates to the way that aggregates fit together, which is an inherent part of aggregate spacing and macrotexture.

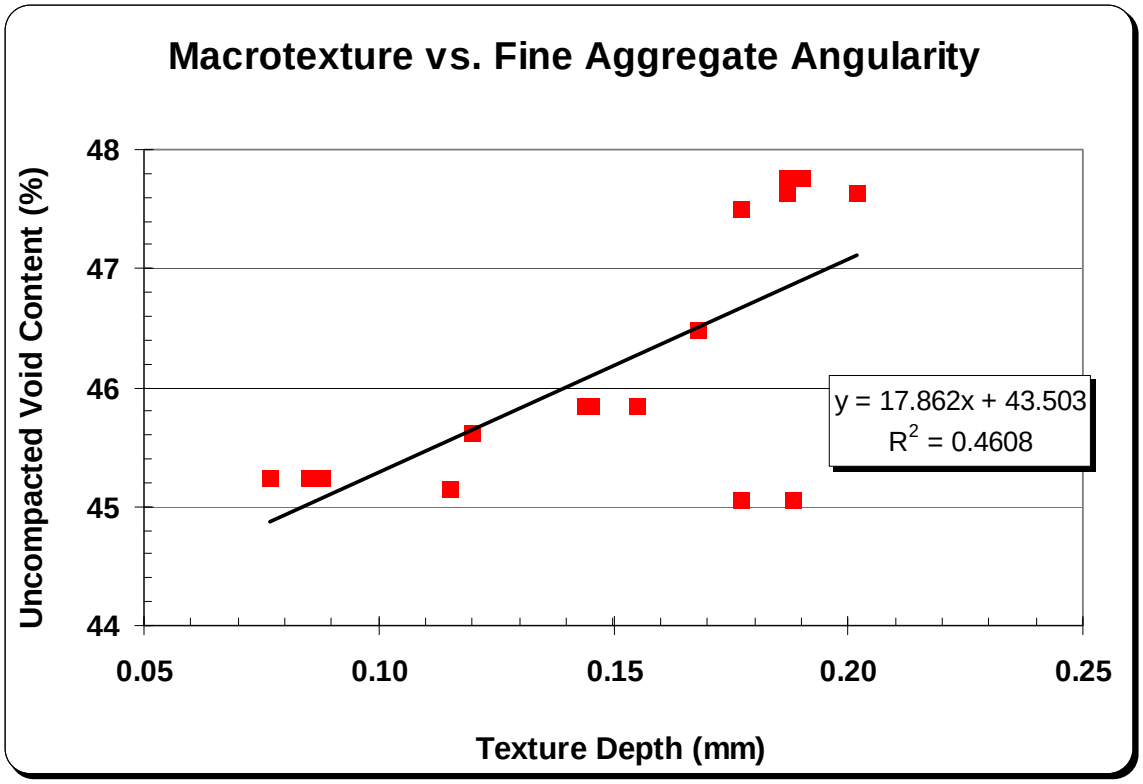

Figure 25. Relationship of Fine Aggregate Angularity to Macrotexture

Micro-Deval

The Micro-Deval abrasion test simulates the wearing of aggregate particles due to their abrasive interactions during production, transportation, and construction activities. Aggregates are known to lose their resistance to skidding when abrasion, wear, and polishing become significant. Thus, the more resistant an aggregate is to abrasion, the greater frictional resistance it should provide. The results for microtexture are shown in Figure 26, and those for macrotexture are shown in Figure 27.

Again, the relationships were weak, but followed the anticipated trends. In general, as percent loss by Micro-Deval decreased (i.e., becomes more abrasion-resistant), both the microtexture and macrotexture increased. The microtexture relationship was the stronger of the two, having an R^2 value of approximately 34 percent. Again, neither of these relationships was sufficient for predictive purposes, but it was noted that a BPN of 65 was consistent with approximately 13 percent loss by Micro-Deval.

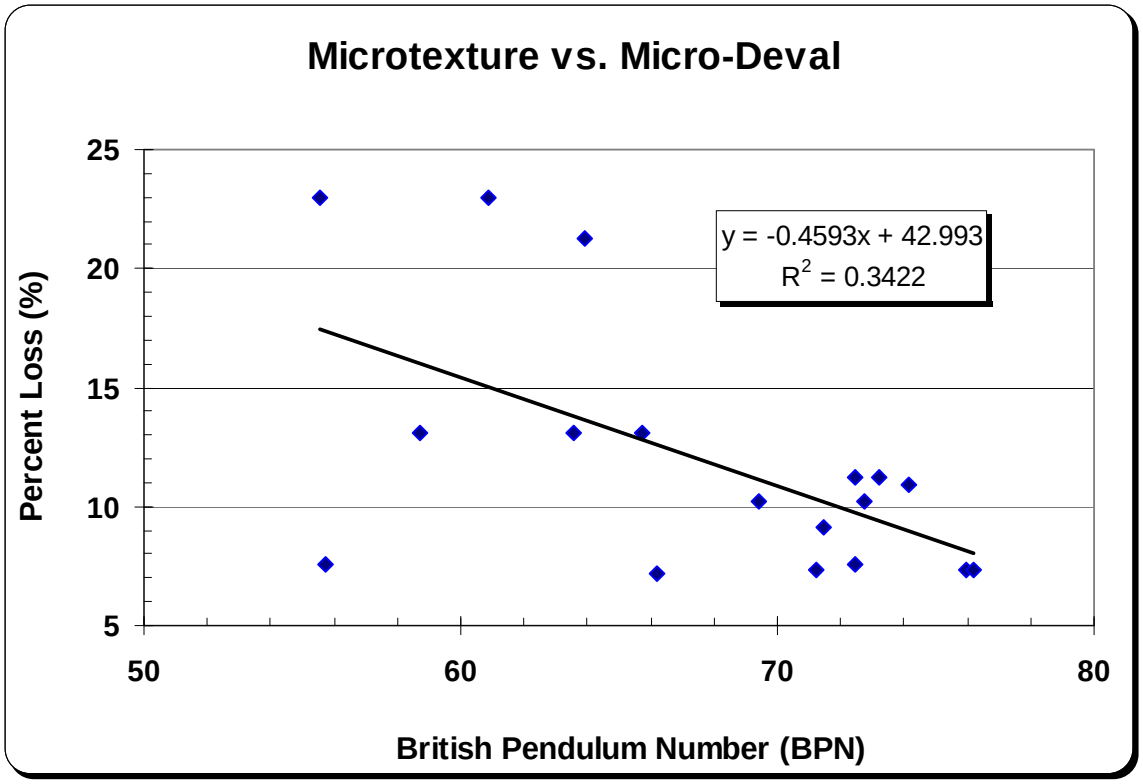

Figure 26. Relationship of Micro-Deval Abrasion to Microtexture

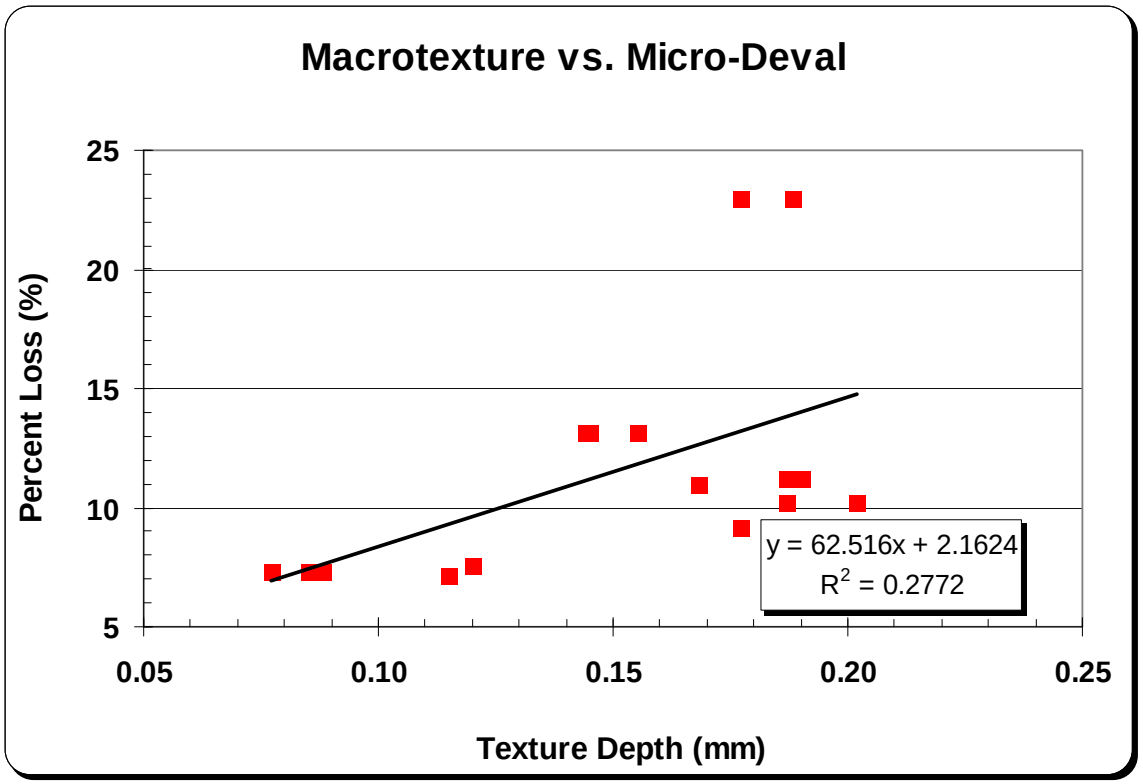

Figure 27. Relationship of Micro-Deval Abrasion to Macrotexture

Sodium Sulfate Soundness

The sodium sulfate soundness test was used as the measure of aggregate durability. This property was used as another method for quantifying the structural integrity of the aggregate particles based on the assumption that a more durable aggregate would possess a greater tendency toward high frictional value. The relationships of aggregate soundness to microtexture and macrotexture are shown in Figures 28 and 29, respectively.

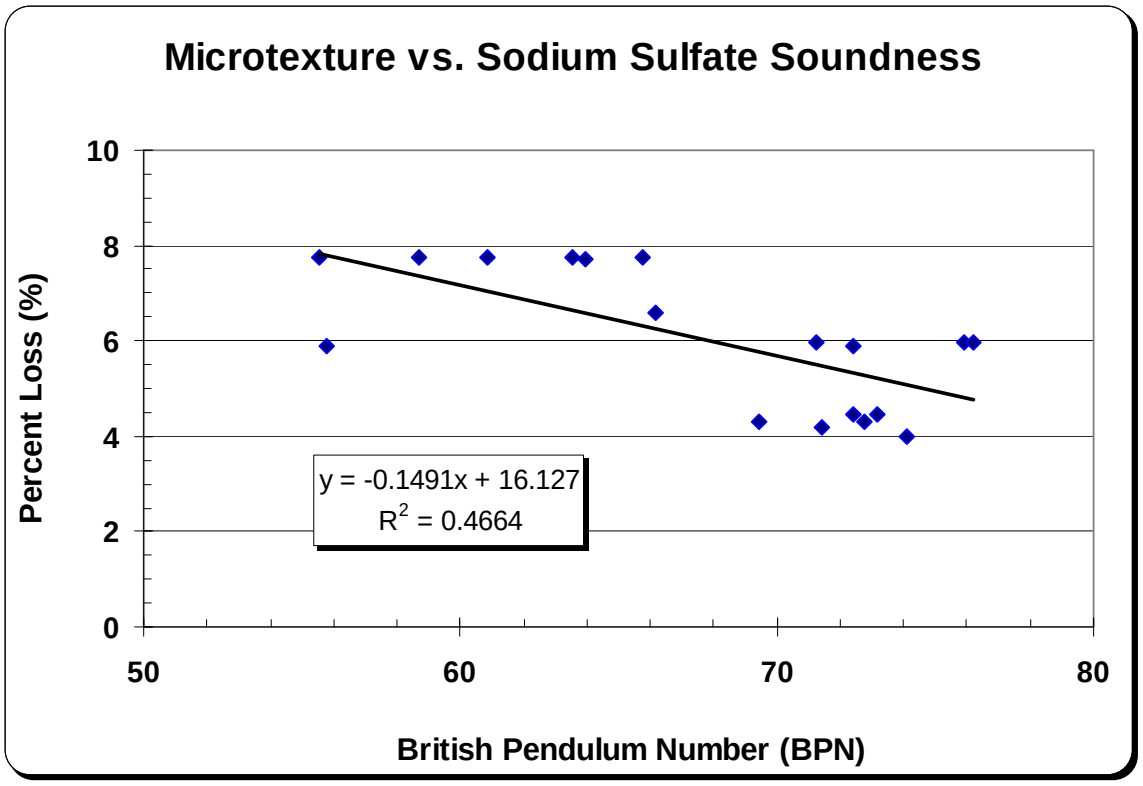

Figure 28. Relationship of Sodium Sulfate Soundness to Microtexture

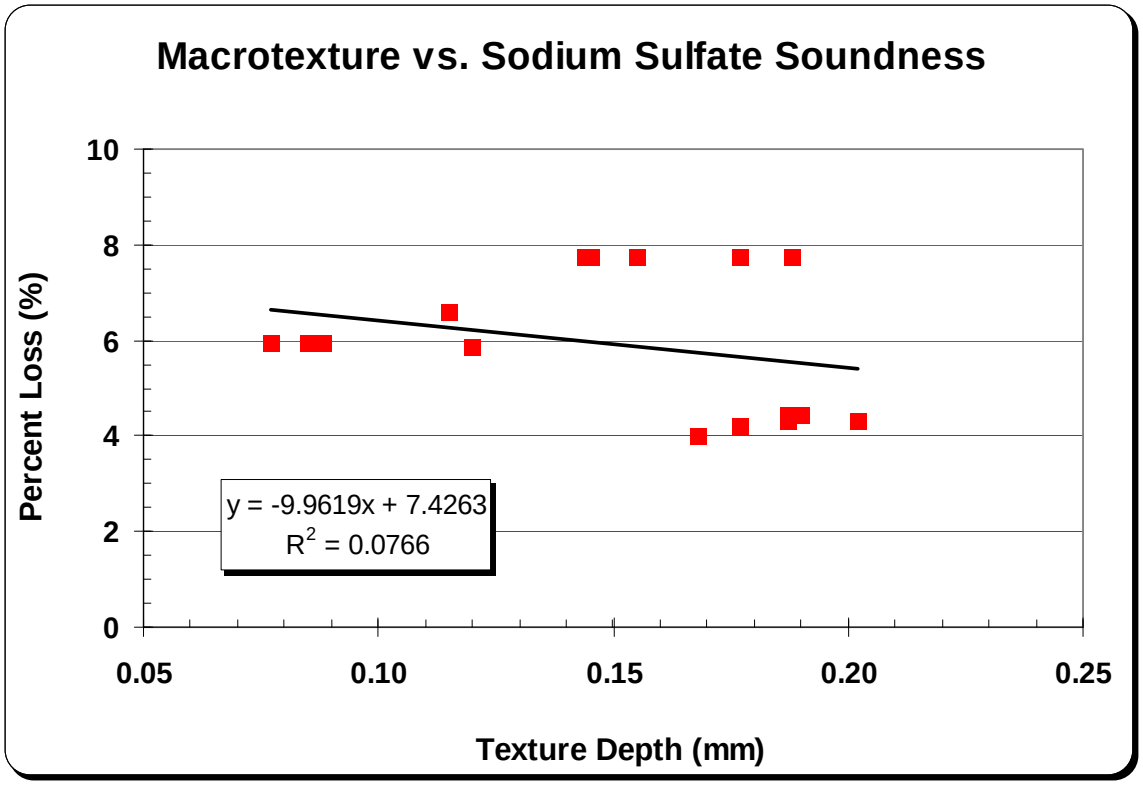

Figure 29. Relationship of Sodium Sulfate Soundness to Macrotexture

The relationship of sodium sulfate soundness to microtexture was negatively correlated and had an R^2 value of just over 46 percent, which was not adequate for predictive purposes. However, the trend appeared to be fairly straightforward in that aggregates having a greater loss by this test method tended to have less frictional resistance to contribute to skid resistance. A BPN of 65 corresponded with approximately 7 percent loss by the sodium sulfate soundness method.

Macrotexture was negatively correlated to percent loss by the sodium sulfate method, but to a much lesser degree than microtexture. The R^2 value for this relationship was approximately 8 percent.

Bulk Aggregate Specific Gravity

The bulk specific gravity of the aggregate blend was investigated next as to its relationship to skid resistance. Denser aggregates are sometimes believed to be better able to withstand the forces that create aggregate wear and decrease the available skid resistance. The relationships of microtexture and macrotexture are given in Figures 30 and 31, respectively.

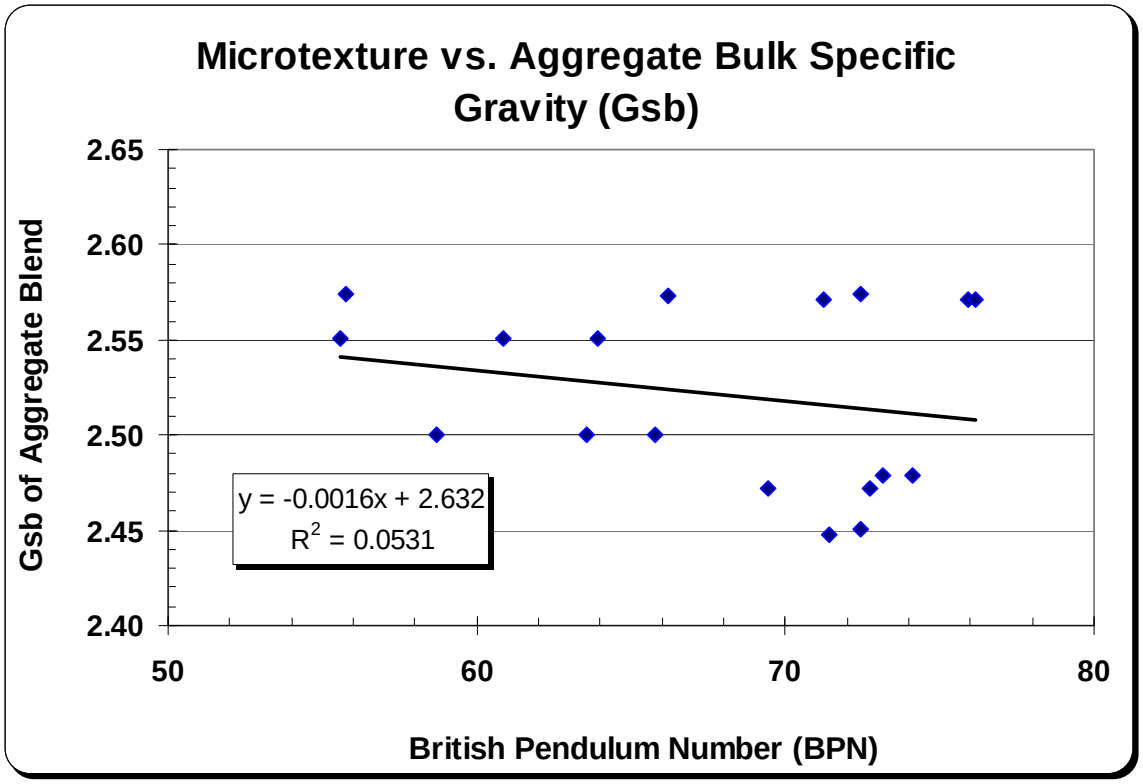

Figure 30. Relationship of Aggregate Bulk Specific Gravity to Microtexture

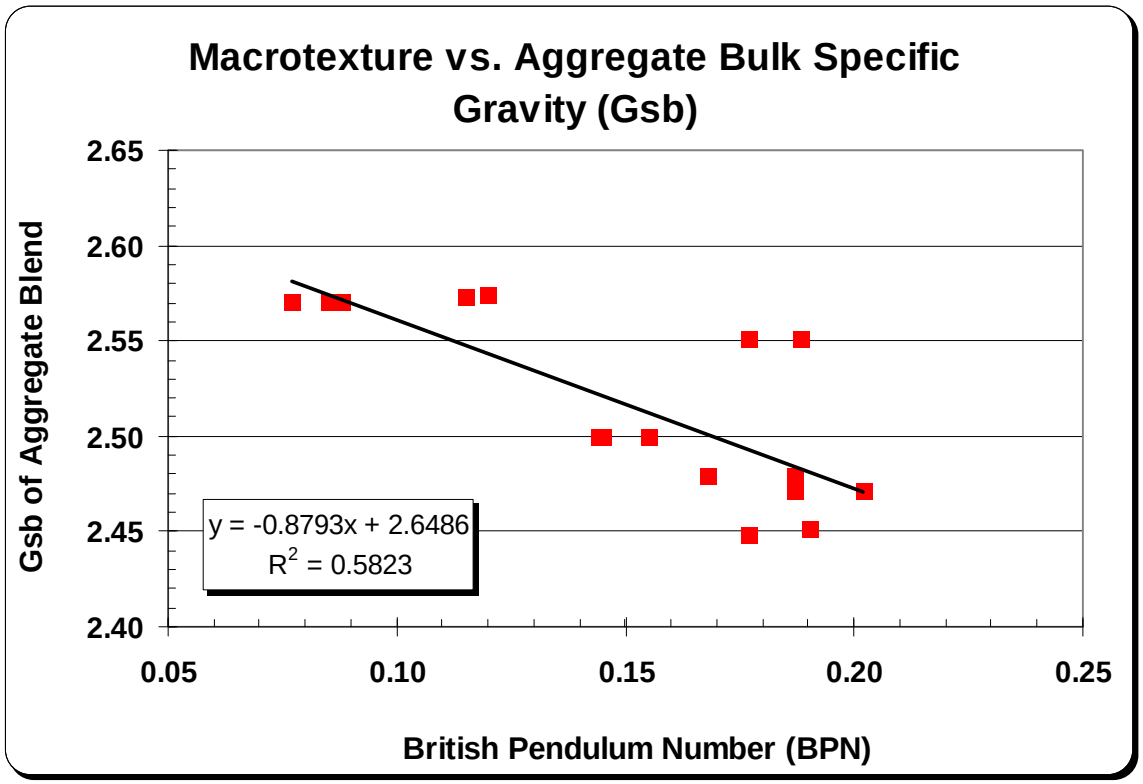

Figure 31. Relationship of Aggregate Bulk Specific Gravity to Macrotexture

Microtexture and macrotexture each displayed a negative correlation with the bulk specific gravity of the aggregate blend, having R^2 values of 5 percent and 58 percent, respectively and macrotexture appeared to be more sensitive to this parameter. This outcome was not consistent with expectations. While this relationship appears to be one of the strongest in the analysis, it is likely that the true differences in macrotexture are more closely related to factors other than specific gravity.

Effective Aggregate Specific Gravity

The effective specific gravity of the aggregate blend was also investigated, and the relationships are given in Figures 32 and 33. Again, the aggregate blends possessing the higher values for density were expected to possess greater skid resistance. This was not the case. The relationships for microtexture and macrotexture were both negatively correlated, with the microtexture relationship having an R^2 value of approximately 35 percent, and the macrotexture relationship having an R^2 value of only 4 percent. No explanation for this relationship was determined, and it was more likely that the relationship was governed by factors other than aggregate density.

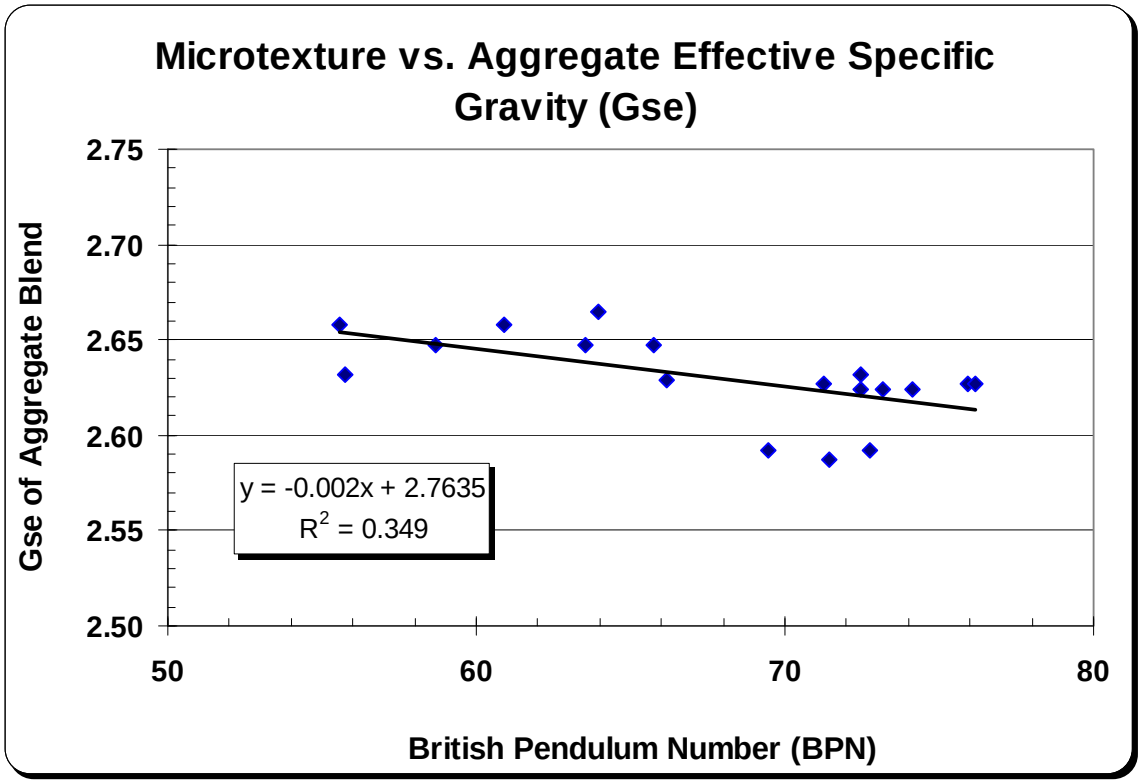

Figure 32. Relationship of Aggregate Effective Specific Gravity to Microtexture

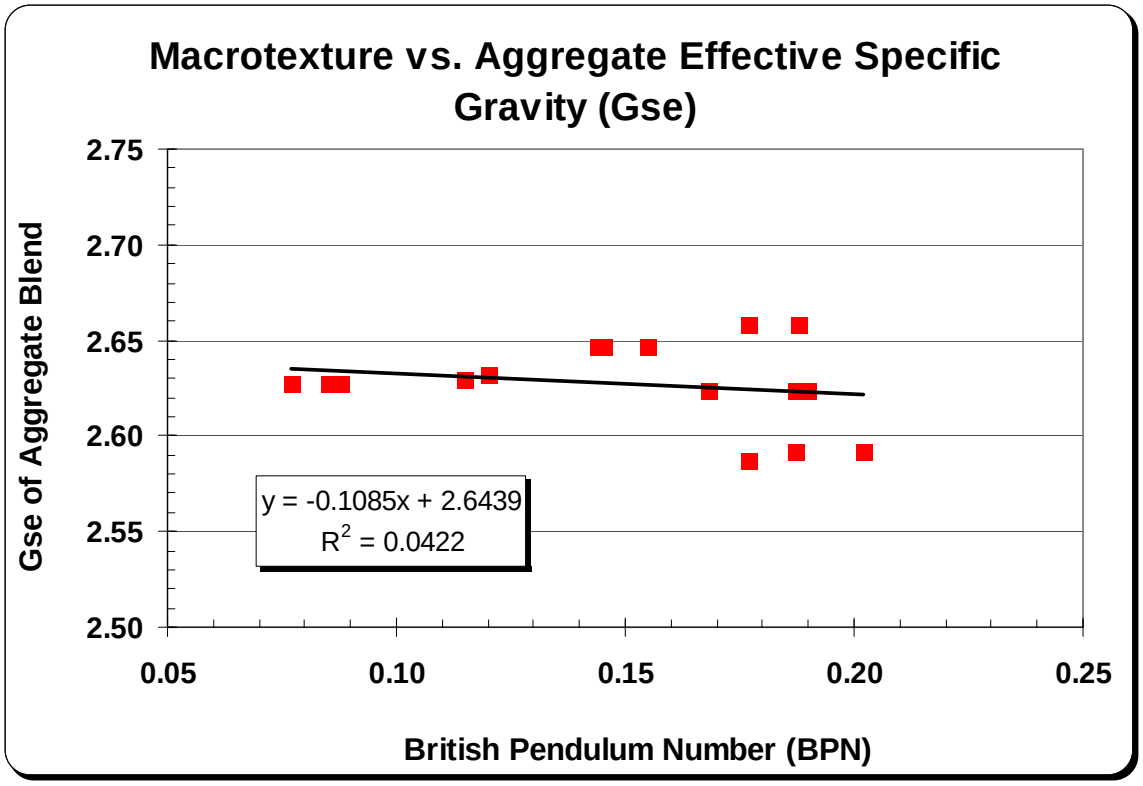

Figure 33. Relationship of Aggregate Effective Specific Gravity to Macrotexture

Aggregate Gradation

Aggregate gradation was evaluated next by studying the relationships of microtexture to the percents passing each sieve size contained in the 4.75mm gradation. The sieve sizes considered were the #8 (2.36mm), #16 (1.18mm), #30 (0.600mm), #50 (0.300mm), #100 (0.150mm), and the #200 (0.075mm). Figures 34 through 39 illustrate the relationships of BPN and percent passing each sieve size.

In terms of BPN, some interesting trends were noted with respect to gradation. For the #8 (2.36mm) sieve, percent passing and BPN were negatively correlated, meaning that microtexture increased as the percent passing decreased. For the #16 (1.18mm) sieve, the trendline was essentially flat, meaning that there was no relationship. For the #30 (0.60mm) sieve (and subsequent smaller sieves), the trend reversed such that microtexture increased with an increase in percent passing. In other words, the slope of the regression line changed from a negative slope to a positive slope as the sieve size decreased. Decreasing the percentage passing the larger sieves in the gradation while increasing the percentage passing the smaller sieves suggests that a gap gradation could be used to maximize the microtexture of 4.75mm HMA mixtures. Although the statistical validity of the individual relationships is weak, aggregate gradation appeared to have a stronger relationship to microtexture than the mixture properties. In fact, some

of the gradation correlations were able to explain over half the variability in the data (as demonstrated by the R^2 values.

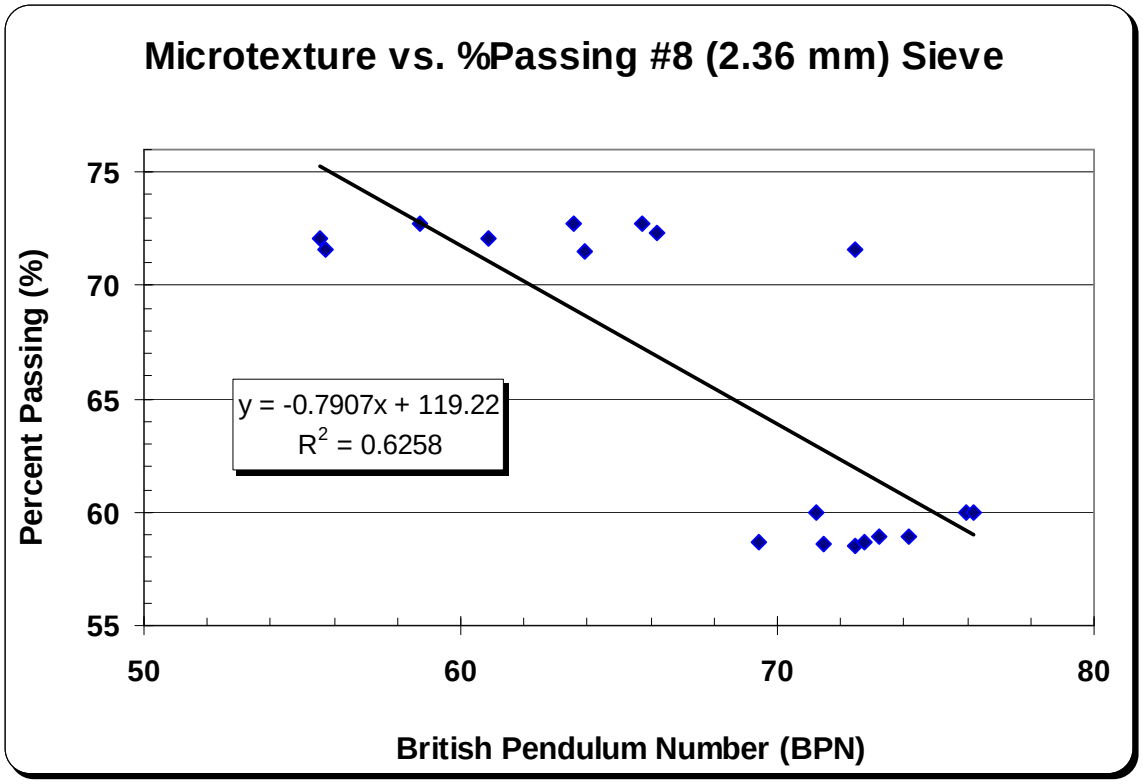

Figure 34. Relationship of Percent Passing the #8 Sieve to Microtexture

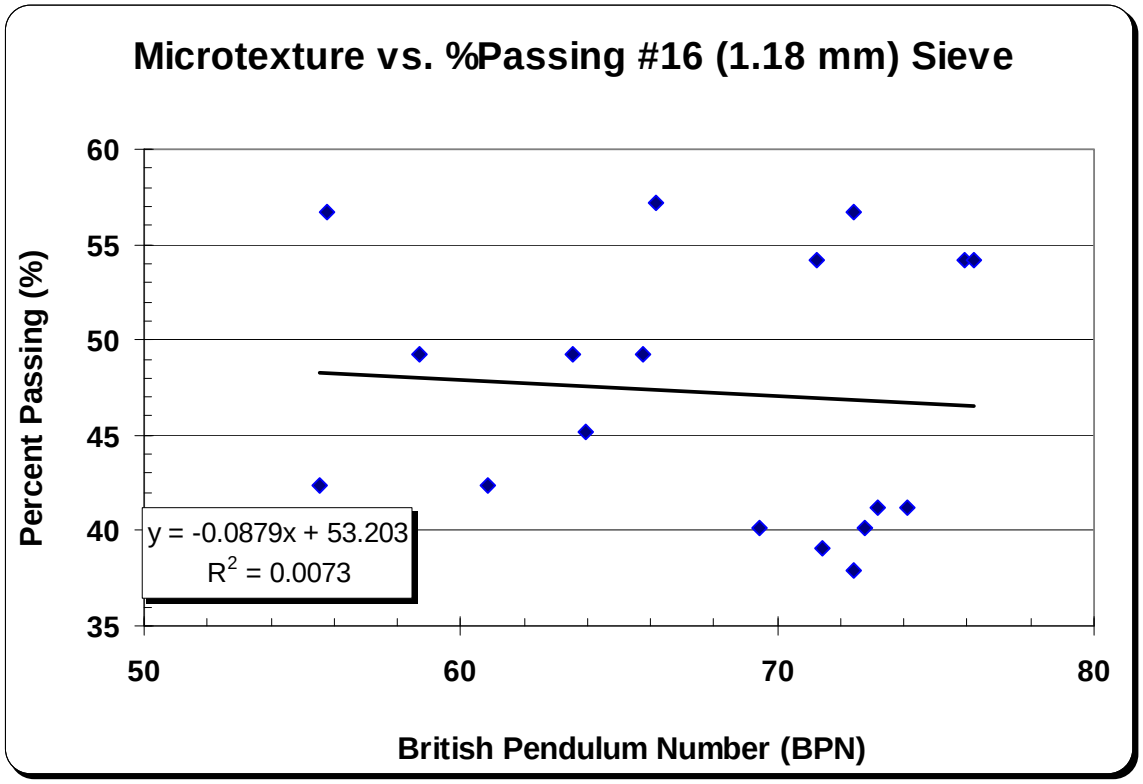

Figure 35. Relationship of Percent Passing the #16 Sieve to Microtexture

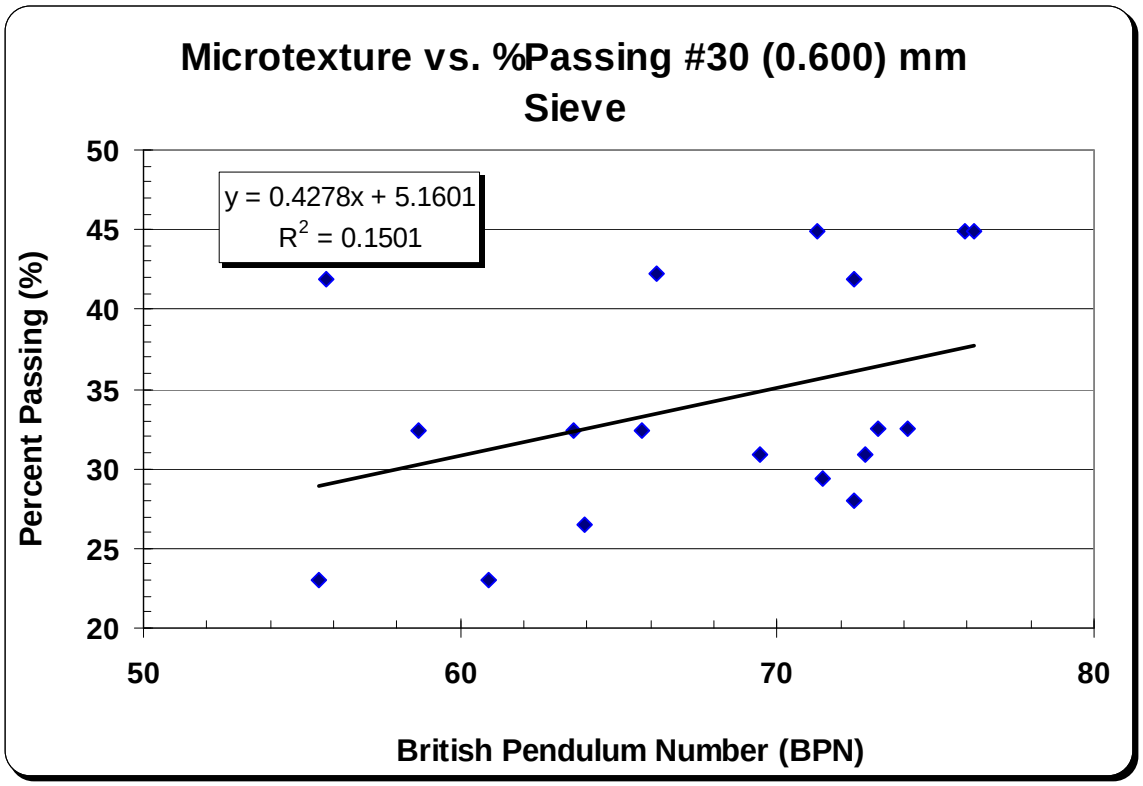

Figure 36. Relationship of Percent Passing the #30 Sieve to Microtexture

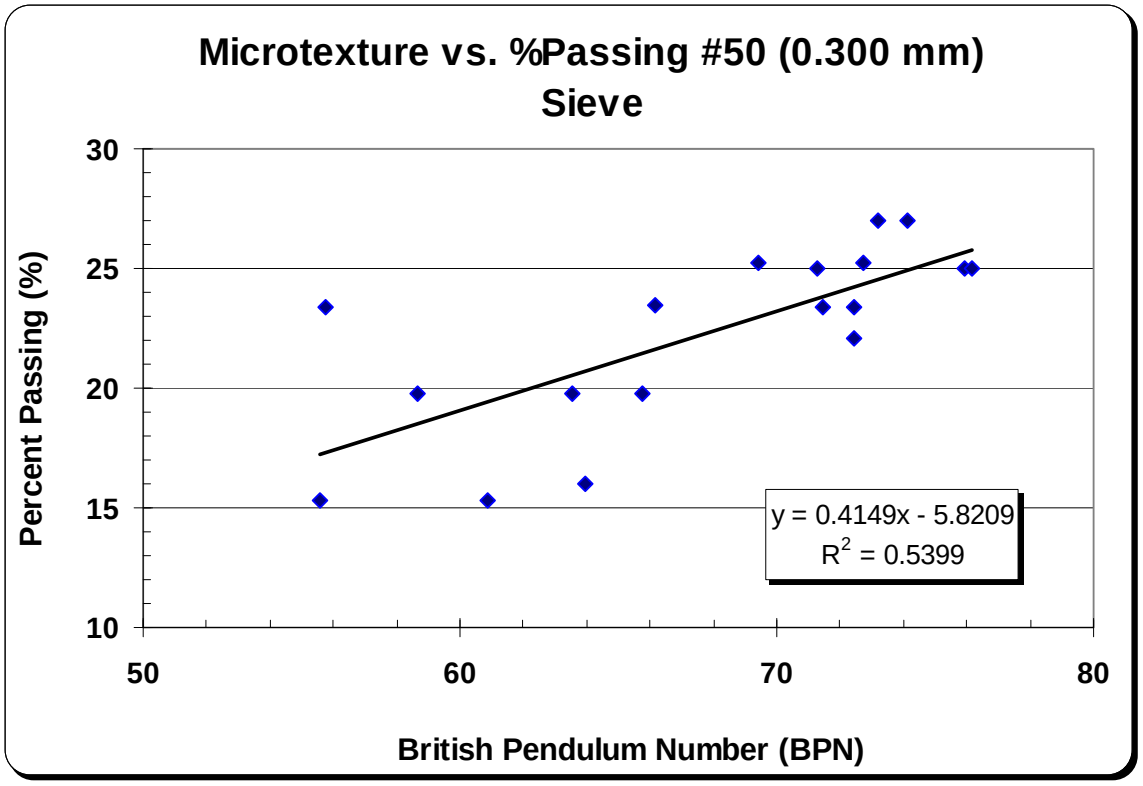

Figure 37. Relationship of Percent Passing the #50 Sieve to Microtexture

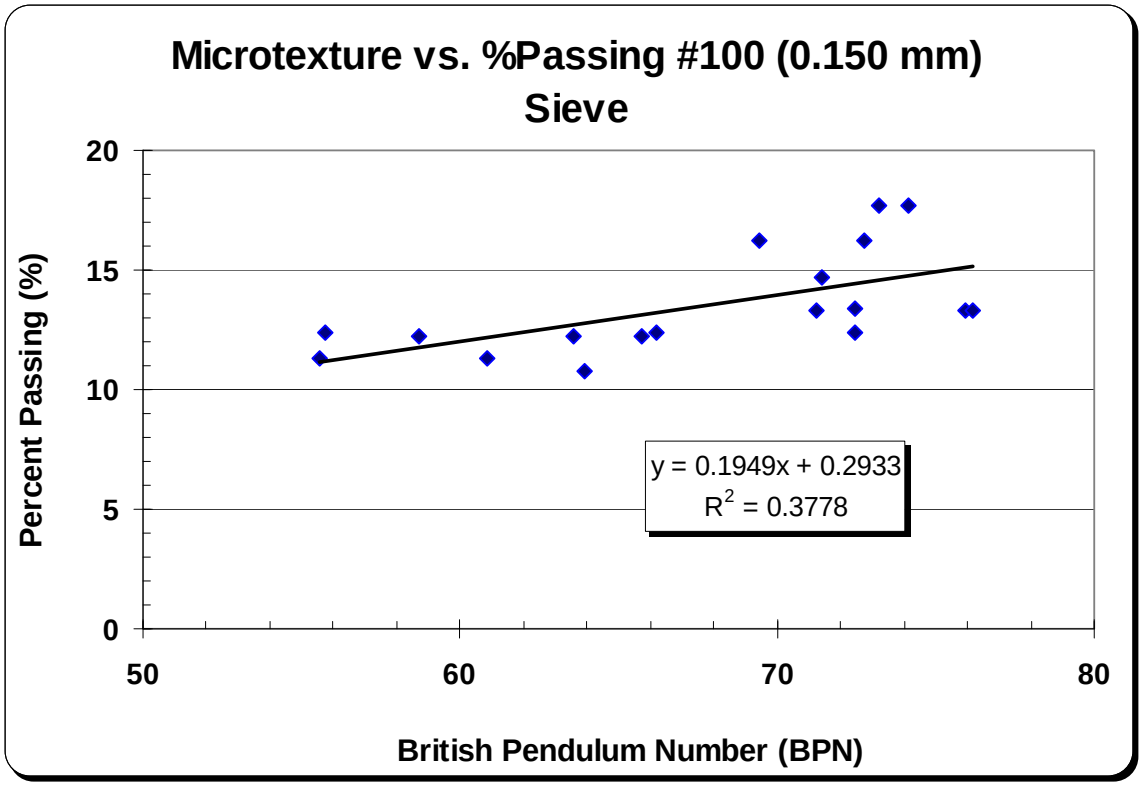

Figure 38. Relationship of Percent Passing the #100 Sieve to Microtexture

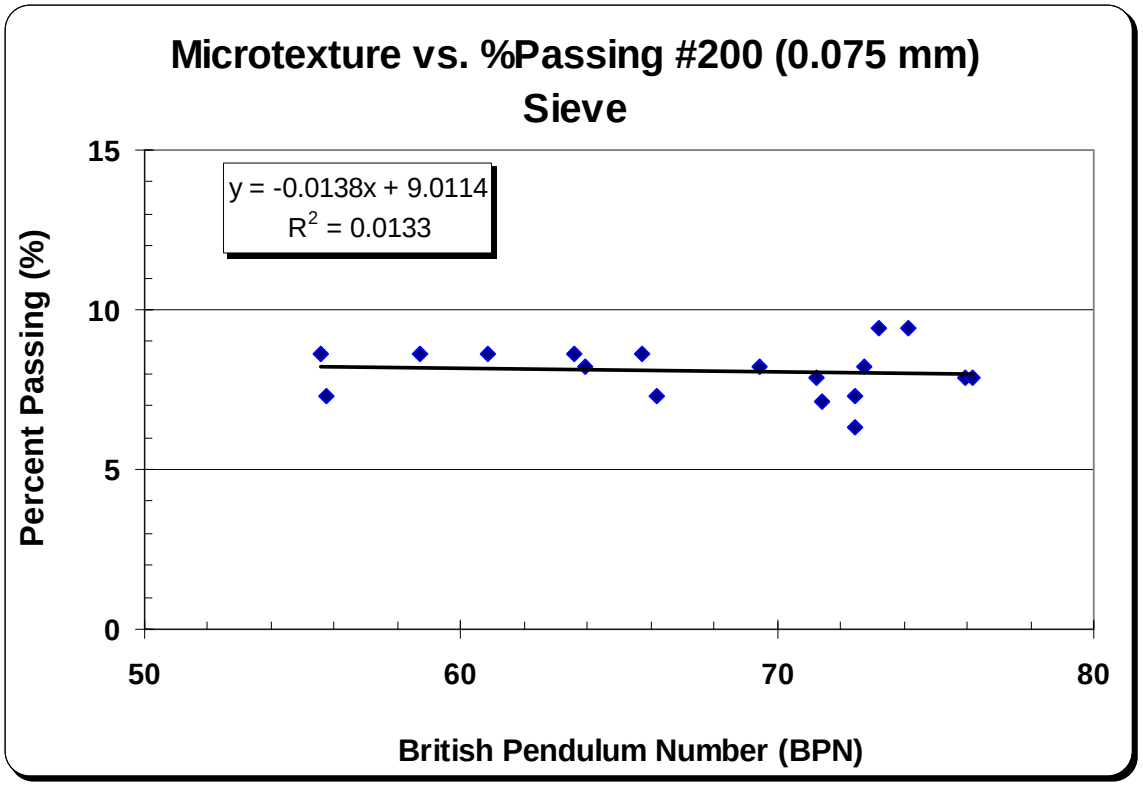

Figure 39. Relationship of Percent Passing the #200 Sieve to Microtexture

A similar routine was used to analyze the effects of gradation on texture depth. The relationships of percent passing and texture depth are plotted for each sieve size, beginning with the #8 (2.36 mm) sieve. These plots are shown in Figures 40 through 45.

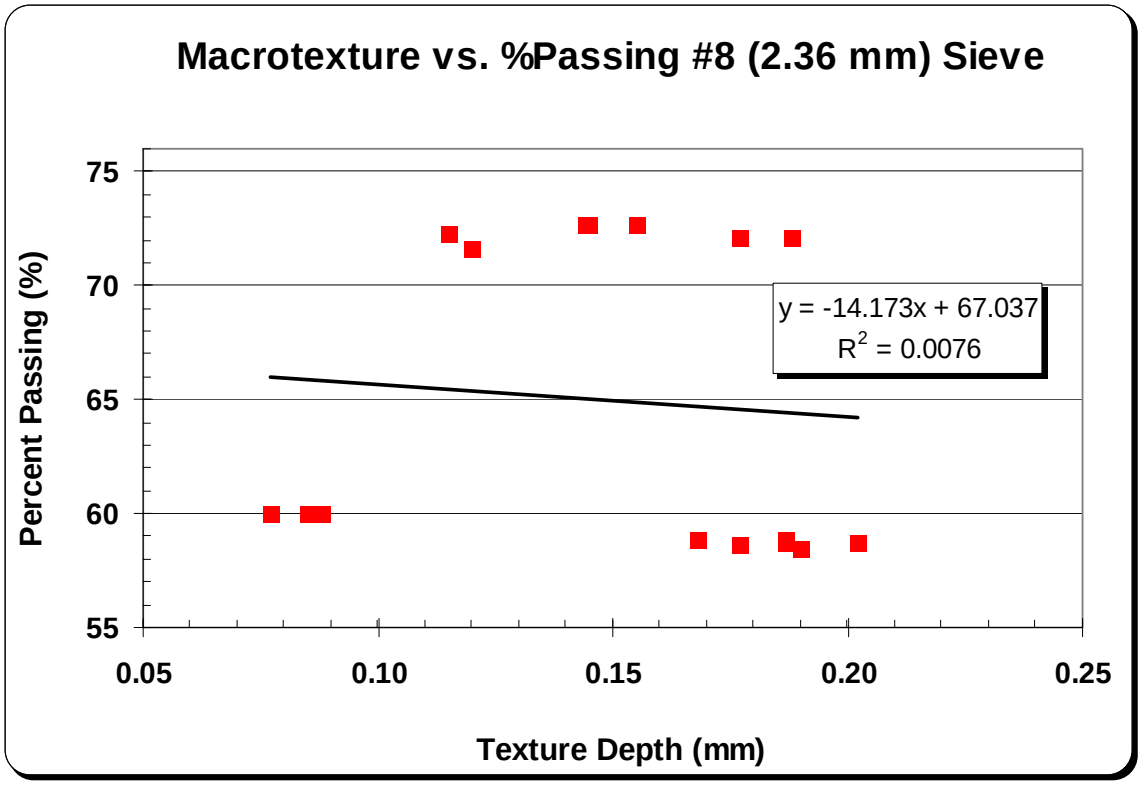

Figure 40. Relationship of Percent Passing the #8 Sieve to Macrotexture

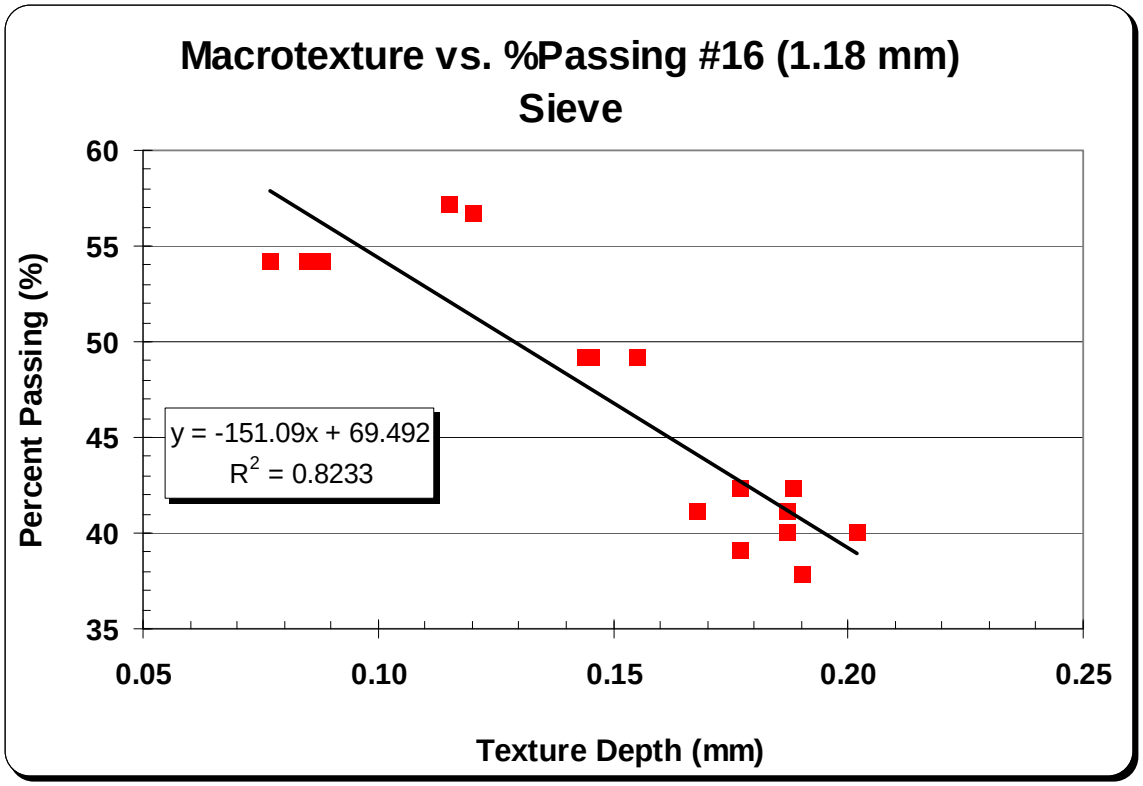

Figure 41. Relationship of Percent Passing the #16 Sieve to Macrotexture

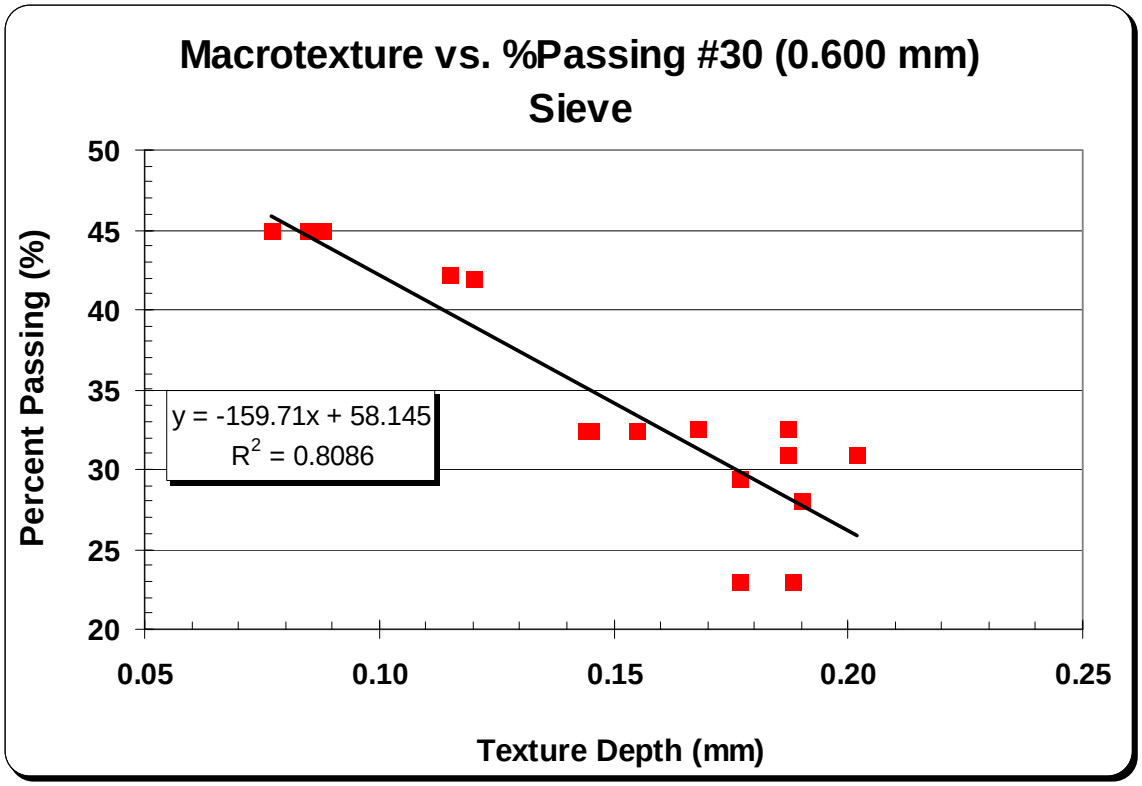

Figure 42. Relationship of Percent Passing the #30 Sieve to Macrotexture

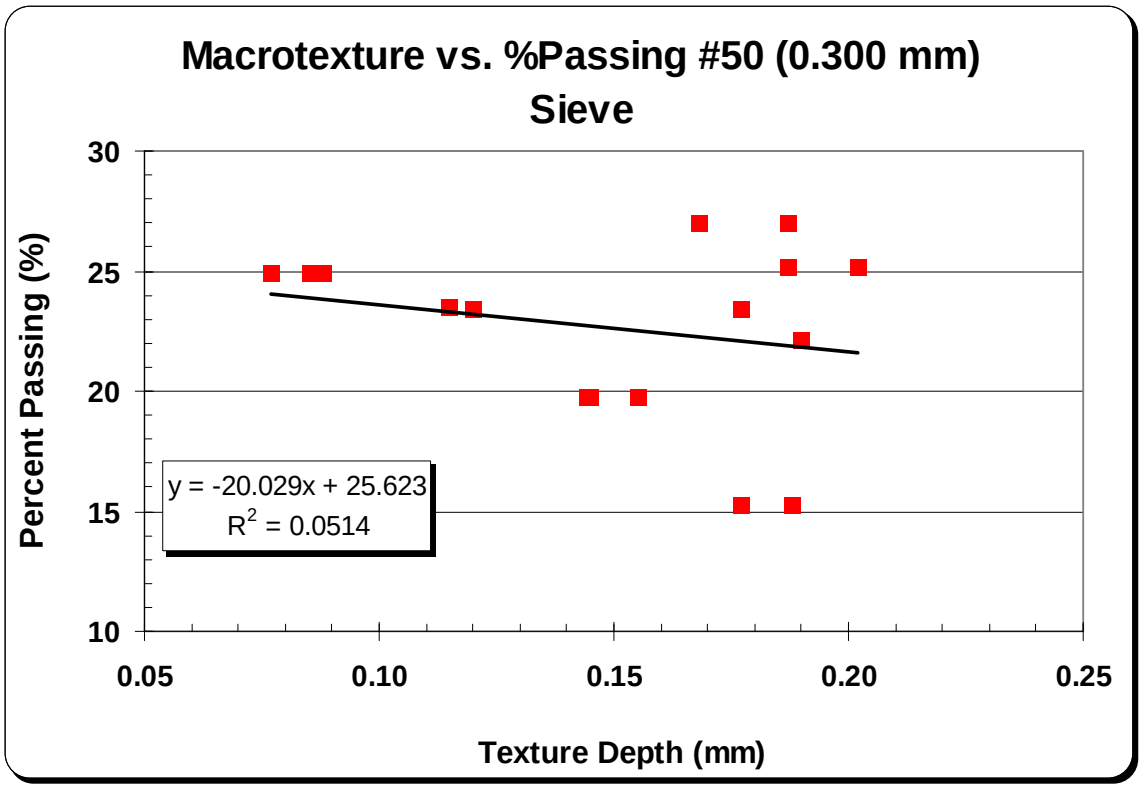

Figure 43. Relationship of Percent Passing the #50 Sieve to Macrotexture

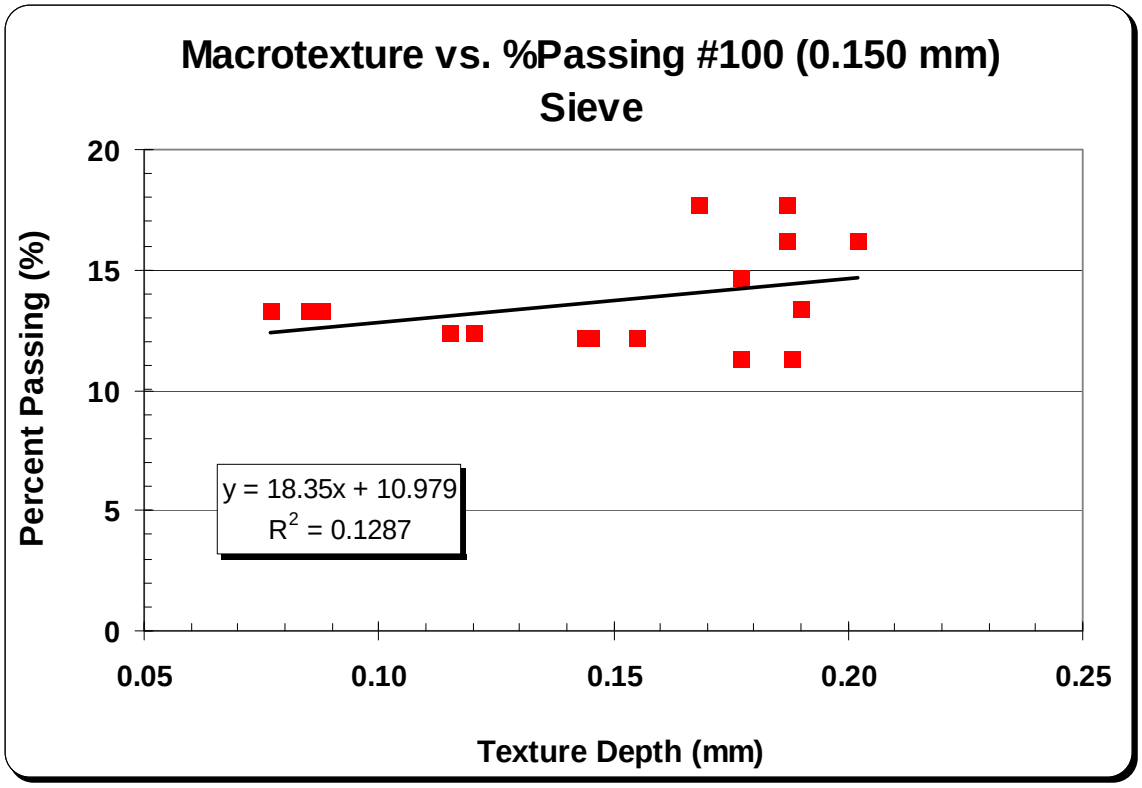

Figure 44. Relationship of Percent Passing the #100 Sieve to Macrotexture

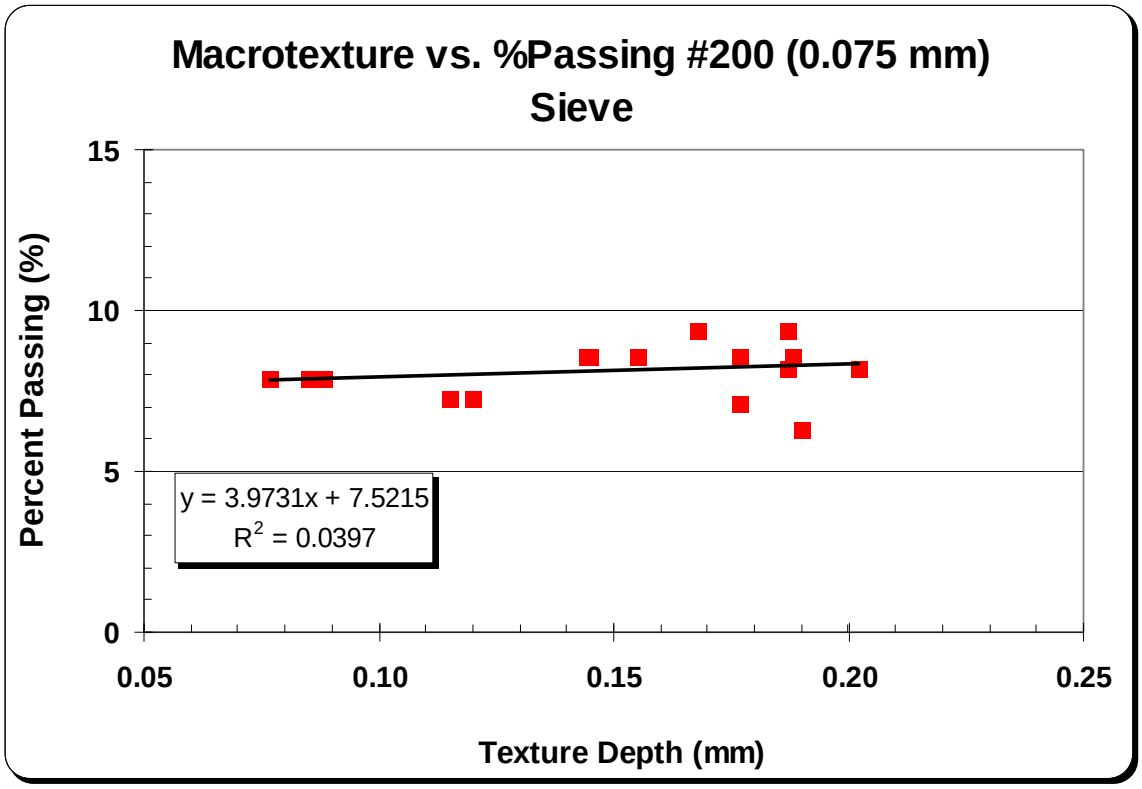

Figure 45. Relationship of Percent Passing the #200 Sieve to Macrotexture

In terms of macrotexture, trends with respect to gradation were similar to those noted for microtexture. The #8 (2.36mm), #16 (1.18mm) and #30 (0.600mm) sieves were negatively correlated with texture depth, and the #50 (0.300mm) sieve showed virtually no correlation. The correlation began to shift positively as sieve size decreased to the #100 (0.150mm). This shifting of trendlines throughout subsequent sieves suggests that a gap-graded aggregate blend may also assist in improving the macrotexture of a 4.75mm HMA mixture.

Fineness Modulus

Fineness modulus is a single aggregate characteristic that takes into account the cumulative gradation of the aggregate blend. The relationships of fineness modulus to microtexture and macrotexture are given in Figures 46 and 47, respectively.

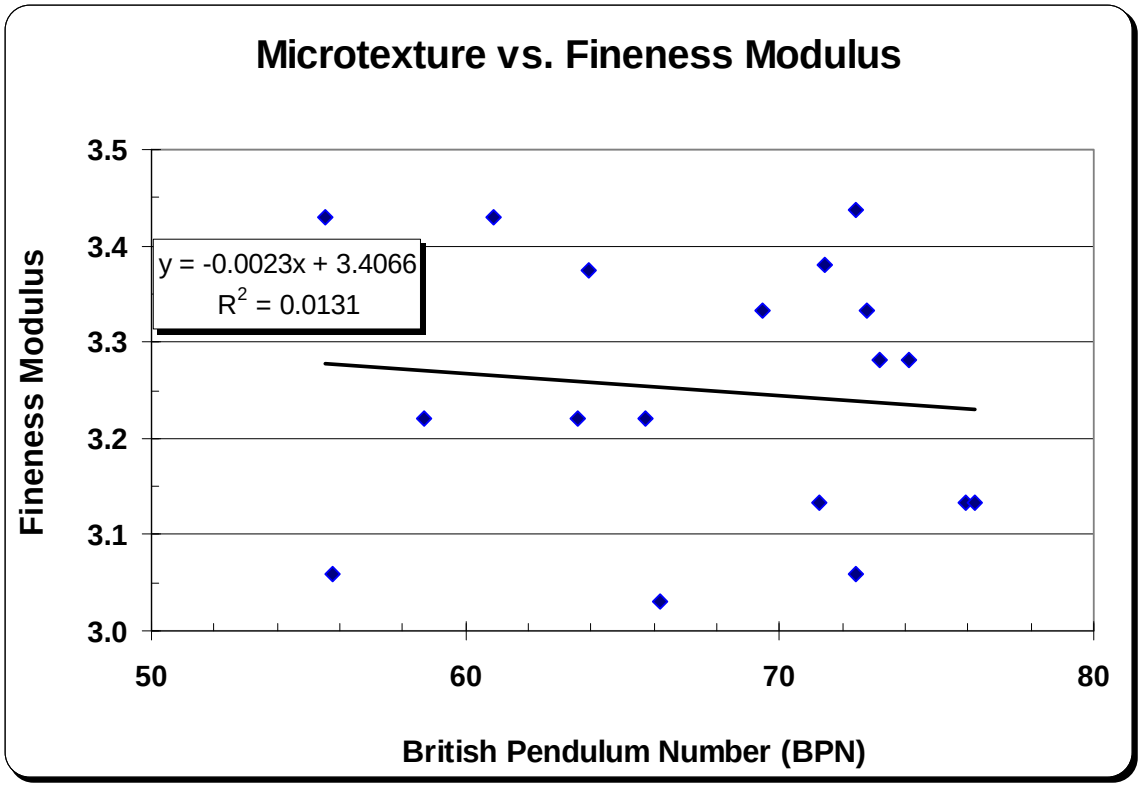

Figure 46. Relationship of Fineness Modulus to Microtexture

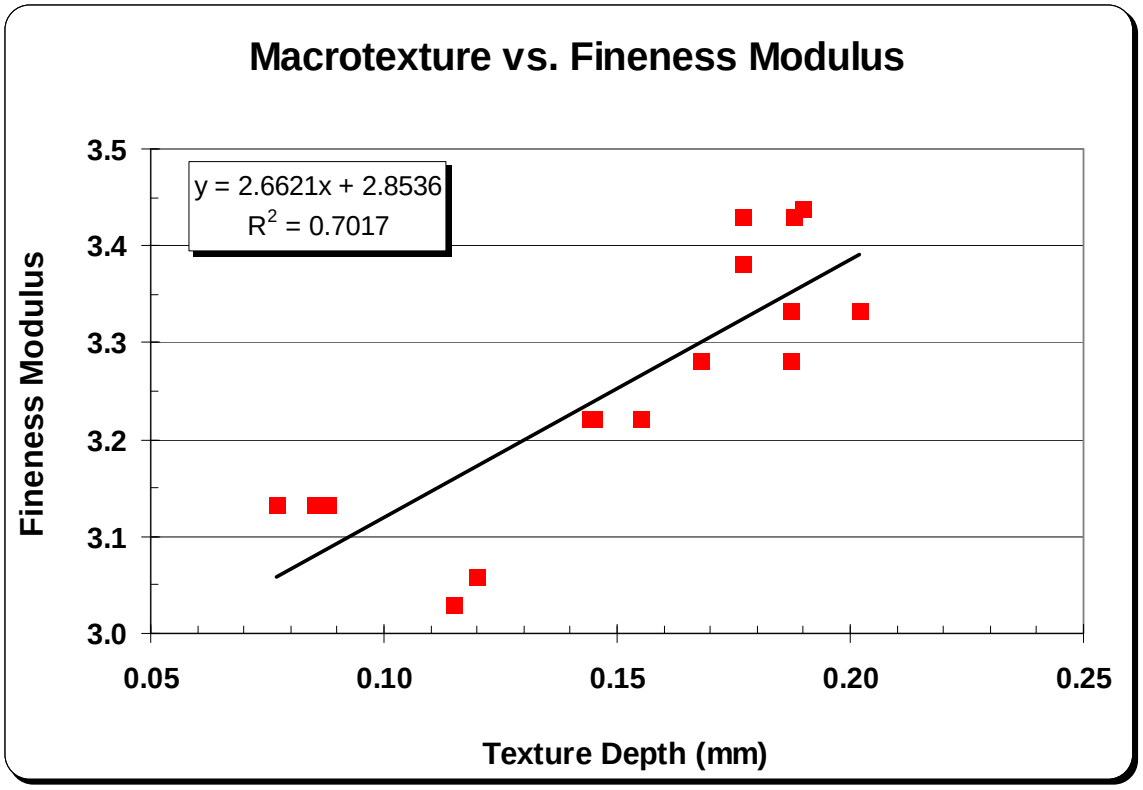

Figure 47. Relationship of Fineness Modulus to Macrotexture

Microtexture was relatively unaffected by changes in fineness modulus (R^2 ~ 0.01), however, macrotexture was significantly correlated. Fineness modulus alone was able to mathematically explain over 70 percent of the variability in texture depth. Specifically, as fineness modulus increased, macrotexture also increased. Increases in fineness modulus are associated with gap-graded mixtures; therefore, this conclusion supports the trends previously noted in the gradation analysis.

Aggregate Shape

Aggregate texture and shape were analyzed using the AIMS technology owned by the Federal Highway Administration (FHWA). Three parameters were quantified for each of the fine aggregate sources used in this study: gradient angularity, radius angularity, and two-dimensional form.

For each aggregate material, multiple fractions of aggregate were tested for texture and shape, and the results were combined mathematically and used to generate overall values for the gradient angularity, radius angularity, and two-dimensional shape of each mix design. Results are summarized in Tables 16 through 18. Based on gradient angularity indexes, all 4.75mm aggregate blends utilized in this study were classified as sub-rounded and sub-angular. The limestone and sandstone/gravel blends were sub-rounded, and the syenite blends were sub-angular. Texture descriptions developed from the Radius Angularity Index tended toward the opposite classifications such that the limestone and sandtone/gravel blends were sub-angular and the syenite blends were sub-rounded. The two-dimensional form index classified aggregate shapes as primarily semi-elongated, with some of the limestone blends as semi-circular.

Aggregate Source	Design Air Voids (%)	Design Compaction (gyr)	Gradient Angularity Index	Texture Classification
LS	4.5	50	3626.2	Sub-Rounded
LS	4.5	75	3622.8	Sub-Rounded
LS	4.5	100	3622.8	Sub-Rounded
LS	6.0	50	3768.3	Sub-Rounded
LS	6.0	75	3768.3	Sub-Rounded
LS	6.0	100	3768.3	Sub-Rounded
SG	4.5	50	3923.9	Sub-Rounded
SG	4.5	75	3828.8	Sub-Rounded
SG	4.5	100	3923.9	Sub-Rounded
SG	6.0	50	3850.8	Sub-Rounded
SG	6.0	75	3777.7	Sub-Rounded
SG	6.0	100	3850.8	Sub-Rounded
SY	4.5	50	4002.7	Sub-Angular
SY	4.5	75	3983.4	Sub-Angular
SY	4.5	100	3983.4	Sub-Angular
SY	6.0	50	4002.7	Sub-Angular
SY	6.0	75	4002.7	Sub-Angular
SY	6.0	100	3983.4	Sub-Angular

Table 16. Gradient Angularity Index Data and Classification Summary

Aggregate Source	Design Air Voids (%)	Design Compaction (gyr)	Radius Angularity Index	Texture Classification
LS	4.5	50	10.667	Sub-Angular
LS	4.5	75	10.821	Sub-Angular
LS	4.5	100	10.821	Sub-Angular
LS	6.0	50	11.260	Sub-Angular
LS	6.0	75	11.260	Sub-Angular
LS	6.0	100	11.260	Sub-Angular
SG	4.5	50	11.367	Sub-Angular
SG	4.5	75	10.988	Sub-Angular
SG	4.5	100	11.367	Sub-Angular
SG	6.0	50	11.417	Sub-Angular
SG	6.0	75	11.467	Sub-Angular
SG	6.0	100	11.417	Sub-Angular
SY	4.5	50	10.630	Sub-Rounded
SY	4.5	75	10.530	Sub-Rounded
SY	4.5	100	10.530	Sub-Rounded
SY	6.0	50	10.630	Sub-Rounded
SY	6.0	75	10.630	Sub-Rounded
SY	6.0	100	10.530	Sub-Rounded

Table 17. Gradient Angularity Index Data and Classification Summary

Aggregate Source	Design Air Voids (%)	Design Compaction (gyr)	2D Form Index	Shape Classification
LS	4.5	50	7.936	Semi-Circular
LS	4.5	75	7.978	Semi-Circular
LS	4.5	100	7.978	Semi-Circular
LS	6.0	50	8.330	Semi-Elongated
LS	6.0	75	8.330	Semi-Elongated
LS	6.0	100	8.330	Semi-Elongated
SG	4.5	50	8.582	Semi-Elongated
SG	4.5	75	8.392	Semi-Elongated
SG	4.5	100	8.582	Semi-Elongated
SG	6.0	50	8.568	Semi-Elongated
SG	6.0	75	8.554	Semi-Elongated
SG	6.0	100	8.568	Semi-Elongated
SY	4.5	50	8.101	Semi-Elongated
SY	4.5	75	8.056	Semi-Elongated
SY	4.5	100	8.056	Semi-Elongated
SY	6.0	50	8.101	Semi-Elongated
SY	6.0	75	8.101	Semi-Elongated
SY	6.0	100	8.056	Semi-Elongated

Table 18. Gradient Angularity Index Data and Classification Summary

Potential correlations between these aggregate shape parameters and skid resistance were investigated. Graphical representations of the relationships to microtexture are shown in Figures 48 through 50, and those to macrotexture are shown in Figures 51 through 53.

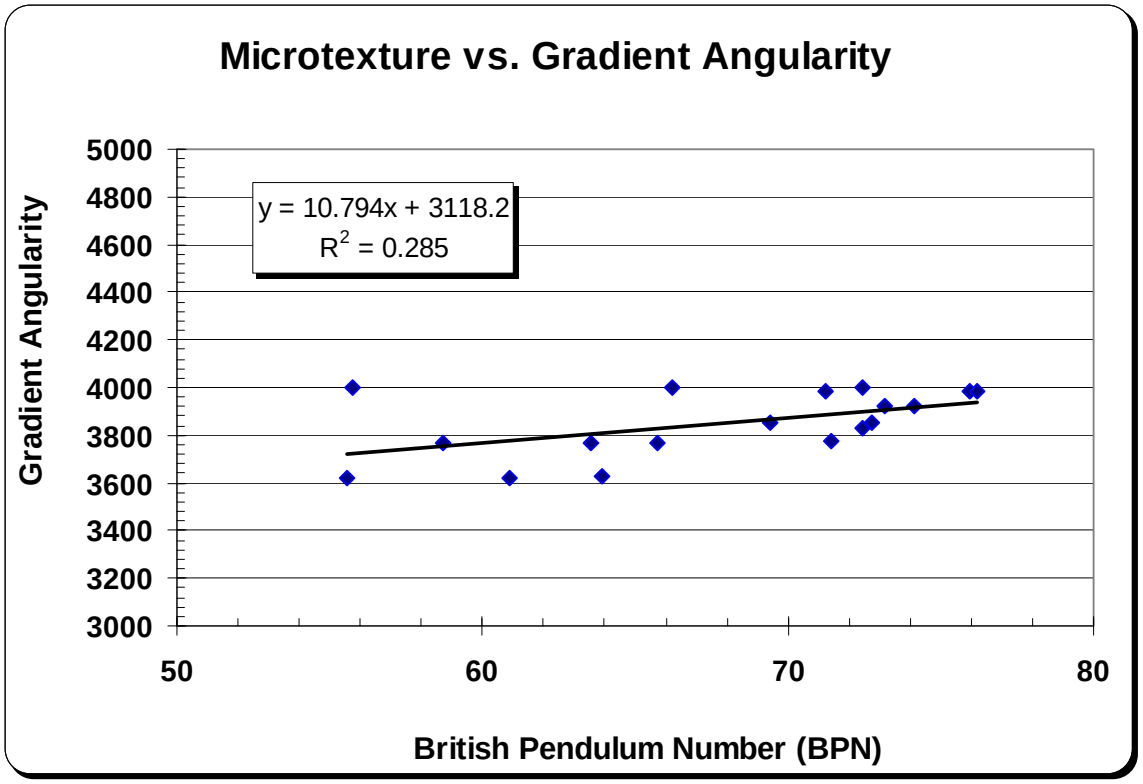

Figure 48. Relationship of Gradient Angularity to Microtexture

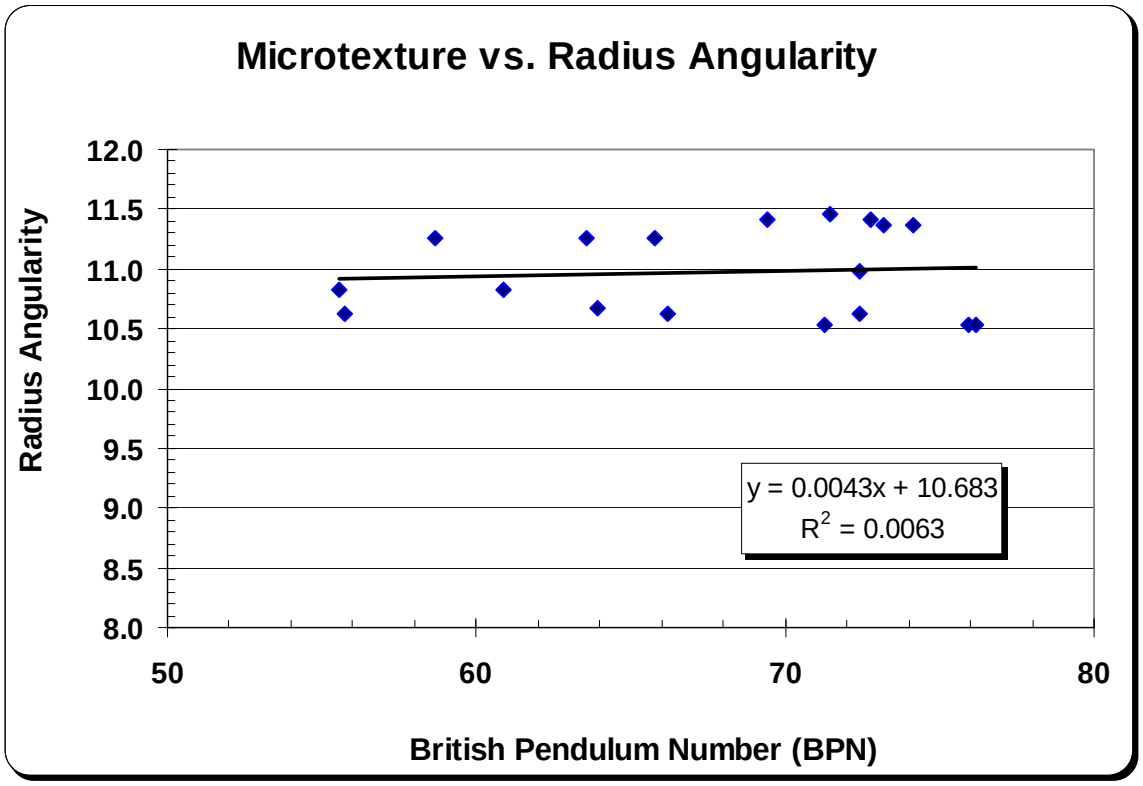

Figure 49. Relationship of Radius Angularity to Microtexture

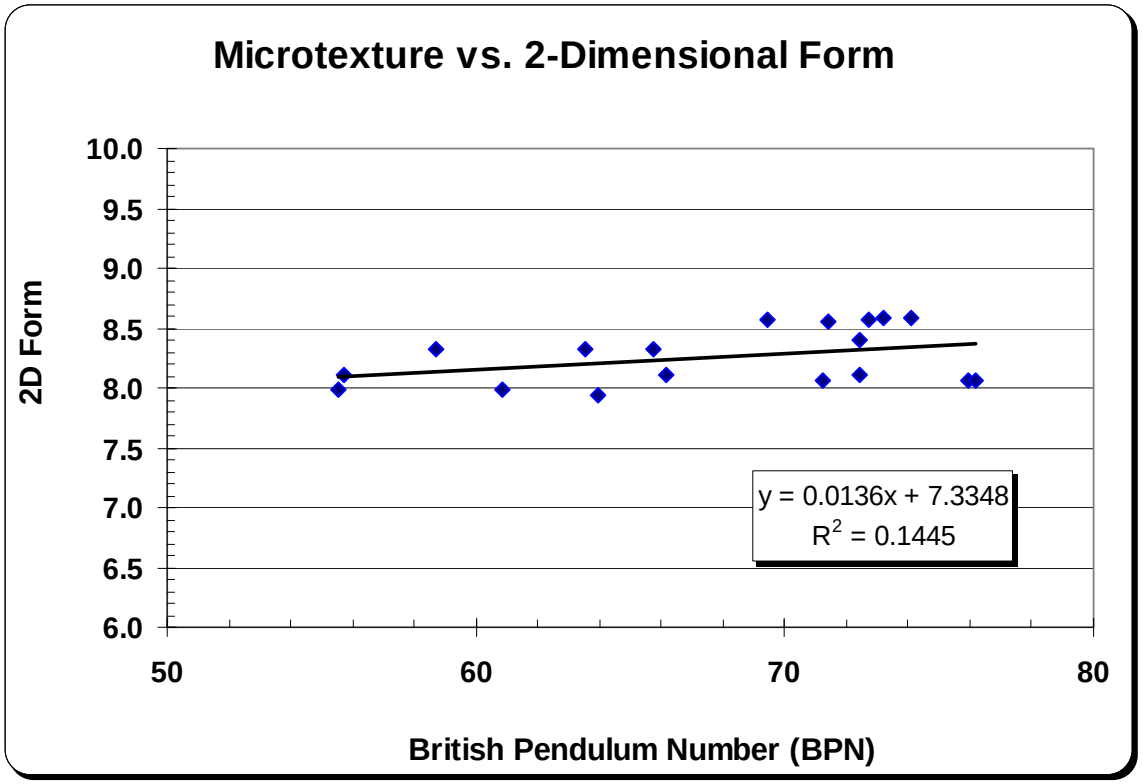

Figure 50. Relationship of Two-Dimensional Shape to Microtexture

Overall, microtexture measurements were relatively insensitive to aggregate texture and shape. The most influential parameter on microtexture was gradient angularity index, in which the R^2 was over 28 percent. While this was certainly not a strong relationship, the trend of increasing microtexture with increasing angularity was present.

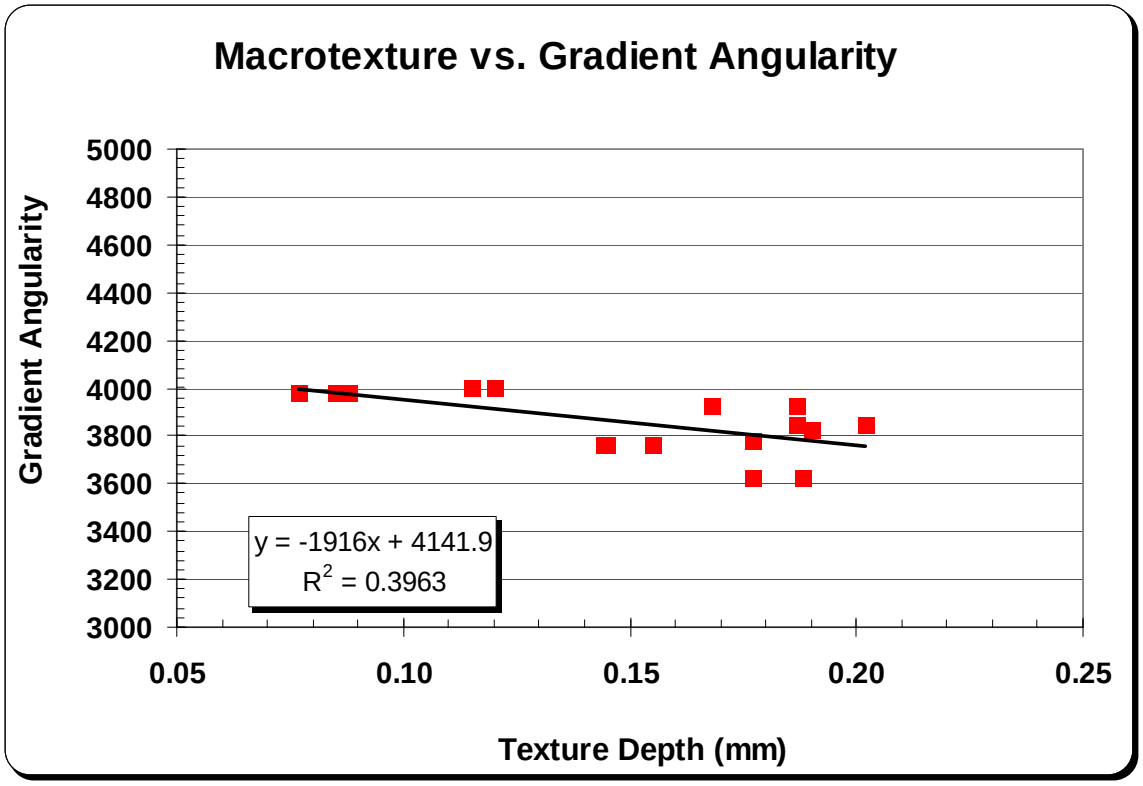

Figure 51. Relationship of Gradient Angularity to Macrotexture

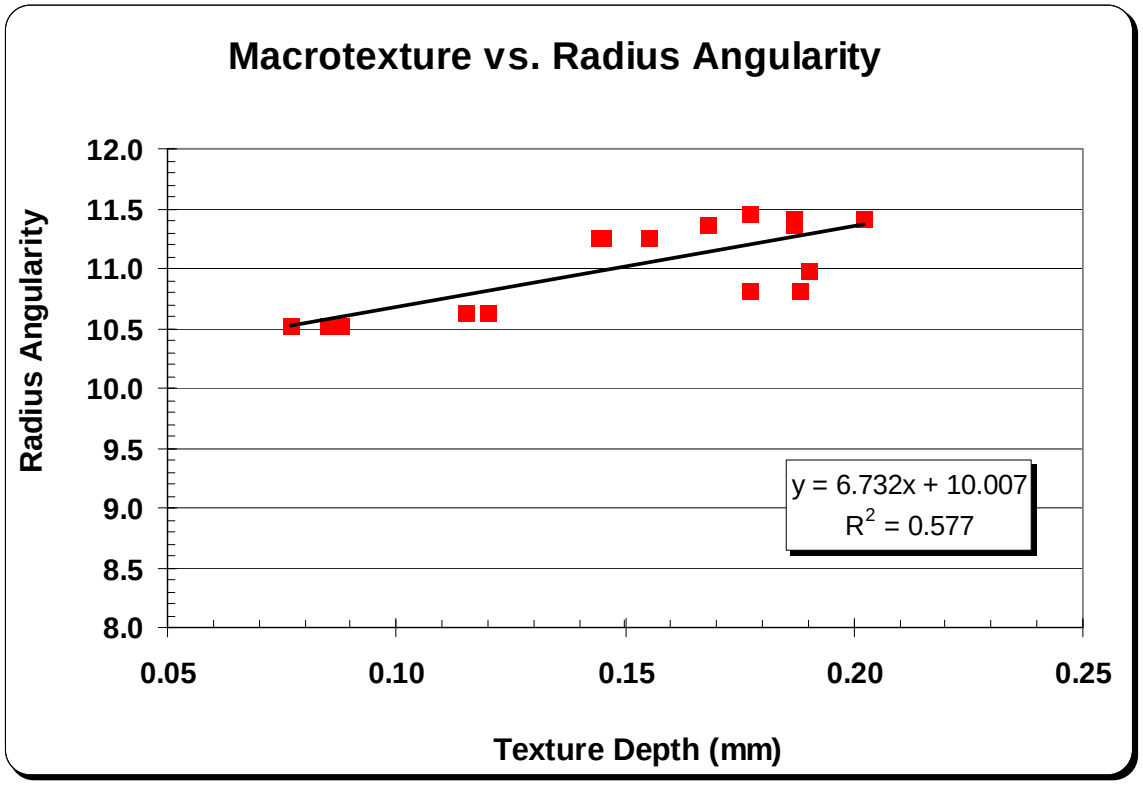

Figure 52. Relationship of Radius Angularity to Macrotexture

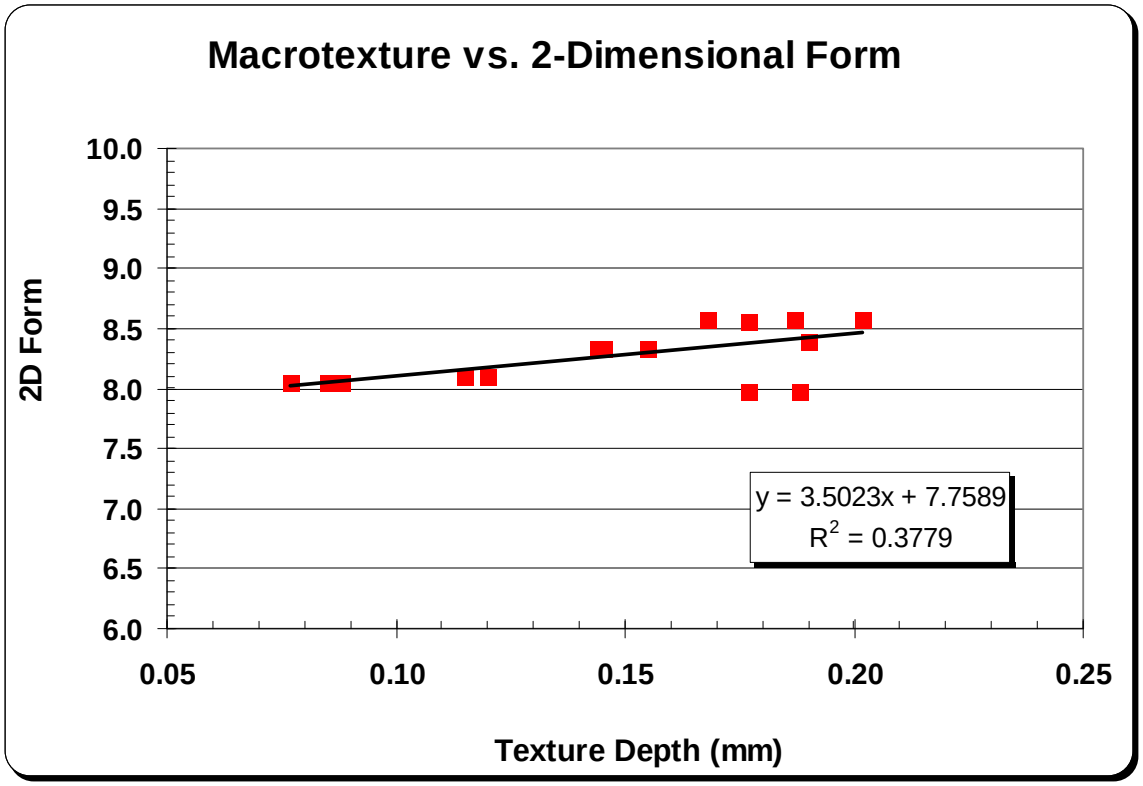

Figure 53. Relationship of Two-Dimensional Shape to Macrotexture

Macrotexture appeared to be most influenced by the radius gradient index, such that almost 60 percent of the variability in MTD could be explained by changes in measured texture. Specifically, a higher radius gradient provided greater macrotexture. Thus, aggregate particles having greater angularity are likely to possess greater texture depths. Overall, macrotexture measurements were more sensitive to changes in shape and texture than microtexture.

Combined Effects of Aggregate and Mixture Properties

While the single regression process provided some insight as to the relationships of mixture and aggregate features to microtexture and macrotexture, a more realistic analysis should combine a number of factors to assess the cumulative effects. Multivariate linear regression procedures were used to determine how well the known mixture and aggregate parameters related to skid resistance, what combinations of factors provided the best correlations, and which properties should be used for the purpose of predicting pavement skid resistance. Table 19 provides a summary of the analyses regarding microtexture.

First, all available parameters were used to determine the most complete relationship of all involved factors. However, two problems existed in this process; 1) the dataset was not sufficient to provide for a full rank model of this size, and 2) a significant number of factors were interrelated, resulting in a problem with multicollinearity. Thus, a number of selection procedures were employed to reduce the number of terms in the model while maintaining the highest possible correlation. These selection techniques were applied simultaneously to all parameters, separately for mixture properties, separately for

aggregate properties, and separately for the aggregate shape parameters measured by the AIMS device.

Coefficients of determination were used to judge the adequacy of model selection techniques, and are also reported in Table 19. The R^2 value indicated the proportion of variability in the dataset that could be explained by the model that included a particular subset of parameters. As the number of parameters in a model increases, the chance for error increases, and the effective R2 is reduced. This reduced R^2, or adjusted R^2 (R^2_{adj}), is the coefficient of determination which accounts for the number of parameters included in the model. An additional reduction should be taken if the model is to be used for predictive purposes. This type of coefficient (R^2_{pred}) describes the ability of the model to predict values based on future data. In other words, the existing dataset may be adequately described by a given model with some level of accuracy, but the ability of the model to accurately *predict a future response* (i.e., a new dataset) should also be considered.

	All Variables				Mix Properties				Aggregate Properties				AIMS	
DP					X		X							
Pbe	X				X			X						
VMA	X		X		X									
VFA	X	X		X	X	X	X	X						
Pb	X				X		X	X						
PDNini	X		X		X	X		X						
FT	X			X	X		X	X						
FAA	X		X						X					
MICROD	X			X					X		X			
SSULFS	X								X		X	X		
P8	X	X	X						X	X				
P16	X		X						X		X			
P30	X		X						X		X			
P50	X								X		X	X		
P100	X		X						X					
P200	X								X		X			
FM	X	X	X						X	X	X			
Gsb	X								X		X	X		
Gse	X			X					X					
GradAng	X			X					X			X	X	
RadAng	X								X				X	X
2Dform	X								X			X	X	X
R^2	0.97	0.76	0.90	0.85	0.78	0.57	0.71	0.73	0.74	0.71	0.74	0.74	0.56	0.54
R^2_{adj}	0.41	0.71	0.81	0.78	0.63	0.51	0.62	0.62	0.36	0.67	0.51	0.63	0.46	0.48
R^2_{pred}	NA	0.59	0.23	0.58	0.33	0.40	0.42	0.37	0.03	0.55	0.10	0.35	0.21	0.37

Table 19. Summary of Results for Factor Selection Process - Microtexture

In general, relationships of the various combinations of parameters and microtexture were poor. A couple of relationships displayed reasonably high R^2 values, but were not

acceptable for predictive purposes. Overall, combinations of mixture and aggregate characteristics appeared to have the most significant effects on microtexture. It was also noted that several subsets of factors could be combined to produce similar levels of correlation. Thus, no particular set of properties was identified as having a significant relationship to microtexture. Also, lack of fit was significant in a number of cases.

The same series of regression techniques were applied to the macrotexture data, and the results are shown in Table 20.

	All Variables				Mix Properties				Aggregate Properties				AIMS	
DP	X				X		X	X						
Pbe	X				X									
VMA	X		X		X	X	X	X						
VFA	X				X	X	X	X						
Pb	X				X	X								
PDNini					X			X						
FT					X		X	X						
FAA	X	X	X	X					X			X		
MICROD	X		X	X					X					
SSULFS	X		X						X		X			
P8									X	X	X			
P16	X	X	X						X	X	X			
P30	X	X	X						X			X		
P50	X	X	X						X		X			
P100	X		X						X					
P200	X		X	X					X		X			
FM	X		X						X		X			
Gsb	X	X	X	X					X			X		
Gse	X		X						X	X	X			
GradAng	X		X						X	X			X	X
RadAng	X		X						X				X	
2Dform	X		X	X					X			X	X	X
R^2	0.99	0.98	0.99	0.98	0.76	0.68	0.67	0.75	0.99	0.97	0.99	0.98	0.83	0.78
R^2_{adj}	0.94	0.97	0.98	0.98	0.56	0.60	0.54	0.62	0.97	0.96	0.97	0.97	0.78	0.75
R^2_{pred}	NA	0.96	0.98	0.96	NA	0.42	0.38	0.28	0.96	0.93	0.92	0.94	0.70	0.66

Table 20. Summary of Results for Factor Selection Process - Macrotexture

The relationships of mixture and aggregate properties to macrotexture were much stronger, as evidenced by the higher R^2 values. Also, it was apparent that aggregate properties alone were better able to model macrotexture than mixture properties; although the AIMS data was not sufficient to model macrotexture without the assistance of other aggregate properties. The most promising relationship (as shown in Table 20) includes the parameters of fine aggregate angularity, percent passing the #30 (0.600mm) sieve, bulk specific gravity of the aggregate blend, and AIMS two-dimensional form. This relationship possessed the least influence by interrelated factors, and provided excellent R^2 values, both adjusted and predictive. It was noted that a number of factor combinations were able to produce similar correlations, and thus,

a large number of aggregate characteristics were believed to have significant influence over macrotexture.

Microtexture and Macrotexture

According to the available literature and general principles, microtexture and macrotexture are both necessary for the provision of adequate skid resistance. Thus, any measures available should be taken to increase both. Increases in microtexture may be achieved by reducing the aggregate particle size as well as the distance between particles, yet both of these adjustments to a mixture would create a decrease in macrotexture. Increases in macrotexture are beneficial to overall skid resistance at high speeds, and texture depth may be increased by coarsening the aggregate structure and extending the separation between particles. Greater macrotexture generates larger void spaces at the surface of the pavement, which reduces the effective contact area of the vehicle tire with the roadway – causing a reduction in microtexture. In Figure 54, macrotexture is plotted as a function of microtexture. Although a large amount of scatter was present in the data, the general trend of decreasing texture depth with increasing BPN was evident. Thus, maximizing both components of skid resistance is not advisable. A balanced approach is more appropriate.

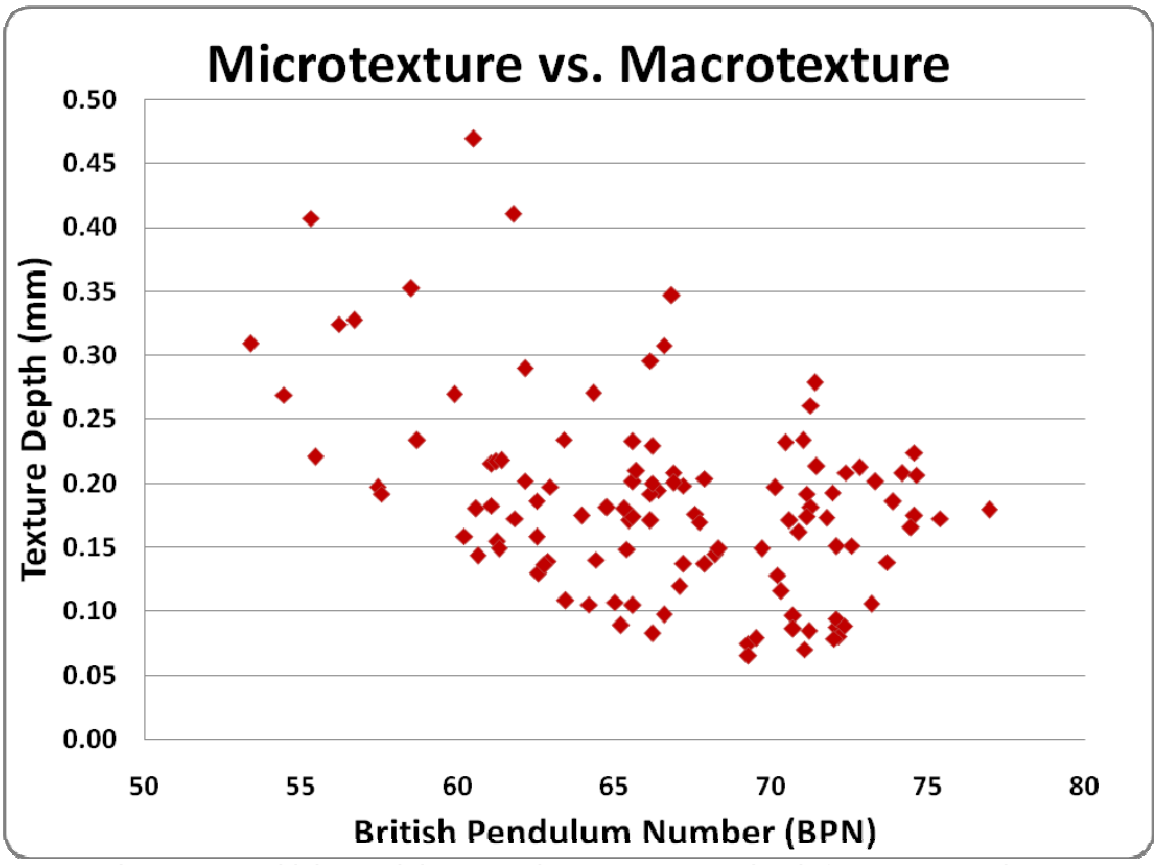

Figure 54. British pendulum Number vs. Texture depth for 4.75mm Mixes

Comparison with Traditional Surface Mixes

At the time of the research project, no 4.75mm mixes had been placed in the state of Arkansas, and thus no field study could be performed in order to validate the findings of the laboratory study. Therefore, a relative comparison of laboratory performance was used to imply the relative field performance of the various nominal maximum aggregate size (NMAS) mixes.

In order to provide a relative comparison of skid resistance, laboratory-compacted specimens of typical surface mixes were prepared and tested. These mixes had NMAS values of 9.5mm and 12.5mm, and were similar to the 4.75mm mixes in terms of aggregate composition. The 9.5mm and 12.5mm mixes were designed at 4.5 percent air voids and 100 design gyrations. Six specimens were prepared for each NMAS from each aggregate source.

Microtexture

Four replicate microtexture tests were performed for each sample. A summary of the BPT results for the larger NMAS mixes, including mean, standard deviation, and coefficient of variation, are given in Table 21. Two samples from the sandstone/gravel source were damaged prior to testing, and were excluded from the analysis.

NMAS	Aggregate Source	Sample #	Side	BPN Mean	BPN Stdev	BPN COV(%)
9.5	LS	1	Bottom	59.88	0.78	1.30
9.5	LS	1	Top	64.31	3.58	5.57
9.5	LS	2	Bottom	57.44	3.78	6.58
9.5	LS	2	Top	57.56	2.41	4.19
9.5	LS	3	Bottom	67.69	2.98	4.41
9.5	LS	3	Top	58.69	3.64	6.21
9.5	LS	4	Bottom	65.56	2.42	3.69
9.5	LS	4	Top	61.06	2.73	4.46
9.5	LS	5	Bottom	71.25	3.99	5.61
9.5	LS	5	Top	66.19	5.74	8.68
9.5	LS	6	Bottom	70.44	2.66	3.77
9.5	LS	6	Top	66.56	4.39	6.59
9.5	SG	1	Bottom	excl	excl	excl
9.5	SG	1	Top	excl	excl	excl
9.5	SG	2	Bottom	excl	excl	excl
9.5	SG	2	Top	excl	excl	excl
9.5	SG	3	Bottom	62.13	1.75	2.82
9.5	SG	3	Top	66.88	1.80	2.69
9.5	SG	4	Bottom	74.56	1.38	1.84
9.5	SG	4	Top	75.38	0.97	1.28
9.5	SG	5	Bottom	69.69	5.55	7.96
9.5	SG	5	Top	67.06	5.70	8.50
9.5	SG	6	Bottom	74.63	3.65	4.90
9.5	SG	6	Top	73.31	6.72	9.16
9.5	SY	1	Bottom	63.44	2.63	4.14
9.5	SY	1	Top	70.13	3.51	5.01
9.5	SY	2	Bottom	66.88	3.07	4.59
9.5	SY	2	Top	64.19	2.33	3.63

9.5	SY	3	Bottom	65.56	2.84	4.33
9.5	SY	3	Top	68.31	1.03	1.51
9.5	SY	4	Bottom	67.88	2.89	4.26
9.5	SY	4	Top	65.31	3.35	5.13
9.5	SY	5	Bottom	67.56	1.95	2.89
9.5	SY	5	Top	65.00	4.13	6.35
9.5	SY	6	Bottom	62.75	4.88	7.77
9.5	SY	6	Top	66.19	4.30	6.50
12.5	LS	1	Bottom	56.69	5.81	10.25
12.5	LS	1	Top	64.81	3.31	5.10
12.5	LS	2	Bottom	55.31	5.15	9.31
12.5	LS	2	Top	63.13	3.75	5.94
12.5	LS	3	Bottom	56.19	3.77	6.70
12.5	LS	3	Top	66.81	3.31	4.95
12.5	LS	4	Bottom	55.44	2.51	4.53
12.5	LS	4	Top	68.44	3.39	4.95
12.5	LS	5	Bottom	54.44	5.49	10.08
12.5	LS	5	Top	58.06	4.79	8.25
12.5	LS	6	Bottom	53.38	4.59	8.61
12.5	LS	6	Top	63.88	5.24	8.20
12.5	SG	1	Bottom	61.19	2.86	4.67
12.5	SG	1	Top	69.19	3.91	5.65
12.5	SG	2	Bottom	58.50	1.54	2.63
12.5	SG	2	Top	67.31	1.98	2.95
12.5	SG	3	Bottom	62.94	2.86	4.54
12.5	SG	3	Top	70.56	2.20	3.12
12.5	SG	4	Bottom	71.38	5.32	7.45
12.5	SG	4	Top	68.31	8.07	11.81
12.5	SG	5	Bottom	60.50	5.13	8.48
12.5	SG	5	Top	58.00	4.27	7.36
12.5	SG	6	Bottom	61.75	3.80	6.15
12.5	SG	6	Top	61.94	2.15	3.48
12.5	SY	1	Bottom	61.38	2.78	4.53
12.5	SY	1	Top	63.06	3.86	6.12
12.5	SY	2	Bottom	62.13	1.75	2.82
12.5	SY	2	Top	65.25	1.58	2.42
12.5	SY	3	Bottom	66.13	4.22	6.38
12.5	SY	3	Top	62.31	2.29	3.68
12.5	SY	4	Bottom	66.81	4.65	6.96
12.5	SY	4	Top	61.56	3.89	6.32
12.5	SY	5	Bottom	66.13	4.63	7.00
12.5	SY	5	Top	57.94	0.83	1.43
12.5	SY	6	Bottom	63.38	4.28	6.76
12.5	SY	6	Top	61.88	4.30	6.96

Table 21. Summary of BPT Results for 9.5mm and 12.5mm Samples

For the 9.5mm mixes, BPN values ranged from 57.44 to 75.38, having an average of 66.36. The average standard deviation was 3.24, and the average COV was 4.88

percent. The BPN values for the 12.5mm mixes ranged from 53.38 to 71.38, with an overall average 62.39. The average standard deviation was 3.73 and the average COV was 6.01. These values indicate a reasonably low level of variability within the test method.

The effect of compaction side (i.e., top vs. bottom) was evaluated for each NMAS using ANOVA techniques. Compaction side was not statistically significant for the 9.5mm NMAS, but it was significant for the 12.5mm mixes, as was reported in the Canadian study. *(5)* Overall, compaction side was not significant for the 4.75mm or 9.5mm samples, but was for the 12.5mm samples. Thus, larger aggregate sizes were believed to be more susceptible to particle fracture during SGC compaction. Due to this significance, the top side BPN results for the 12.5mm mixes (which have been reported to exhibit unrealistically high BPN values) were removed from the dataset.

Next, an ANOVA was performed to determine whether the effect of NMAS on microtexture was statistically significant. The results of this analysis are given in Table 22, and a graphical comparison of average microtexture for each NMAS by aggregate source is shown in Figure 55.

Factor	df	F-calc	P-value
NMAS	2	70.27	**<0.0001**
Aggregate Source	2	104.63	**<0.0001**
Error	255		

Table 22. ANOVA Results – Effects of NMAS on BPT

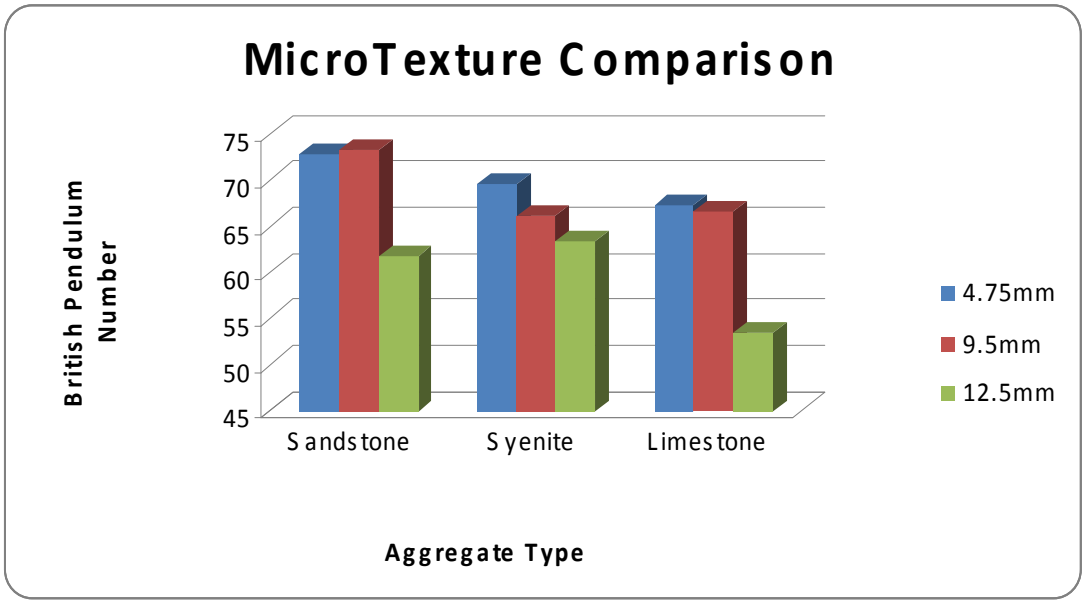

Figure 55. Effect of Nominal Maximum Aggregate Size on Microtexture

In terms of microtexture, NMAS was significant. In fact, the differences in the three NMAS values were statistically significant, meaning that the 4.75mm mixes displayed the greatest microtexture, the 9.5mm mixes displayed significantly less microtexture, and the 12.5mm mixtures possessed significantly less microtexture than either the 4.75mm or 9.5mm mixes. For all aggregate sources, the 12.5mm mixes possess the least amount of microtexture, with the greatest differences exhibited for the limestone aggregate source. Although no design criteria currently exists for BPN, 12.5mm mixtures are routinely used as surface mixes and lack of microtexture has not been reported as a common problem. Since the 4.75mm mixes were obviously the better performers, it was concluded that 4.75mm mixtures clearly possess adequate microtexture.

Macrotexture

A similar analysis was performed to provide a comparison of macrotexture for the various NMAS values. Triplicate measures of texture depth were performed for each sample. Table 23 provides a summary of the macrotexture data collected for the 9.5mm and 12.5mm samples. Average values for texture depth, standard deviation, and coefficient of variation are presented. Again, two samples were excluded from the analysis due to sample damage.

NMAS	Aggregate Source	Sample #	Side	MTD Mean	MTD Std. Dev.	MTD COV (%)
9.5	LS	1	Bottom	0.270	0.006	2.11
9.5	LS	1	Top	0.270	0.005	1.75
9.5	LS	2	Bottom	0.197	0.005	2.56
9.5	LS	2	Top	0.192	0.009	4.44
9.5	LS	3	Bottom	0.170	0.006	3.25
9.5	LS	3	Top	0.234	0.010	4.07
9.5	LS	4	Bottom	0.233	0.006	2.76
9.5	LS	4	Top	0.215	0.007	3.09
9.5	LS	5	Bottom	0.261	0.008	2.89
9.5	LS	5	Top	0.229	0.009	3.73
9.5	LS	6	Bottom	0.232	0.003	1.32
9.5	LS	6	Top	0.308	0.007	2.11
9.5	SG	1	Bottom	excl	excl	excl
9.5	SG	1	Top	excl	excl	excl
9.5	SG	2	Bottom	excl	excl	excl
9.5	SG	2	Top	excl	excl	excl
9.5	SG	3	Bottom	0.202	0.007	3.47
9.5	SG	3	Top	0.208	0.004	2.00
9.5	SG	4	Bottom	0.224	0.006	2.68
9.5	SG	4	Top	0.173	0.007	3.77
9.5	SG	5	Bottom	0.149	0.006	3.74
9.5	SG	5	Top	0.119	0.005	3.96
9.5	SG	6	Bottom	0.207	0.007	3.22
9.5	SG	6	Top	0.201	0.008	3.73

9.5	SY	1	Bottom	0.108	0.007	6.01
9.5	SY	1	Top	0.197	0.007	3.39
9.5	SY	2	Bottom	0.201	0.006	3.16
9.5	SY	2	Top	0.105	0.005	4.78
9.5	SY	3	Bottom	0.105	0.007	6.25
9.5	SY	3	Top	0.149	0.003	2.32
9.5	SY	4	Bottom	0.204	0.007	3.27
9.5	SY	4	Top	0.180	0.005	2.79
9.5	SY	5	Bottom	0.176	0.005	2.95
9.5	SY	5	Top	0.107	0.008	7.06
9.5	SY	6	Bottom	0.136	0.005	3.89
9.5	SY	6	Top	0.200	0.008	3.77
12.5	LS	1	Bottom	0.328	0.003	0.93
12.5	LS	1	Top	0.576	0.005	0.80
12.5	LS	2	Bottom	0.407	0.007	1.67
12.5	LS	2	Top	0.598	0.009	1.44
12.5	LS	3	Bottom	0.324	0.007	2.10
12.5	LS	3	Top	0.406	0.006	1.37
12.5	LS	4	Bottom	0.221	0.010	4.32
12.5	LS	4	Top	0.358	0.005	1.48
12.5	LS	5	Bottom	0.269	0.005	1.93
12.5	LS	5	Top	0.460	0.008	1.63
12.5	LS	6	Bottom	0.309	0.007	2.27
12.5	LS	6	Top	0.449	0.005	1.12
12.5	SG	1	Bottom	0.217	0.005	2.13
12.5	SG	1	Top	0.473	0.002	0.49
12.5	SG	2	Bottom	0.352	0.011	3.01
12.5	SG	2	Top	0.379	0.008	2.05
12.5	SG	3	Bottom	0.197	0.005	2.39
12.5	SG	3	Top	0.477	0.006	1.35
12.5	SG	4	Bottom	0.279	0.006	2.00
12.5	SG	4	Top	0.318	0.010	3.03
12.5	SG	5	Bottom	0.469	0.008	1.63
12.5	SG	5	Top	0.301	0.006	1.94
12.5	SG	6	Bottom	0.411	0.008	1.86
12.5	SG	6	Top	0.240	0.011	4.42
12.5	SY	1	Bottom	0.218	0.009	3.97
12.5	SY	1	Top	0.284	0.004	1.47
12.5	SY	2	Bottom	0.290	0.007	2.26
12.5	SY	2	Top	0.310	0.005	1.53
12.5	SY	3	Bottom	0.171	0.005	3.09
12.5	SY	3	Top	0.147	0.003	2.08
12.5	SY	4	Bottom	0.347	0.004	1.15

12.5	SY	4	Top	0.231	0.005	2.04
12.5	SY	5	Bottom	0.296	0.007	2.25
12.5	SY	5	Top	0.206	0.004	1.75
12.5	SY	6	Bottom	0.234	0.005	1.96
12.5	SY	6	Top	0.166	0.004	2.17

Table 23. Summary of MTD Results for 9.5mm and 12.5mm Samples

Measures of macrotexture for the 9.5mm mixes ranged from 0.105mm to 0.308mm, and had a grand average of 0.193mm. The average standard deviation was 0.006, and the average COV was 3.45 percent, which is an acceptable level of testing variability. The 12.5mm mixes had MTD values ranging from 0.147 to 0.598 with an overall average of 0.326. The average standard deviation and average COV were 0.006 and 2.03 percent, respectively.

The effect of compaction side was also evaluated for the macrotexture of the 9.5mm and 12.5mm mixes. As was the case for microtexture, the 9.5mm mixes were not sensitive to compaction side, but the 12.5mm mixes were. Although previous research had indicated that macrotexture of the top side of gyratory-compacted samples more closely matched field values, bottom side values were lower, and thus more conservative. The top side data was removed from the 12.5mm dataset, and only the data corresponding with the bottom of the samples was used.

An ANOVA procedure was performed in order to determine the statistical significance of NMAS on macrotexture. The results of the ANOVA are shown in Table 24, and an average macrotexture comparison is illustrated in Figure 56.

Factor	**df**	**F-calc**	**P-value**
NMAS	2	256.10	**<0.0001**
Aggregate Source	2	95.86	**<0.0001**
Error	255		

Table 24. ANOVA Results – Effects of NMAS on MTD

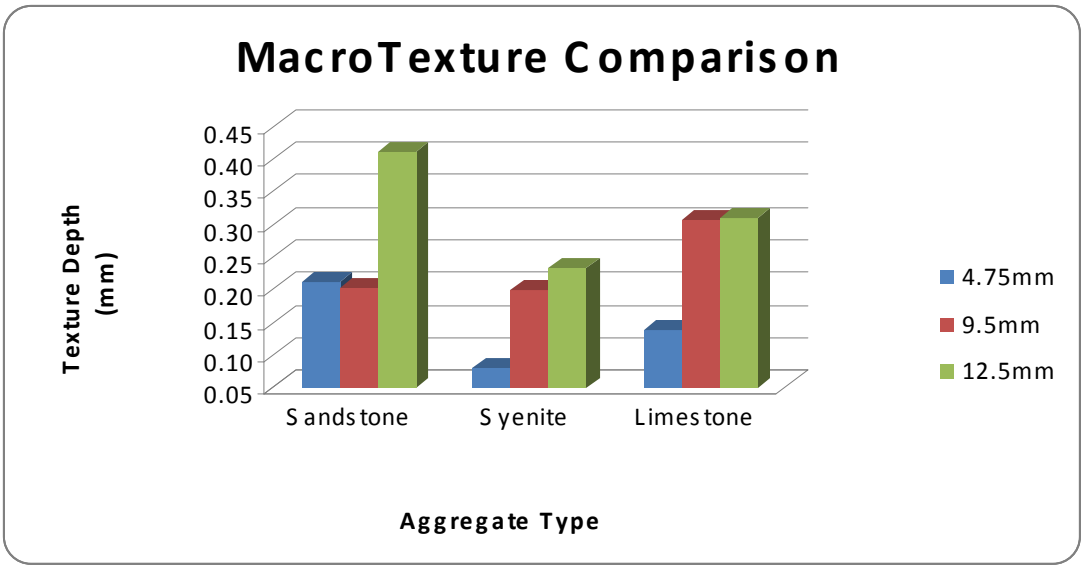

Figure 56. Effect of Nominal Maximum Aggregate Size on Macrotexture

In terms of macrotexture, NMAS was significant such that no two NMAS values were statistically similar. Aggregate source was also significant. In general, the LS and SG mixes were similar, but the macrotexture of the SY mixes was significantly lower.

For all aggregate sources, the 12.5mm mixes were the best performers, and possessed a texture depth that was significantly greater than that of the 4.75mm mixes. On average, the 12.5mm mixes possessed about twice the texture depth of the 4.75mm mixes, which is consistent with the ratio of NMAS. This conclusion was not unexpected, but is important to consider when designing a 4.75mm mixture for a relatively high speed roadway. Roadway geometry for 4.75mm mix applications should include grades and cross-slopes that facilitate the removal of water.

As noted previously, the texture depths measured in this research were lower than those published in the available literature. However, this was likely due to the variation in the types of mixes tested and the use of a modified laboratory procedure for this study. By and large, 12.5mm NMAS mixes are known to possess adequate skid resistance for high-speed roadways. Thus, conclusions regarding these measurements were based on a relative comparison to the 12.5mm mixes rather than to texture depths reported by others.

Field Testing

Near the end of the study, one 4.75mm mixture was constructed using the syenite aggregate source, and a very limited amount of microtexture testing was performed according to the BPT. At the time of construction, six laboratory-compacted samples and 6 field testing locations were tested. The results are shown in Table 25.

Laboratory-compacted specimens		**Field-compacted specimens**	
BPT Values		BPT Values	
66.6	Average 67.5	69.5	Average 68.3
65.0		81.5	
68.8	Standard Deviation 2.31	76.5	Standard Deviation 9.21
71.3		62.5	
67.6	Coefficient of Variation (%) 3.4	61.5	Coefficient of Variation (%) 13.5
65.5		58.3	

Table 25. BPT Results for Laboratory-Compacted and Field-Compacted 4.75mm Mix

The average BPN values for each sample set were similar, and had less than 1 BPN unit difference. The field tests in this comparison exhibited slightly greater microtexture. However, there was approximately 4 times more variability present in the field data than the laboratory data. Thus, laboratory and field measures of BPN may be similar, provided the sample size is sufficiently large.

Effects of Sample Conditioning

Samples were conditioned using the ERSA wheel-tracking machine in order to simulate the loss of microtexture over time. Triplicate BPT measurements were taken for the newly compacted samples, and then again after 50, 150, 650, 1650, and 6650 wearing cycles. The average results are plotted for each of the aggregate sources in Figure 57. In general, the samples exhibited most of the microtexture loss within the first 1000 – 2000 cycles, after which a fairly "steady-state" microtexture value was reached. On average, samples exhibited approximately five BPN units before reaching an asymptotic rate of loss, which was not affected by aggregate type.

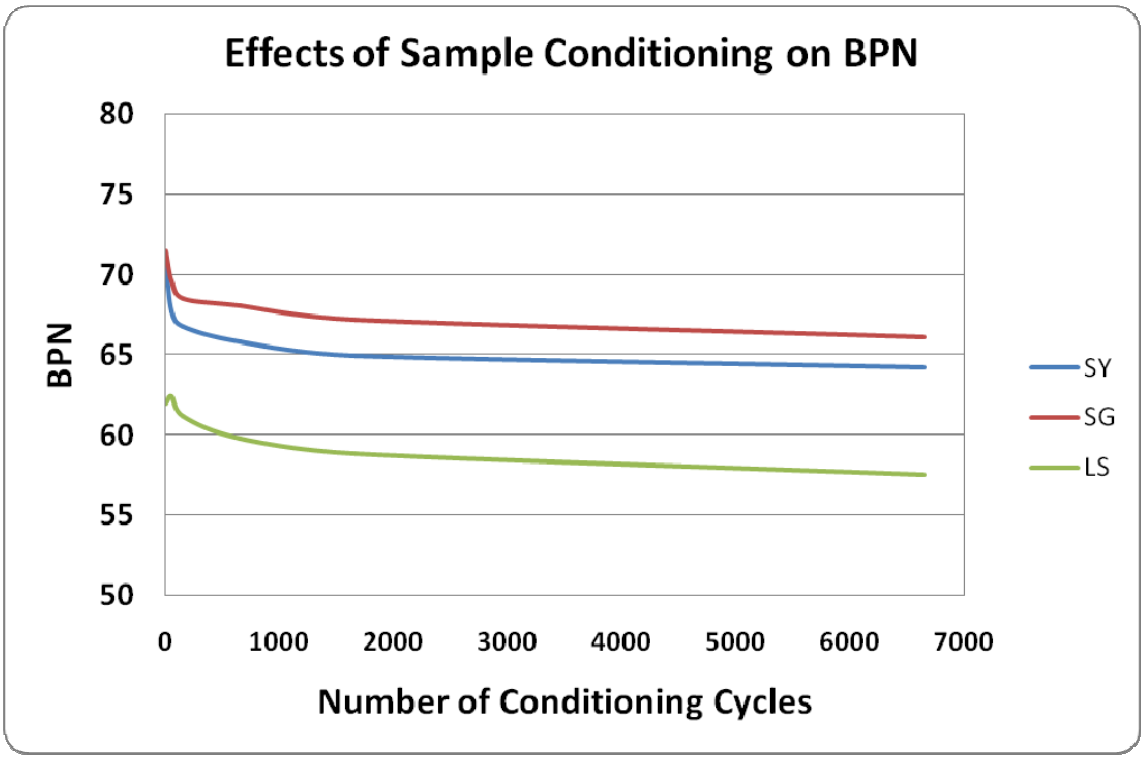

Figure 57. Effect of Specimen Conditioning on Microtexture

Hydroplaning

The drainage characteristics of a roadway are largely a function of the roadway geometry and surface characteristics. The ability of a vehicle to safely maneuver when water is present on the roadway is a function of many factors, including the depth of water, vehicle speed, tire tread, tire wear, and roadway surface characteristics. Wet skid resistance is often thought of as a resistance to hydroplaning, but hydroplaning is not the same as wet skidding. Hydroplaning occurs when the entire footprint of the vehicle tire is separated from the pavement, essentially removing all potential for skid resistance. Thus, pavement characteristics no longer play a factor in skid resistance. Roadway geometry and surface characteristics do, however, influence the amount of water on the roadway, which can lead to hydroplaning.

To compare 4.75mm and 12.5mm mixes relative to depths of water present on a roadway, an analysis was conducted to model the change in depth of water during a storm over time. Several assumptions were made in modeling this relationship, but the general process involved the following steps.

First, rainfall intensities of 1 in/hr, 2 in/hr, and 3.5 in/hr were chosen. Next, two roadway geometries were assumed. The flat roadway was assumed to have a 1 percent cross-slope and a 0.5 percent grade. The steep roadway was assumed to have 2 percent cross-slope and a 7 percent grade. Runoff velocities were calculated according to Manning's equation, assuming a Manning's coefficient, n, of 0.013 for the 4.75mm mix and 0.015 for the 12.5mm mix. The perimeter value in the equation was taken to be the width of the driving lane (i.e., the width influencing the driving lane), and a value of 12 feet was used. Based on the rainfall intensity, the depth of accumulating water was calculated as a function of time. Simultaneously, the quantity of water leaving the roadway was determined. This quantity was determined as a function of velocity, which increases as depth increases. In essence, a running total of water on the roadway (i.e., water accumulated – water removed) was calculated for 1 second time increments. The time required for the available texture depth to become filled with water was also considered. Macrotexture values used were based on the values measured in this research; a value of 0.15mm was used for the 4.75mm mixes, and a value of 0.33mm was used for the 12.5mm mixes. The results were plotted as net depth of water in millimeters per time in seconds. The results for the 4.75mm mixes are presented in Figures 58, 59, and 60 for 1 in/hr, 2 in/hr, and 3.5in/hr rainfall intensities, respectively. Results for the 12.5mm mixes are presented in Figures 61, 62, and 63.

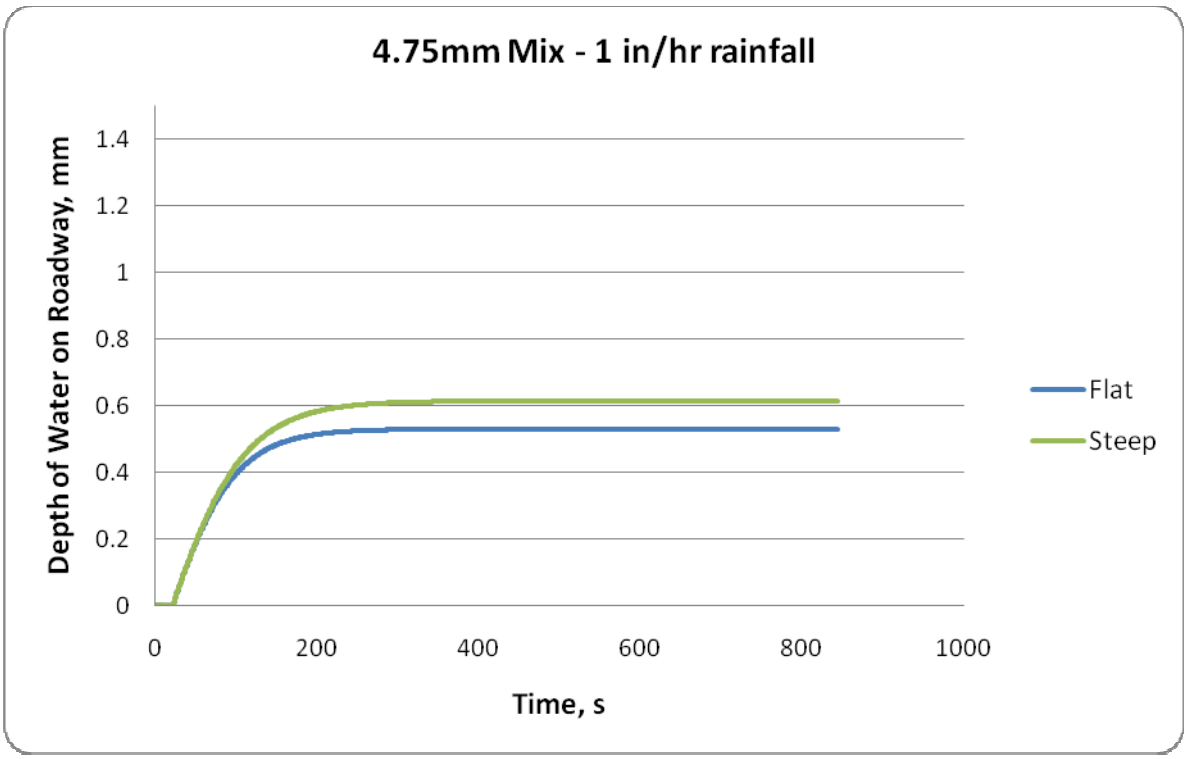

Figure 58. Net Depth of Water on Roadway vs. Time – 4.75mm Mix, Rainfall = 1 in/hr

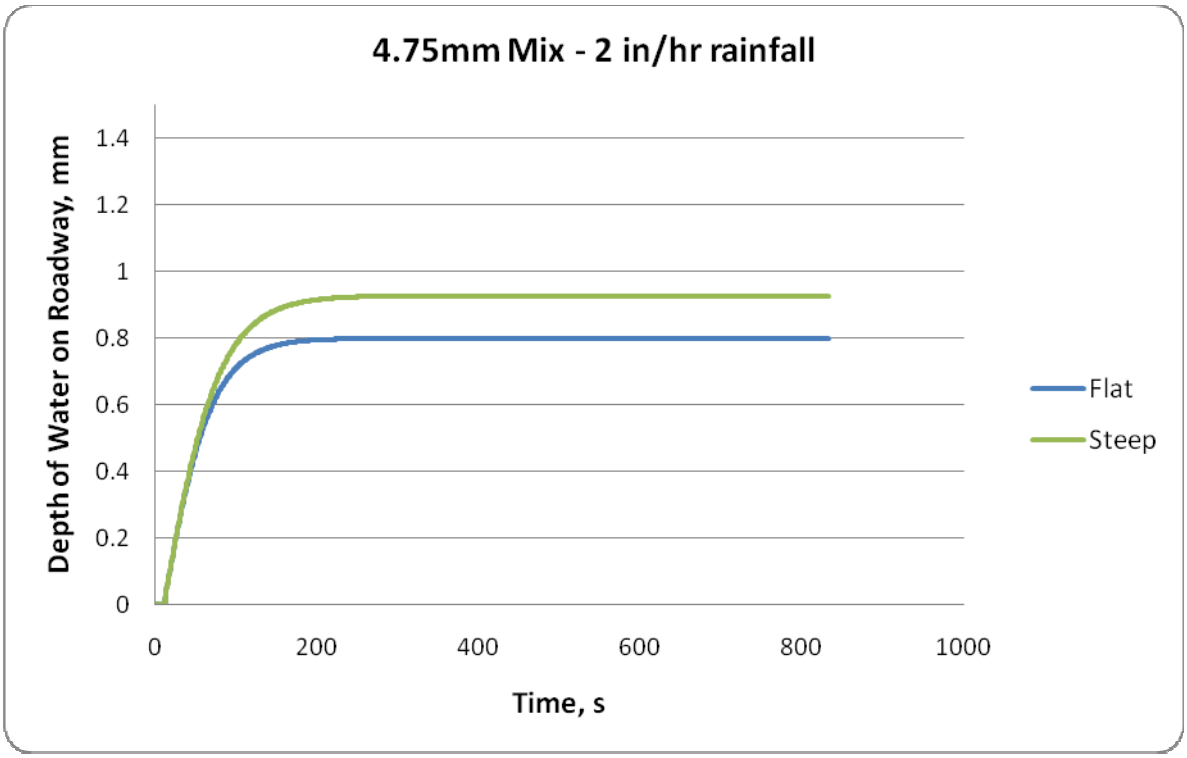

Figure 59. Net Depth of Water on Roadway vs. Time – 4.75mm Mix, Rainfall = 2 in/hr

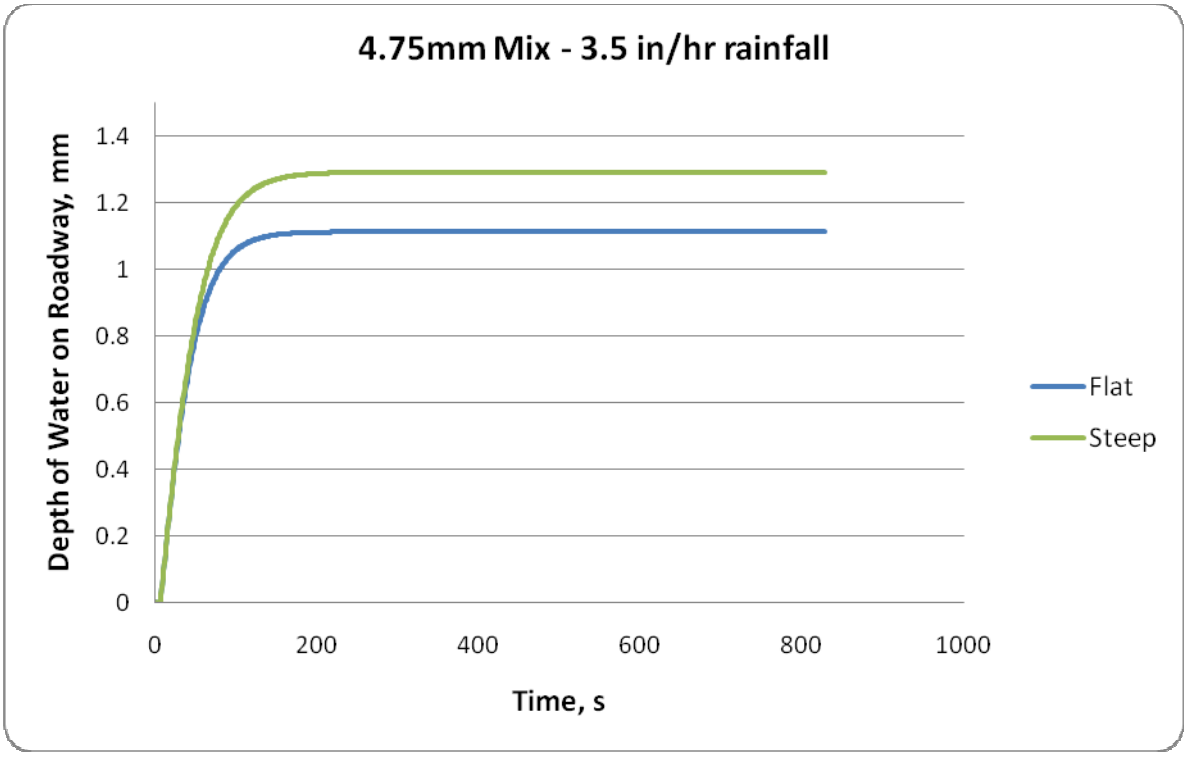

Figure 60. Net Depth of Water on Roadway vs. Time – 4.75mm Mix, Rainfall = 3.5 in/hr

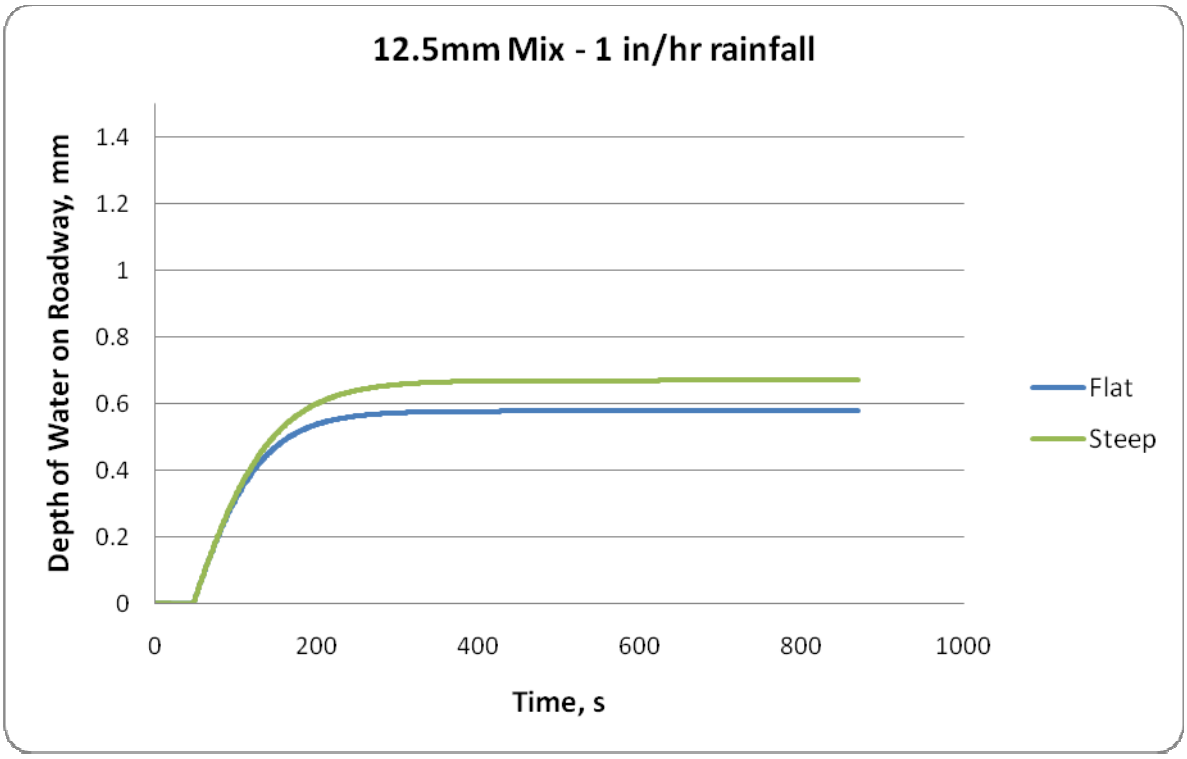

Figure 61. Net Depth of Water on Roadway vs. Time – 12.5mm Mix, Rainfall = 1 in/hr

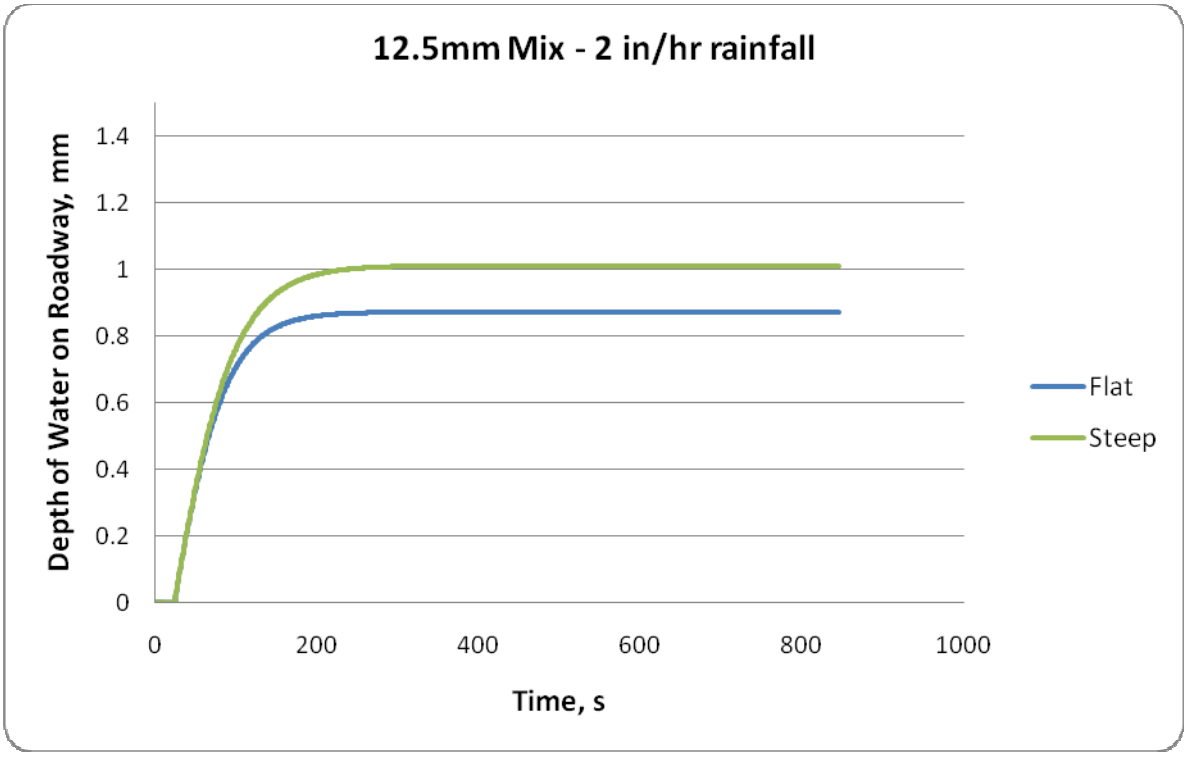

Figure 62. Net Depth of Water on Roadway vs. Time – 12.5mm Mix, Rainfall = 2 in/hr

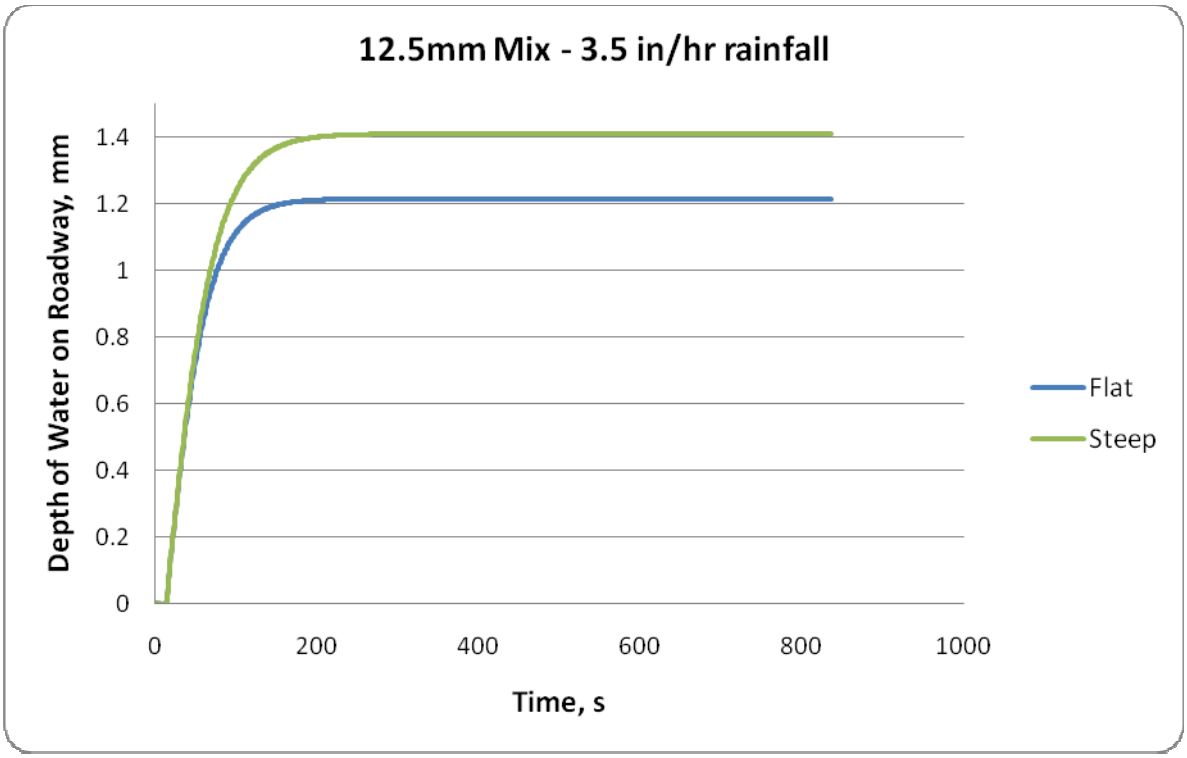

Figure 63. Net Depth of Water on Roadway vs. Time – 12.5mm Mix, Rainfall = 3.5 in/hr

For each graph, the depth of water on the roadway increases with time, then stabilizes at a maximum depth, with the steep roadway geometry holding 0.1 to 0.2 mm more water than the flat slopes. While a steep slope might be expected to shed water more quickly, it must be recognized that a steep grade creates a longer effective distance required for the water to traverse before leaving the traveled way, thereby increasing the overall quantity of water on the surface.

Interestingly, the 4.75mm mixtures appeared to have a lesser net water depth than the 12.5mm mixes, which is, in part, due to the values of Manning's coefficient assumed for each mix. The 4.75mm mixtures, however, reached the maximum net water depth in a shorter amount of time.

This analysis indicated that 4.75mm mixtures should have a maximum of approximately 0.8mm of water present on the roadway surface at any given time, but the ability of a vehicle to drive safely with this amount of water present depends on many other factors. This analysis was not intended to completely model the ability of a vehicle to maneuver safely on a wet surface. However, it does provide some insight as to the relative depth of water that could be present on the roadway surface. Further research is needed to more accurately model these interactions.

CONCLUSIONS AND RECOMMENDATIONS

The microtexture and macrotexture of 4.75mm NMAS mixtures from three aggregate sources were evaluated with respect to mix design parameters, mixture properties, and aggregate characteristics with the intention of determining specific steps that may be taken during mixture design to maximize the skid resistance of 4.75mm mixes. The skid resistance properties of the 4.75mm mixes were then compared to those of more traditional surface mixes having a NMAS of 9.5mm and 12.5mm. In addition, specimens were conditioned in order to estimate the long-term effects of traffic on microtexture. The following conclusions were made.

Mix Design

Eighteen 4.75mm mix designs were analyzed with respect to changes in design air void content and compaction level. Two measures of skid resistance (microtexture and macrotexture) were significantly impacted by changes in design air void content such that designing mixes at 4.5 percent air voids (rather than 6.0 percent) produced a slight increase in skid resistance. These increases were not felt to have practical significance, however, and no mix design changes for 4.75mm mixes were recommended.

Mixture Properties

A number of mix design properties were reviewed to assess their effects on microtexture and macrotexture, and linear regression techniques were used to determine the significance of any relationships. No mixture properties, whether used singly or in combination with other factors, were determined to be significant predictors of skid resistance. Some slight trends were observed.

- As percent density at $N_{initial}$ increased, microtexture decreased.
- As binder content increased, macrotexture increased.
- As dust proportion increased, macrotexture increased.
- Binder content, effective binder content, VMA, VFA, and dust proportion exhibited almost no correlation with microtexture.
- Film thickness, VFA, and percent density at $N_{initial}$ displayed virtually no relationship to macrotexture.

Aggregate Properties

Skid resistance was influenced to a much greater extent by aggregate properties than mixture properties. Test results by the Micro-Deval, sodium sulfate soundness, and fine aggregate angularity related to skid resistance as expected, such that as toughness, durability, and angularity increased, skid resistance also increased.

Aggregate gradation was determined to be one of the most influential factors on skid resistance. When measures of skid resistance were compared to the percent of aggregate blend passing each sieve, the correlation changed from negative to positive as sieve size decreased. This suggests that a gap-graded aggregate blend could prove

beneficial in generating additional microtexture and macrotexture. When all aggregate characteristics were considered simultaneously, the parameters of fine aggregate angularity, percent passing the #30 sieve, bulk specific gravity of the aggregate blend, and two-dimensional particle shape (as measured by the Aggregate Imaging System) were the most significant predictors of macrotexture.

Nominal Maximum Aggregate Size

Because no 4.75mm mixtures had been constructed in Arkansas at the time of the research project, adequate levels of skid resistance were based on a relative comparison with traditional surface mixes with a history of satisfactory skidding performance. When compared to 9.5mm and 12.5mm mixes, the 4.75mm mixes were superior in terms of microtexture. 12.5mm mixtures possessed the greatest levels of macrotexture, which were approximately twice that of the 4.75mm mixes. Specific comparisons were dependent upon aggregate type.

Field Testing

Late in the study, a 4.75mm mix was constructed in Arkansas. Limited data suggested that field and laboratory measures of microtexture by the British Pendulum Test were similar.

Sample Conditioning

In order to simulate the effects of wearing under traffic loadings, samples were conditioned using modified wheel on the ERSA wheel-tracking device. Periodically during the conditioning process, microtexture was measured. Most of the microtexture loss occurred during the first 1000 to 2000 conditioning cycles, then reached a relatively steady-state.

Hydroplaning

An analysis was performed to model the anticipated depth of water present on the roadway at a given time for various rainfall intensities. 12.5mm mixes were determined to generate greater maximum net water depths, but 4.75mm mixes reached maximum depths in a shorter time frame.

Recommendations

For low-speed roadways, microtexture is the critical feature of skid resistance, but as speed increases, macrotexture becomes increasingly important. Based on the results of this study, 4.75mm mixtures are recommended for use on low speed roadways as an efficient use of resources for maintenance and other applications. If used on high-speed roadways, roadway grade and cross-slope must be accurately constructed in order to ensure the adequate removal of water from the roadway during rain events.

REFERENCES

1. Williams, S.G., “Development of 4.75mm Superpave Mixes”, *Final Report, MBTC-2030*, University of Arkansas, May, 2006.
2. (Z) Smith, T.E., Chen, X., Song, W., and A. Hedfi, “Investigation of Skid Resistance of Hot-Mix-Asphalt-Surfaced Pavements in Maryland State Highway Network System”, *Proceedings CD from the 85th Annual Meeting of the Transportation Research Board*, Washington D.C., January, 2006.
3. Design Manual for Roads and Bridges, Pavement Design and Maintenance, Pavement Maintenance Assessment, Volume 7, Section 3, Part 1, HD 28/04, The Highways Agency, Scottish Executive, Welsh Assembly Government, The Department for Regional Development Northern Ireland, August 2004.
4. Woodward, W.D.H., Woodside, A.R., and J.H. Jellie, “Early and Mid Life SMA Skid Resistance”, *Proceedings, International Conference on Surface Friction, Christchurch*, New Zealand, May, 2005.
5. Goodman, S.N., Hassan, Y., and A.O. Abd El Halim, “Preliminary Estimation of Asphalt Pavement Frictional Properties from Superpave Gyratory Specimen and Mix Parameters”, *Transportation Research Record #1949*, Transportation Research Board, Washington, D.C., 2006.
6. Kuennen, T. “Creating Friction Where Rubber Meets the Road”, *Better Roads*, October, 2003.
7. Henry, J.J., “Evaluation of Pavement Friction Characteristics”, *NCHRP Synthesis 291,* National Cooperative Highway Research Program, Transportation Research Board, National Research Council, Washington, D.C., 2000.
8. Janoo, V.C., and C Horhonen, “Performance Testing of Hot-Mix Asphalt Aggregates”, *Special Report 99-20*, U.S. Army Corps of Engineers Cold Regions Research & Engineering Laboratory, December 1999.
9. Ergun, M.D., Agar, A., “Optimization of Road Surface Friction from Macro and Micro Texture Point of View”, *SURF 2000: Fourth International Symposium on Pavement Surface Characteristics on Roads and Airfields*, World Road Association, 2000.
10. McDaniel, R., and B.J. Coree, “Identification of Laboratory Techniques to Optimize Superpave HMA Surface Friction Characteristics”, *Phase I Final Report*, Purdue University / Indiana Department of Transportation JTRP, FHWA, Washington, D.C., 2003.
11. Kennedy, C.K, Young, A.E., and I.C. Butler, “Measurements of Skidding Resistance and Surface Texture and the Use of Results in the United Kingdom”, *Surface Characteristics of Roadways: International Research and Technologies*, ASTM STP 1031, American Society for Testing and Materials, Philadelphia, PA, 1990.
12. Specification for Skid Resistance Investigation and Treatment Selection, *TNZ T10:2002, SP/ST10:020821*, Transit New Zealand, 2002.

13. Flintsch, G.W., Luo, Y., and I.L. Al-Qadi, “Analysis of the Effect of Pavement Temperature on the Frictional Properties of Flexible Pavement Surfaces”, *Proceedings CD from the 84th Annual Meeting of the Transportation Research Board*, Washington D.C., January, 2005.
14. Mansour, F., and E. Amoosoltani, “Skid Resistance Assessment of Chip Seal Mixtures”, *Proceedings, International Conference on Surface Friction*, Christchurch, New Zealand, May, 2005.
15. Kulakowski, B.T., and D.W. Harwood, “Effect of Water-Film Thickness on Tire-Pavement Friction” *Surface Characteristics of Roadways: International Research and Technologies*”, ASTM STP 1031, American Society for Testing and Materials, Philadelphia, PA, 1990.
16. Owen, M.T., and J. Donbavand, “There’s a Fraction Too Little Friction”, *Proceedings, International Conference on Surface Friction*, Christchurch, New Zealand, May, 2005.
17. Hall, G., “Aggregate Characteristics Pertinent to Skid Resistance”, report prepared by Hall Consulting, P.L.L.C. Tulsa, Oklahoma, acquired 2004.
18. Liu, Y., Fwa, T.F., and Y.S. Choo, “Finite Element Modelling of Skid Resistance Test”, *ASCE Journal of Transportation Engineering*, Vol 129, No. 3, 2003.
19. Bullas, J.C., “Slippery When Dry? – Low Dry Friction and Binder-rich Road Surfaces”, *Proceedings, International Conference on Surface Friction*, Christchurch, New Zealand, May, 2005.
20. Bullas, J.C., and N. Hounsell, “Bituplaning: The Truth and the Friction Concerning Dry Friction and New Bituminous Road Surfaces”, *Proceedings, International Safer Roads Conference*, Cheltenham, England, May 2008.
21. Wambold, J.C., and J.J Henry, “NASA Wallops Tire/Runway Friction Workshops: 1993-2002”, *2450-BP-14 Final Report*, Montreal, Quebec, Canada, September, 2002.
22. Leu, M.C. and J.J. Henry, “Prediction of Skid Resistance as a Function of Speed from Pavement Texture”, *Transportation Research Record #946*, Transportation Research Board, National Research Council, Washington, D.C., 1983.
23. “Calculating International Friction Index of a Pavement Surface”, ASTM E1960, *Annual Book of ASTM Standards*, Volume 04.03, American Society for Testing and Materials, West Conshohocken, Pennsylvania, 2007.
24. “Standard Practice for Calculating Pavement Macrotexture Mean Profile Depth”, ASTM E1845, *Annual Book of ASTM Standards*, Volume 04.03, American Society for Testing and Materials, West Conshohocken, Pennsylvania, 2007.
25. Saito, K., Horiguchi, T., Kasahara, A., Abe, H., and J.J. Henry, “Development of Portable Tester for Measuring Skid Resistance and its Speed Dependency on Pavement Surfaces, *Transportation Research Record #1536*, Transportation Research Board, Washington, D.C., 1996.
26. Marek, C.R., “Review, Selection and Calibration of Accelerated Wear and Skid Resistance Testing Equipment, *Interim report – Phase 1*, Project IHR-406, Illinois

Cooperative Highway Research Program, University of Illinois at Urbana-Champaign, 1972.
27. Sullivan, B.W., "Development of a Fundamental Skid Resistance Asphalt Mix Design Procedure", *Proceedings, International Conference on Surface Friction*, Christchurch, New Zealand, May, 2005.
28. Vollor, T.W., and D.I. Hanson, "Development of Laboratory Procedure for Measuring Friction of HMA Mixtures – Phase I", *NCAT Report No. 06-06*, National Center for Asphalt Technology, Auburn, Alabama, 2006.
29. Woodward, W.D.H, Woodside, A.R., and Jellie, J.H., "Higher PSV and Other Aggregate Properties", *Proceedings, International Conference on Surface Friction, Christchurch*, New Zealand, May, 2005.
30. Fwa, T.F., Choo, Y.S., and Y. Liu, "Effect of Aggregate Spacing on Skid Resistance of Asphalt Pavement", *ASCE Journal of Transportation Engineering*, Vol. 129, No. 4, 2003.
31. Roe, P.G., and L. Caudwell, "Skid Resistance Policy in the UK – Where Did It Come From and Where Is It Going?", *Proceedings, International Safer Roads Conference*, Cheltenham, England, May 2008.
32. Kowalski, K.J., McDaniel, R.S., and J. Olek, "Development of a Laboratory Procedure to Evaluate the Influence of Aggregate Type and Mixture Proportions on the Frictional Characteristics of Flexible Pavements", *Journal of the Association of Asphalt Paving Technologists*, Vol. 77, 2008.
33. Indiana Test Method, ITM 214: "Acceptance Procedures for Polish Resistant Aggregates", Indiana Department of Transportation Materials and Tests Division, Indianapolis, Indiana, September, 2006.
34. West, T.R., Choi, J.C., Bruner, D.W., Park, H.J., and K.H. Cho, "Evaluation of Dolomite and Related Aggregates Used in Bituminous Overlays for Indiana Pavements", *Transportation Research Record #1757*, Transportation Research Board, Washington, D.C., 2001.
35. Superpave Mix Design, *Superpave Series No. 2 (SP-2)*, The Asphalt Institute, Lexington, Kentucky, 2001.
36. Goodman, S.N., Hassan, Y., and A.O.A. Abd El Halim, "Estimating Asphalt Pavement Texture Depth Using Superpave Gyratory Specimens and Mix Properties", *Proceedings of the 2005 Canadian Technical Asphalt Association Annual Conference*, Victoria, British Colombia, 2005.
37. Lee, Y.P.K., Yurong, L., Ying, L., Fwa, T.F., and Y.S. Choo, "Skid Resistance Prediction by Computer Simulation", *Conference Proceedings, Eighth International Conference, Applications of Advanced Technologies in Transportation Engineering*, 2004.
38. Standard Specifications for Transportation materials and Methods of Sampling and Testing, American Association of State Highway and Transportation Officials, 25th Edition, Washington, D.C., 2007.
39. Cooley, Jr., L.A., James, R.S., Buchanan, M.S., "Development of Mix Design Criteria for 4.75mm Superpave Mixes – Final Report", *NCAT Report No. 02-04*,

National Center for Asphalt Technology, Auburn University, Alabama, February 2002.
40. Standard Specifications for Highway Construction, Arkansas State Highway and Transportation Department, 2003 Edition.
41. Masad, E.A., “Aggregate Imaging System (AIMS): Basics and Applications”, *Report #FHWA/TX-05/5-1707-01-1*, Texas Transportation Institute, College Station, Texas, October, 2005.
42. Wessex Skid Tester S885, Operating Instructions, Version 4.1, Wessex Enigneering Ltd., Weston-Super-Mare, United Kingdom, October, 2004.
43. Tremblay, G., Julian, S., Leclerc, A., and B. Auger, “The Role of Aggregates in Road Surfacing Texture and Skid Resistance”, *Proceedings, Transportation Association of Canada*, Victoria, British Columbia, 1995.
44. Yager, T.J., “An Overview of the Annual NASA Tire/Runway Friction Workshop and Lessons Learned”, *Proceedings, International Conference on Surface Friction*, Christchurch, New Zealand, May, 2005.
45. Williams, S.G., “Development of Wheel-Tracking Test Method and Performance Criteria for Asphalt Pavements”, Doctoral Dissertation, University of Arkansas, Fayetteville, Arkansas, 2001.
46. Mackey, G., “Road Surface Friction: Measurement, Testing and Accuracy”, *Proceedings, International Conference on Surface Friction*, Christchurch, New Zealand, May, 2005.